TITLE: **DYNAMIC ACOUSTIC INTENSITY SCANNING FOR THE DETECTION OF FATIGUE IN OFFSHORE STRUCTURES**

FINAL REPORT

Work on this project was conducted under the auspices of the Department of Energy, Mines and Resources

DSS FILE NUMBER: 03SQ.23440-6-9208

DSS CONTRACT NUMBER: 23440-6-9208/01-SQ

EMR SCIENTIFIC AUTHORITY: Dr.D.K.Mak
Metals Technology Laboratories
555 Booth St, Ottawa

MICROMEDIA

C-CORE Contract Number 89-C4
March 1989

C-CORE
Centre for Cold Ocean Resources Engineering
Memorial University of Newfoundland
St.John's, NF, A1B 3X5, Canada
Tel (709) 737-8354 Fax 709-737-4706

90-07109/

The correct citation for this report is:

Guigné, J.Y. and Williams, P.G. (1989) "Dynamic Acoustic Intensity for the Detection of Fatigue in Offshore Structures".Contract report for the Department of Energy, Mines and Resources, C-CORE Contract Number 89-C4

Project Team

Jacques Guigné, Ph.D.
Group Leader

Gareth Williams, B.A.
Research Engineer

CONTENTS

		PREFACE	1
SECTION I		EXECUTIVE SUMMARY	2
SECTION II		REPORT TO CANMET ON DYNAMIC ACOUSTIC INTENSITY SCANNING	
	1.0	INTRODUCTION	4
	1.1	Context of research	4
	1.2	"What is DAIS ?"	5
	1.3	Marketing Potential	8
	2.0	RESEARCH STATUS	9
	2.1	Project Tasks and Status	9
	2.2	Time Scheduling Status	11
	2.3	Product Status	11
	3.0	CONCLUSION	12
	4.0	ACKNOWLEDGEMENTS	13
SECTION III		RESEARCH COMPENDIUM	14
	I	A concept for the detection of fatigue cracks in welded steel nodes	
	II	Analysis of the deformation in partially cracked welded T-plate	
	III	An introduction to the application of dynamic acoustic intensity scanning for non-contact detection of fatigue cracks	
	IV	Acoustic imaging using a DAIS technique for non-destructive testing	
	V	Stationarity of acoustical intensity measurement on steel plates	
	VI	Hydrophone phase matching for underwater intensity measurement	
	VII	Detection of in-service fatigue damage in offshore structures using dynamic acoustic intensity scanning	
	VIII	Characterization of steel plates containing machined defects using the DAIS technique	

CONTENTS cont.

SECTION IV APPENDIX A: LABORATORY EQUPMENT AND PROCESSORS

A.1 INTENSITY ANALYSER
A.2 TRANSDUCERS

A.2.1 Microphones
A.2.2 Hydrophones

A.3 CALIBRATION

PREFACE

This presentation is in four major sections. The first is an executive summary which provides a review of the content and direction of the research program. Section two details the research program and outlines the current research status in the context of the contractual obligations. The third section provides the reader with a research compendium made up of reviewed and published papers that have arisen from the project. These are based on the data collected over the period of the contract, and provide a reference to the collection techniques and the inferences drawn from the data. The final section describes the equipment utilized in this investigation. Their functions are described in view of their limitations and resolutions. Also highlighted in this section are the calibration techniques and standards used in establishing the DAIS methodology.

EXECUTIVE SUMMARY

Current in-service inspection of offshore steel structures tends to fall into three categories [1]:

i) global monitoring for establishing overall integrity

ii) specific defect location

iii) the gauging of the severity of defects when located

Detection of defects presents the most costly part of inspection and a number of different techniques are used: magnetic particle inspection, ultrasound, eddy-current, acoustic emission and alternating current potential difference (ACPD). These techniques are applied either through divers or through remotely operated robot systems. Of these techniques, only acoustic emission has the ability to remotely detect and locate defects, and even this technique has the disadvantage that a large number of transducers are required to fully instrument a structure.

An innovative energy flow mapping approach called Dynamic Acoustic Intensity Scanning (DAIS) has been developed at the Centre for Cold Ocean Resource Engineering (C-CORE). The technique measures the energy flow in a structure, as radiated by ambient vibration, to provide an early indication of fatigue cracking [2,3]. The radiated acoustic energy is measured and mapped using acoustic intensity scanning, and the DAIS logic relates changes in acoustic intensity maps measured over a structure to changes within the structure [4] such as the initiation and development of fatigue cracks. The DAIS methodology is applied through software control of data collection and vectorial analysis.

Work is currently being focussed on applying DAIS to underwater measurements in association with NORDCO Ltd. The design of suitable transducers for the DAIS is the primary emphasis of the underwater research. The phase matching of a set of hydrophones has been carried out [5] and this has allowed the measurement of intensity in an underwater environment to be successfully performed [6].

A number of reports and data are now in preparation for publishing, including a paper on the stationarity of acoustical intensity measurements [7] which illustrates the reproducibility and sensitivity of the DAIS approach for NDT. This report is a compendium to collectively present the ideas, experiments and data performed or collected under the terms of the

CANMET contract, Ref DSS File No. 03SQ.23440-6-9208.

The objectives of the contract were to:

i) investigate the use of an innovative acoustic intensity scanning technique

ii) detect fatigue cracks using acoustic intensity scanning

iii) quantify fatigue cracking using acoustic intensity scanning

iv) initiate the application of the DAIS for underwater mapping

The conclusions drawn from the research are as follows:

i) intensity mapping in the context of the DAIS technique is a powerful tool for structural engineering applications

ii) fatigue cracks have been shown to be detectable through the DAIS approach

iii) underwater measurement of acoustic intensity has been shown to be feasible

References

1. Anderson, M.R., "Nondestructive testing of offshore structures", NDT International, Vol.20 No. 1 Feb 1987

2. Guigne, J.Y., Williams, P.G. and Chin, V.H. "A Concept for the detection of fatigue cracks in welded steel nodes", Marine Technology, Vol 18 No. 4 Dec 1987

3. Guigne, J.Y., Williams, P.G. and Chin, V.H. "Analysis of the deformation in a partially cracked welded T-plate", Marine Technology, Vol. 18 No. 4 Dec 1987

4. Guigne, J.Y., Williams, P.G. and Mak, D.K. "Acoustical imaging using a DAIS technique for non-destructive testing", Proceedings of 17th International Symposium on Acoustical Imaging, Publ. Plenum 1988

5. Guigne, J.Y. and Williams, P.G. "Hydrophone phase matching for underwater intensity measurements", Proprietary Report to NORDCO Ltd. 1988

6. Guigne, J.Y., Williams, P.G. and Adams, J.G. "Detection of in-service fatigue damage in offshore structures using Dynamic Acoustic Intensity Scanning", To be presented at the 12th World Conference on Non-destructive Testing, Amsterdam, 1989.

7. Guigne, J.Y., Williams, P.G. and Adams, J.G. "Stationarity of Acoustic Intensity Measurements on Steel Plates", Submitted to JASA, Feb. 1989

RESUME GENERAL

L'inspection en service des structures marines en acier peut être rangée actuellement en trois catégories [1]:

i) surveillance globale destinée à vérifier l'intégrité d'ensemble

ii) détection des défauts singuliers

iii) appréciation de l'importance des défauts aprés détection.

La détection des défauts représente la partie la plus coûteuse et plusieurs techniques peuvent être utilisées: inspection magnétique par particules, ultra-sons, courants de Foucault, émission acoustique et différence de potentiel en courant alternatif (ACPD en anglais). Ces techniques sont mises en oeuvre soit par des plongeurs soit par des systèmes robotisés télécommandés. Parmi ces techniques seule l'émission acoustique peut détecter et localiser les défauts à distance, et même cette technique offre l'inconvénient de nécessiter la pose d'un grand nombre de capteurs pour instrumenter complètement une structure.

Une approche originale de cartographie du flux d'énergie, appelée Balayage Dynamique de l'Intensité Acoustique (BDIA ou DAIS en anglais) a été développée au Centre d'ingénieurie des océans froids (C-CORE en anglais). Cette technique mesure le flux d'énergie émis par la vibration ambiante d'une structure et fournit une première indication sur les fissures de fatigue[2]. L'énergie acoustique émise est mesurée et cartographiée par balayage de l'intensité acoustique et le logiciel inclus dans DAIS relie les variations d'intensité acoustique le long de la structure aux changements internes comme la création et le développement de fissures de fatigue[3]. La méthodologie du systéme DAIS repose sur une acquisition de données par ordinateur et une analyse vectorielle.

A l'heure actuelle le travail est concentré sur l'application sous-marine du système DAIS, en coopération avec NORDCO Ltd. La conception de capteurs appropriés au systéme est la première priorité de la recherche en cours. La synchronisation en phase d'un ensemble d'hydrophones a été effectuéee[4] et a permis de mesurer avec succès des intensités acoustiques dans un environnement marin[5].

Plusieurs rapports et ensembles de données sont actuellement en voie de publication, dont un papier sur la stabilité des mesures d'intensité acoustique[6] qui illustre le caractére reproductible et la sensibilité du

système DAIS. Le présent rapport tente de présenter globalement les idées, expériences et données développées ou recueillies lors de l'exécution du contrat CANMET (Réference dossier DSS No. 03SQ.23440-6-9208).

Les objectifs du contrat étaient les suivants:

i) évaluer les possibilités d'une nouvelle technique de balayage d'intensité acoustique.

ii) détecter des fissures de fatigue en utilisant cette technique.

iii) quantifier le degré de fissuration par fatigue.

iv) démarrer l'application du systéme DAIS à l'environnement marin.

Les conclusions tirées de cette recherche ont été les suivantes:

i) la technique de balayage d'intensité mise en oeuvre par le système DAIS est un instrument approprié à l'analyse des structures.

ii) il est possible de détecter des fissures de fatigue par ce système.

iii) la mesure d'intensité acoustique en milieu sous-marin est réalisable.

RESEARCH REPORT AND STATUS

1.0 INTRODUCTION

1.1 Context of Research

More than 1.5 billion barrels of recoverable light crude oil is probably contained in the nine significant offshore discoveries around Newfoundland and Labrador, including Hibernia. Many of these offshore field developments are expected to utilize floating production systems consisting of semi-submersible units, shuttle tanker fleets and sub-sea wells/flowlines, because the oil and gas reserve sizes are not significantly high to favour the use of a massive gravity structure. The majority of these structures would be entirely constructed of steel plates, beams and tubulars joined together by welding; they have to operate in an environment frequented by drifting first-year or multi-year ice, mobile bergy-bits/growlers and extreme hostile waves. Consequently, they will be subjected to considerable deterioration and damage due to corrosion fatigue cracking at the welded joints and impact with the drifting ice field or mobile ice masses. Furthermore, the commercial transport of oil and gas across the ice-bound northern regions of Canada and along the coasts of Newfoundland and Labrador would require ice-transiting ships capable of breaking through 4-5m thick ice and larger ice ridges. Areas of research pertaining to these two areas, viz., corrosion fatigue and impact, need to be developed to yield further insights into the mechanisms and procedures that would assist in formulating better prediction procedures, design methodologies and classification rules devised with Canadian East Coast waters in mind, but applicable worldwide.

The recent disasters of Alexander Kielland, Ocean Ranger and Piper Alpha have heightened the need for accurate monitoring of the safety of these offshore structures. A well-coordinated international effort is under way to develop inspection procedures and techniques to detect and quantify cracks and defects at welded joints of offshore structures using diver assisted Magnetic Particle Inspection (MPI), Alternating Current Field Measurement (ACFM), Eddy Current (EC) and Ultrasonic Techniques. Detailed underwater tests are in progress to establish technique reliabilities and the probability of detection and of the sizing of these

cracks. One identified shortcoming of these techniques is that they have been found to be limited in application because they must operate in the close vicinity of welded joints; they become useless at a little distance away from the zone of damage. Hence the development of a different procedure is required which would easily identify and quantify the damaged/cracked zone at a distance. One method amenable to global detection is the sound intensity measurement technique using the Dynamic Acoustic Intensity Scanning (DAIS) procedure, which is the primary product and subject of this CANMET funded investigation.

1.2 "What is DAIS ?"

Acoustic monitoring applications are based on the measurement of sound pressure levels. These are scalar quantities and hence no directional information is revealed. Acoustic intensity is a vector quantity indicating both the magnitude and direction of acoustic energy flow and is therefore a better descriptor of active sound fields. In general, a sound field will have both active and reactive components. Ambient noise is predominantly reactive and tends to have low particle velocities. Vibrational energy radiated from structures forms active fields with high particle velocities. Signal-to-noise ratios thus have the potential for a gain of up to 20 dB through intensity mapping instead of pressure measurement because of the high particle velocity and directional nature of an active field over the reactiveness of noise environments.

Applications of sophisticated signal processing techniques to the measurement of acoustic intensity [1,2] have led to the practical measurement of intensity using real-time digital filtering intensity analyzers.Intensity techniques are currently being employed for sound power measurement and source location in environments with a high background noise level. Bennett [3] utilises this technique to identify excessive noise levels radiating from a rotary pump set on an offshore production platform. The directionality of acoustic intensity allows for meaningful measurements to be made in the presence of high background noise. Recent refinements in the post processing of acoustic intensity data are enhancing the adoption of the approach to analyze repetitive, non-stationary signals to determine the timing of acoustic events [4]. This allows noise measurements in, for

example, marine diesel engines, to be relate to particular locations and times within the operating cycle.

An innovative energy flow mapping approach called Dynamic Acoustic Intensity Scanning (DAIS) has been developed at the Centre for Cold Ocean Resource Engineering (C-CORE). The technique measures the energy flow in a structure, as radiated by ambient vibration, to provide an early indication of fatigue cracking [2]. The radiated acoustic energy is measured and mapped using acoustic intensity scanning, and the DAIS algorithms relate changes in acoustic intensity maps measured over a structure to changes within the structure [3] such as in the initiation and development of fatigue cracks. The DAIS methodology is applied through software control of data collection and vectorial analysis.

In summary, DAIS is an iterative adaptive technique whereby the non-local or far-field physical characteristics of an object being analyzed can be determined through a theoretical manipulation and adaptive focussing of the vector energy flow which emerges from localised regions. The algorithms utilised by the DAIS, including continuous error analysis, are incorporated into the following descriptive steps:

Step 1

- Obtain the intensity at a point to isolate the maximum and minimum energy directions and the corresponding spectra.

- Define the measurement parameters from this initial step, e.g. the trigger cycle and signal averaging. This information can also be used to select an appropriate gated trigger for the measurements and to provide an estimate of the number of samples and their duration required for the trigger gate.

Step 2

- Perform a continuous scan over the surface using a one octave analysis to produce a power spectrum averaged over an area.

- Compare the frequency bands of the spectrum obtained from step 1 with the area averaged spectrum. This produces a first look at the natural flexing of the material. The frequency bands which are not associated with flexing are identified and classed as indicative bands. These are the first highlighted signs of anomalous zones.

Step 3

- Design and implement a coarse grid matrix enclosing the anomalous

zones.

- A one octave analysis is superseded by a one-third octave analysis and a comparison of the bands is made between the two octaves.

- The power spectrum averaged over this coarse grid is executed and mirrored against step 2.

- The preliminary indicative bands noted in step 2 are now confirmed by comparison with the one-third octave analysis. A two-dimensional energy flow vector map is created by sampling each of the grid points in two orthoganol directions. The vector map is then processed against the intensity maps.

Step 4

- Identify the following from steps 1, 2 and 3:

  a) Sources and sinks along the structure,

  b) Anomalies and associated frequency bands,

  c) Two- and three-dimensional spatial maps at the indicative frequency bands and at other frequencies not associated with the anomaly such as those related to the natural flexing behaviour of the structure.

  d) Two-dimensional vector directions of the energy flowing in the structure.

- Delineate the targets of interest, define their frequency band and decide on a grid spacing for a more detailed spot investigation.

Step 5

- Establish a finer measurement grid over the anomalous area.

- Optimise the microphone spacing and configuration to the indicative frequency bands of step 4.

- Construct spatial contour maps at these frequencies. Vector plots can be performed at this stage.

- Compare the grid point power spectra with the area averaged power spectrum as obtained over the finer grid.

- Statistically quantify the spatial changes.

Step 6

- Further investigation into the morphology of the crack, including depth, width and shape, can now be initiated using a 1/12 octave

examination via a Fast Fourier Transform (FFT) analysis. The logic now retraces steps 3, 4, and 5. This step is a tentative suggestion yet to be validated experimentally.

The measurement of an acoustic intensity vector allows for direct identification of sound sources including the direction of acoustic energy flow. This energy flow is due to acoustic/vibrational excitation of the test piece, either artificially induced or due to natural sound sources such as machinery operating aboard an oil production platform. At any time, the energy flow at a localised region will depend upon the physical state of both the near field and the far field. This is analogous to the flow of water at a point in a river, which depends both upon the shape of the river bed at the point in question, and also on the condition of the river bed upstream and downstream of the point. DAIS determines a "zero" or reference energy flow map, corresponding, for example, to the oil production platform in a newly operational condition, and measures changes to this energy flow map as the oil production platform physically changes (i.e. as work is done at a particular node during the formation of a fatigue crack). Remote changes to the physical structure of the oil production platform will affect the local energy characteristics. Hence, the energy mapping does not have to occur at a point where a fatigue crack is forming; mathematical manipulation of the local energy flow data will detect distant defects. Through the DAIS technique the possibility of the non-detection of small, but potentially dangerous, cracks will be reduced and the monitoring of the entire structure from a few strategic points becomes feasible.

1.3 Marketing Potential

The advantages of the DAIS techniques have not been unrecognized by the industry. The offshore oil sector, as represented by the industrial associates of C-CORE, have displayed great interest in DAIS; in particular for the detection of fatigue cracks in oil platforms. NORDCO Ltd., a profit motivated company, sees DAIS based defect detection as a profitable enterprise, and are involving themselves in its development, especially in underwater applications. Collaborative work with C-CORE to marry the DAIS techniques with their own areas of expertise is being actively pursued. It is this industrial interest, from both primary and support industry, which

is fueling the DAIS development at C-CORE.

2.0 RESEARCH STATUS

2.1 Project tasks and status report

The research followed an exacting set of schedules and project management tasks as stated in the contract (DSS File No. 03SQ.23440-6-9208). A synopsis of the study status is tabulized into the following summary.

PART I DESIGN OF EXPERIMENTS

Task 1 Design of the steel plate and preparation of equipment

i) Fabrication of the plates
Five plates will be used, four in air and one in water

Each plate is:
11.6 cm. wide x 61 cm long x 1.9 cm. thick

Status: Complete

ii) Calibration of the MTS test frame including load cells and accelerometers

Status: Complete

iii) Building of water jacket around steel plates for intensity scanning in water medium

Status: Complete

Task 2 Installation of the Acoustic Intensity scanning equipment an control instrumentation

i) Optimization of microphone configuration in air and hydrophone configuration in water

Status: Complete

ii) Construction of positioning apparatus

Status: Complete

iii) Establishment of a scanning grid

Status: Complete

iv) Installation of computer network

Status: Complete

Task 3 Instrumentation Trials

i) Evaluation of MTS frame, microphones and analyzer

Status: Complete

ii) Refinement of data acquisition assembly and support software

Status: Complete

iii) Final interfacing with test run

Status: Complete

PART II SCIENTIFIC INVESTIGATION

Task 4 Preliminary data evaluation

Power spectra at different points will be inspected to choose the appropriate intensity parameter, i.e. frequency band and interval for time averaging. This procedure will be repeated for different plates under different conditions, i.e. different incision an appropriate fixed loads.

Status: Complete

Task 5 Acoustic data collection

i) The steel plates will be scanned two-dimensionally at pre-determined grid points. At each grid point, two pairs of microphone readings will be collected, each pair will be taken at 90^{o} from each other

Status: Complete

ii) The plates will then be scored as specified and then re-scanned

Status: Complete

iii) In addition, one of the five plates will be scanned in water medium

Status: Complete

Task 6 Post Processing

i) Sound power analysis - sound power (dB) will be plotted versus frequency

Status: Complete

ii) Spatial acoustic intensity, frequency magnitude and phase analysis (2D contour mapping and 3D plot)

Status: Complete

Task 7 Interpretation and Analysis of Results

i) Correlating the acoustic intensity, frequency and phase scans with incisions of different width and depths and at different fixed load conditions

Status: Complete

ii) Establishing confidence levels and errors

Status: Complete

Task 8 Presentation of results

i) Exploration of tubular T-joint application and analysis and reporting results

Status: Complete

ii) Establishing the significance of the results

Status: Complete

iii) Publication of the results

Status: Ongoing

iv) Recommendation of future work, including application to concrete, non-ferrous metals and ice

Status: Ongoing

2.2 Time scheduling status

The time scheduling is presented in Table A and exhibits the proposed, revised and actual times taken for the various tasks.

2.3 Product status

This research project has had a high level of productivity as measured

by its peer reviewed publications (see Section III for a research compendium).

2.3.1 Journal Papers

Guigne, J.Y., Williams, P.G. and Chin, V.H. "A Concept for the detection of fatigue cracks in welded steel nodes". Marine Technology, Vol 18 No. 4 Dec 1987

Guigne, J.Y., Williams, P.G. and Chin, V.H. "Analysis of the deformation in a partially cracked welded T-plate". Marine Technology, Vol. 18 No. 4 Dec 1987

Guigne, J.Y., Williams, P.G. and Chin, V.H. An Introduction to the Application of Dynamic Acoustic Intensity Scanning for Non-Contact Detection of Fatigue Cracks. Monograph, Publ. Brüel & Kjaer Denmark Ltd.

Guigne, J.Y., Williams, P.G. and Adams, J.G. "Stationarity of acoustical intensity measurements on steel plates". Submitted for review to the Journal of the Acoustical Society of America (1988)

2.3.2 Conference Submissions

Guigne, J.Y., Williams, P.G. and Mak, D.K. "Acoustical imaging using a DAIS technique for non-destructive testing". Proceedings of 17th International Symposium on Acoustical Imaging, Publ. Plenum 1988

Guigne, J.Y., Williams, P.G. and Adams, J.G. "Detection of In-Service Fatigue Damage in Off-shore Structures using Dynamic Acoustic Intensity Scanning". 12th World Conference on Non-Destructive Testing, Amsterdam 1989

2.3.3 Technical Reports

Guigne, J.Y. and Williams, P.G. Hydrophone phase matching for underwater intensity measurements. Report to NORDCO Ltd. 1988

Guigne, J.Y. and Williams, P.G. Application of Acoustic Intensity Scanning for Fatigue Prediction and Crack Detection. Final Report to EMR (CANMET) 1988

3.0 CONCLUSION

The Dynamic Acoustic Intensity Scanning is an innovative application of acoustic intensity mapping which applies an iterative and adaptive methodology developed at C-CORE to relate changes in acoustic intensity maps measured over a structure to changes within the structure, such as the initiation and development of fatigue cracks. The DAIS methodology is

applied through software control of data collection and vectorial analysis. Canadian and overseas industries, especially from the oil sector, are displaying considerable interest in the development of the DAIS techniques, and are encouraging an accelerated program of research and calibration.

On this basis, C-CORE, with its associate NORDCO Ltd., will direct research involving the Dynamic Acoustic Intensity Scanning technique for a wide variety of applications, such as:

i) the remote sensing technique on offshore structures to monitor fatigue at welded nodes.

ii) an on-line inspection procedure in metal; casting and rolling mills,

iii) a method of monitoring the integrity of pressure vessels, turbine shafts, pipe work and ship hulls without withdrawal from service,

iv) a cost effective system for monitoring concrete structures such as bridges, dams and concrete gravity based oil platforms.

4.0 ACKNOWLEDGEMENTS

Special thanks are due to Mr. Gunnar Rasmussen and Mr. Gary Burns (Bruel & Kjaer Ltd.) for their scientific support of this program; to Dr.A.S.J.Swamidas (Memorial University of Newfoundland) for his interest and help in making the welded T-plate and tubular specimens available; to Drs. Robert Thompson and Don Mak of CANMET for their encouragement and advice throughout the work and to NORDCO Ltd for their financial support of the underwater intensity trials.

Reference

1. Fahy, F.J., Measurement of acoustic intensity using the cross spectral density of two microphone signals. J.Acoust. Soc. Am. 62, pp 1057-1059, 1977

2. Chang, J.Y., Cross-spectral method of measuring acoustic intensity without error caused by instrument phase mismatch. J. Acoust. Soc. Am. 64, pp 1613-1616, 1978

3. Bennett, I., AIA points to the noisy parts. CME pp 48-50, 1987

4. Rasmussen, G. and Rasmussen, P. Localization of sound fields. SENLIS 1985

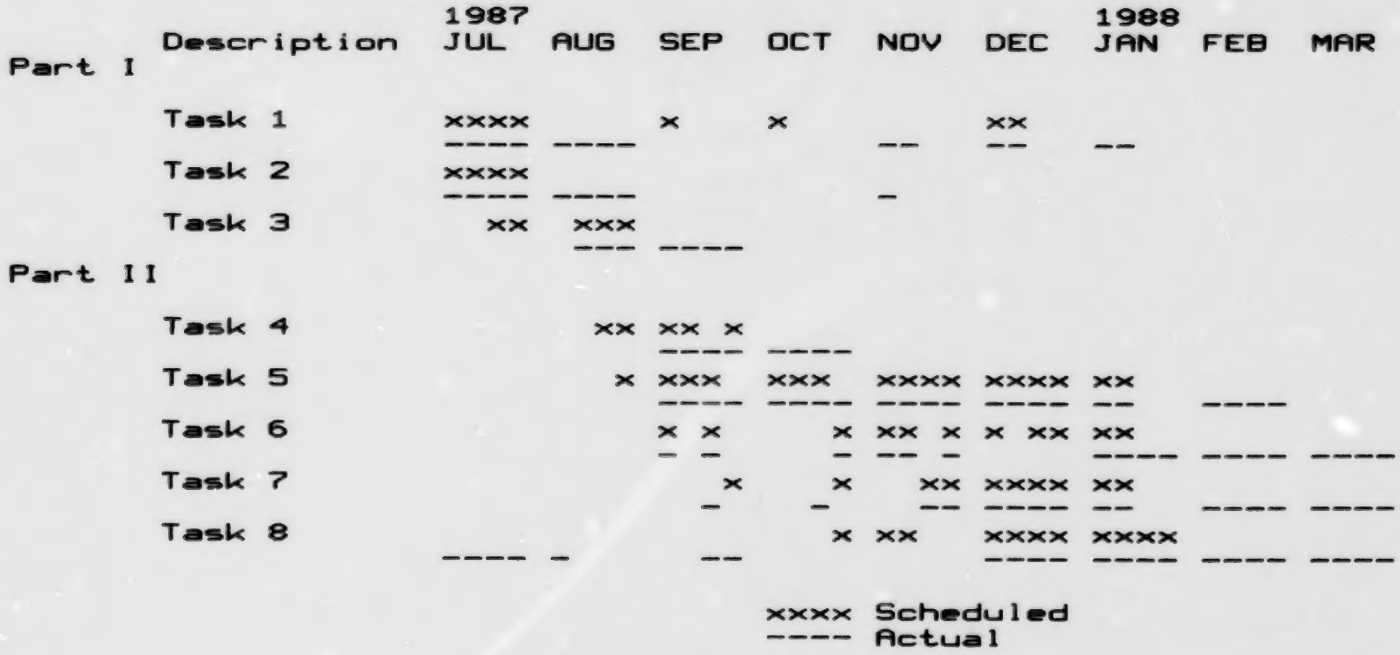

Time Scheduling Status
Table A

RESEARCH COMPENDIUM

This research compendium is presented in the form of peer reviewed papers which cover the initiation and development of the Dynamic Acoustic Intensity Scanning technique for the detection of fatigue cracking.

The first application of acoustic intensity scanning was made on large scale tubular joints undergoing fatigue testing at Memorial University of Newfoundland, and these results are presented in Paper I, "A Concept for the Detection of Fatigue Cracks in Welded Steel Nodes", which was published in Marine Technology (Dec. 1987). The data were studied and compared with crack data obtained using AC Field Measurement (ACFM) techniques for fatigue crack sizing, and the location of the defect correlated well between the two techniques. The technique was also applied to small scale welded T-plate specimens also undergoing fatigue cracking. In addition to the crack detection, the ability of the technique was demonstrated for the measurement of modal deformation. These results are presented in Paper II, "Analysis of the Deformation in a Partially Cracked Welded T-Plate", also published by Marine Technology (Dec. 1987).

Paper III is a monograph, based on the work done in the previous two papers. This monograph will be published and circulated by Brüel & Kjaer Ltd. Denmark. It is expected that a wide readership will occur. The title of the monograph is: An Introduction to the Application of Dynamic Acoustic Intensity Scanning for Non-Contact Detection of Fatigue Cracks.

Paper IV, "Acoustic Imaging Using a DAIS Technique for Non-Destructive Testing" was presented at Acoustical Imaging 88 in Sendai, Japan (1988). This paper exhibits a new data processing technique called the Residual Factor*. The Residual Factor quantifies changes in acoustic energy flow and facilitates these changes to be correlated with the development and progression of fatigue cracking.

The stationarity of the acoustic mapping was also investigated, primarily to determine how consistent the energy flow maps are when repeated readings are made with the same test conditions. The study is described in Paper V, "Stationarity of Acoustical Intensity Measurements on Steel Plates", which has been submitted for publication to the Journal of

---

*renamed in Paper V as the Remnant Factor

the Acoustical Society of America.

The initial work was carried out using microphones in air; hydrophones were subsequently evaluated for the underwater measurement of acoustic intensity in collaboration with NORDCO Ltd. This aspect of the project required the phase matching of a set of hydrophones to permit the measurement of acoustic intensity and these results are presented in Paper VI, "Hydrophone Phase Matching for Underwater Intensity Measurements". This piece of work was submitted as a propriety Technical Report to NORDCO Ltd. (Oct. 1988) and reflects their financial and equipment contribution. Once the hydrophones were phase matched and calibrated, they were used in the DAIS technique to scan a flat plate held in fresh water in a small tank. The results are presented in Paper VII, "Detection of In-Service Fatigue Damage in Offshore Structures using Dynamic Acoustic Intensity Scanning". This paper has been accepted for oral and written presentation at the World Conference on Non-Destructive Testing, to be held in The Netherlands in April 1989.

The final paper of the report, paper VIII, presents a study using the DAIS techniques as developed to date characterizing, in air, steel plates containing different machined defects. The paper is titled: "Characterization of Steel Plates Containing Machined Defects using the DAIS Technique". The final manuscript will be submitted to the Canadian Metallurgical Quarterly for potential publication of the results. Intensity maps are displayed and evaluated, and the Residual Factors illustrated. In addition, the modal damping of the specimens was measured using DAIS. The modal frequencies were identified and noted within the illustrations.

Submitted to Marine Technology/Meerestechnik (Germany)
Published December 1987 Vol. 18 No. 4

A CONCEPT FOR THE DETECTION OF FATIGUE CRACKS IN WELDED STEEL NODES

BY

J. Y. Guigné[+*], P. G. Williams, and V. H. Chin[+]

Centre for Cold Ocean Resources Engineering,
Memorial University of Newfoundland,
St. John's, A1B 3X5

+ C-CORE, Memorial University of Newfoundland,
St. John's, Newfoundland.

* NORDCO LTD., St. John's, Newfoundland.

ABSTRACT

An innovative dynamic acoustic intensity scanning concept is introduced for the remote non-contact detection of fatigue cracks in the welded steel nodes of offshore platforms. The physics of the approach were verified on a large steel node mounted in a test frame and subjected to a cyclic, tension-tension loading in the axial direction. The crack growth was monitored using this new technique of dynamic acoustic intensity mapping and the results were validated against AC field data. The crack position and shape were revealed coherently and unambiguously. From the cross-referencing routines of the interrogation logic, insight was obtained of the response of the structure to loading. Dynamic acoustic intensity scanning is a promising approach to rapid, non-contact monitoring of fatigue in offshore structures in both air and water. It also yields structural information which cannot be obtained directly through current non-destructive testing techniques.

INTRODUCTION

This paper presents the results obtained by using an innovative acoustic intensity scanning approach to detect fatigue cracking in a large scale laboratory specimen. The objective of this investigation was to explore the use of the energy flow in a structure, as radiated by ambient vibration, to provide an early indication of fatigue cracking. Most current non-destructive testing (NDT) techniques, such as ultrasound or magnetic particle inspection, rely on the defect to produce measurable perturbations of an introduced pulse or field within finite spatial and temporal resolution limits. In contrast, the concept described here measures the spatial flow of energy over the entire area of the structure. A dynamic intensity analysis of the structure differentiates between its modal behaviour and anomalous charac-teristics. The anomalies highlight and correspond to discrete sources and sinks in the energy field. The location of a defect is revealed after the energy spectra have been processed and the resultant acoustic signatures have been exhibited in the context of the natural flexing mode of the structure.

With the advent of sophisticated real-time analyzers for digital filtering and Fourier analysis, the practical measurement of intensity is now possible [1,2,3]. Dedicated computer processors and the use of self-calibrating acoustic manipulations [4] allow for the structure to be interrogated.

A significant aspect of this passive approach is that the receivers can be microphones, hydrophones or accelerometers. Since measurements can be made without surface contact and in most fluid media, the method is not affected by surface finish or environment and yet it is highly sensitive.

It is envisioned that the concept of dynamic acoustic intensity scanning could lead to an early predictive monitoring NDT tool which would help direct more effective usage of other NDT techniques and result in substantial cost saving.

I PHYSICS OF INTENSITY

Definition

The classic definition for sound intensity is a vector quantity that describes the net amount and direction of flow of acoustic power at a given point in space (where intensity is in W/m^2 and the intensity level is in dB re $1pW/m^2$). It is well established and stated in physics that if the intensity vector $\vec{I}$ (the energy flow vector) is the net rate of flow of energy per unit area at the given position, then the acoustic power, W, passing through a surface, S is:

$$W = \int_S \vec{I}.\, d\vec{S} \qquad (1)$$

$$W = \int_S I_n.\, dS \qquad (2)$$

where I_n is the vector component normal to the surface. In a medium without flow or bulk movement, the intensity vector $\vec{I}$ is equal to the time averaged product of the instantaneous pressure p(t) and the corresponding particle velocity $\vec{v}(t)$ at the same point. This is expressed mathematically as:

$$\vec{I} = \lim_{T\to\infty} \frac{1}{T} \int_{-T/2}^{+T/2} p(t).\vec{v}(t)dt \qquad (3)$$

Hence the intensity vector component in a given direction I_r is:

$$I_n = \lim_{T\to\infty} \frac{1}{T} \int_{-T/2}^{+T/2} p(t).v_r(t)dt \qquad (4)$$

It should be noted that our concept incorporates these fundamentals. The application of expression (4) is described in the following section.

Measurement of Intensity

From Eulers equation we know that, for a sound field propagating in a fluid, the particle acceleration A is given by the ratio of the pressure gradient to the fluid density ρ :

$$A = \frac{1}{\rho} \frac{\partial p}{\partial r} \qquad \text{(Eulers equation)} \qquad (5)$$

The particle velocity can thus be obtained by integrating the particle acceleration:

$$V = \frac{1}{\rho} \int \frac{\partial p}{\partial r} \, dt \qquad (6)$$

The pressure gradient is a continuous function which for two closely spaced microphones can be approximated using a finite difference method [5],[6] :

$$\frac{\partial p}{\partial r} = \frac{P_b - P_a}{\Delta r} \qquad (7)$$

where P_a and P_b are the pressures measured at the two microphones, and Δr is the receiver spacing; see Figure 1.

This gives an approximation for the pressure gradient at the centre of the microphone pair. The pressure at this point is derived from the average pressure of the two microphones:

$$P = \frac{P_a + P_b}{2} \qquad (8)$$

Substituting expressions (6), (7) and (8) into (4) we find that intensity can in practice be computed from:

$$I = \frac{P_a + P_b}{2\rho\Delta r} \int (P_b - P_a)\, dt \qquad (9)$$

Our dynamic intensity scanning approach uses sophisticated electronic equipment which applies Eulers equation and the supporting theory directly through the use of digital filtering and integration. The operations are executed in real time as shown in Figure 1.

Limitations

There are inherent limitations in measuring intensity using two closely spaced microphones and a finite pressure difference approximation for the derivation of the particle velocity [7]. The use of this technique in the measurement of sound intensity introduces a number of errors which limit the useful frequency range of the system. These errors have been well studied [8],[9],[10], and can be synthesised into the following categories:

i) a finite difference approximation error at high frequencies,

ii) an error due to the phase mismatch when the phase difference between the two element positions is small,

iii) a random error.

Errors can be minimized by optimising the receiver array and its configuration, and by having high transducer performance in accordance with IEC, ISO and ANSI standards (e.g. ANSI S1.12 1967 type XL, M). Signal averaging, as dictated by the ambient back-ground conditions, will substantially reduce the random error. For the detection of fatigue cracks, the application of a continuous calibration and a collective learning

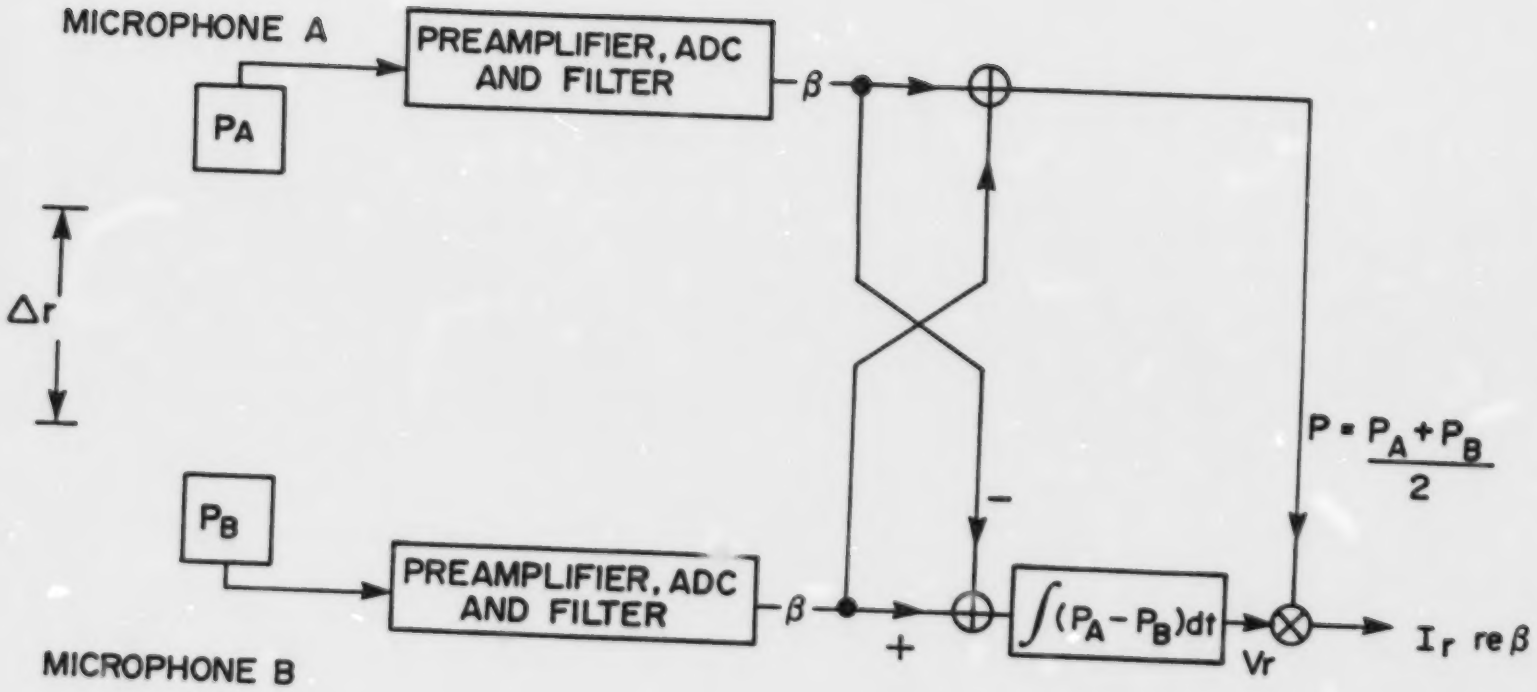

β Referenced to a Selected Frequency Band

Block Diagram for Real Time

Intensity Measurements

Figure 1

feedback diminishes the effect of errors and meets operational specifications and standards [4]. Continuous optimization of the measurement system yields high levels of precision.

Attenuation of Intensity

As energy propagates through a medium it can be redistri-buted as reflections, back-scatter and attenuation. The flexing of the specimen is displayed by the first two redistribution modes while the fatigue cracking of the node is revealed by the absorption that occurs. Changes in the mediums shear viscosity and bond relaxation, will cause an energy conversion into heat. The resultant intensity will be a negative direction seen as a sink. For instance, if we examine the intensity of a plane wave passing through an homogeneous steel plate, then we can express the absorption component classically by:

$$\frac{dI}{I} = -n\ dx \qquad (10)$$

where I is the intensity at some distance having a range R_1; dI is the loss of intensity in travelling a small distance, dx, having a range R_2; n is a proportional constant with a minus sign to indicate a negative change of intensity at dI. Upon integration between the two ranges, we find that the relationship between the two intensities is simply:

$$I_2 = I_1 \exp(-n(R_2 - R_1)) \qquad (11)$$

Expressed in dB, equation (11) becomes:

$$10 \log_{10} (I_2) - 10 \log_{10} (I_1) = - 10\ n(R_2 - R_1) \log_{10} (e) \qquad (12)$$

If we substitute $\alpha = 10\ n \log_{10}(e)$ we can now obtain a change of intensity level between R_2 and R_1 as:

$$10 \log_{10} (I_2) - 10 \log_{10} (I_2) = -\alpha(R_2 - R_1) \qquad (13)$$

or in other words:

$$\alpha = \frac{10 \log_{10} (I_1) - 10 \log_{10} (I_2)}{R_2 - R_1} \qquad (14)$$

Therefore expression (14) establishes the logarithmic absorption coefficient in decibels per metre (dB/m). For each metre travelled the intensity is diminished through absorption by α dB. The absorption is frequency dependant. Extensive studies and investigations into sound attenuation in fluids and sedi-mentary media have been widely reported and acknowledged in the literature [4]. This frequency factor is important and is exploited during our intensity interrogations of a specimen.

II LABORATORY INVESTIGATION

Laboratory Test Specimen

The fatigue behaviour of large offshore structures is being investigated by the Civil Engineering group of Memorial University's Faculty of Engineering and Applied Science in conjunction with CANMET, Arctec Canada Ltd. and Waterloo University. The specimen used to validate our concept was one of a series of welded tubular T-joints studied by the group; see Figure 2 for dimensions. The steel nodes were mounted in a test frame and subjected to a cyclic, tension-tension loading in the axial direction using an MTS 600 kip servo-hydraulic actuator. Fatigue cracking started at the weld toe in the region of the saddle point and the crack grew around the weld toe and through the thickness of the chord until near-complete failure had occurred [11]. The crack growth was monitored using an AC field measurement technique as part of the ongoing base research. This provided an opportunity to have a reliable and calibrated baseline to register the sensitivity of our experimental NDT approach and verify the validity of monitoring intensity dynamically.

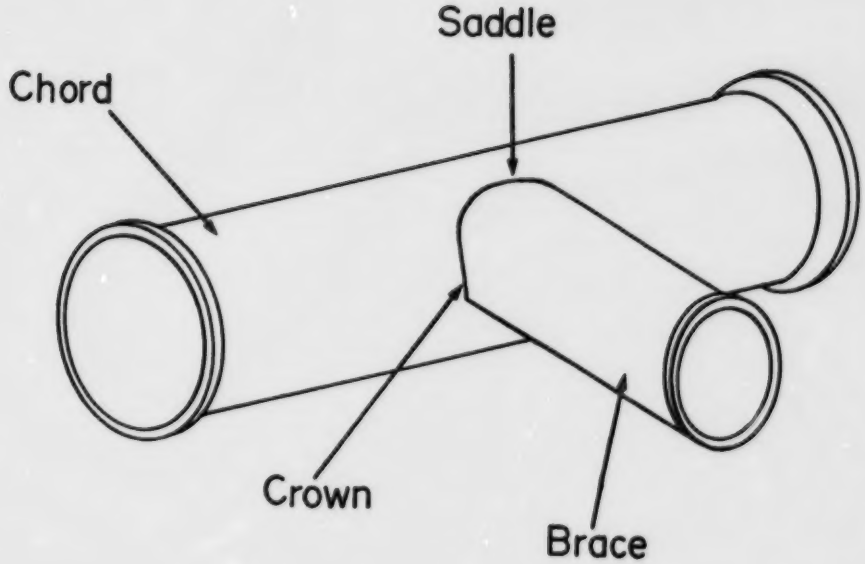

Chord diameter	= 914 mm
Brace diameter	= 457 mm
Plate thickness	= 19 mm
Chord length	= 2896 ± 5mm

Dimensions of Welded
Tubular T-Joints

Figure 2

Experimental Setting

The MTS system, and in particular the hydraulic power system and servo-valve, were employed as a source of energy. This energy propagated through the actuator and linkage to the specimen. It is this energy, freely flowing through the structure, that was targeted by our intensity scans. Measurements were taken for three different loading states:

i) a static load of 3 kN (nominally zero),

ii) a static load of 315 kN (maximum test load),

iii) a cyclic load between 51 kN and 315 kN at a frequency of 4 Hz.

The intensity measurements were made using the Brüel and Kjaer type 3360 sound intensity analyzing system using two 1/2" microphones (ANSI S1.12 1967 type XL) and a reference pistonphone for calibration.

Scanning Methodology

The interrogation logic utilised in the dynamic intensity scans, including continuous error analysis, is described by the following steps:

Step 1

- Obtain the intensity at a point to isolate the maximum and minimum energy directions and the corresponding spectra.
- Define the measurement parameters from this initial step, e.g. the trigger cycle and signal averaging. This information can also be used to select an appropriate gated trigger for the measurements and to acquire an estimate of the number of samples and their duration required for the trigger gate.

Step 2

- Perform a continuous scan over the surface using a one octave analysis to produce a power spectrum averaged over an area.
- Compare the frequency bands of the spectrum obtained from step 1 with the area averaged spectrum. This produces a first look at the natural

flexing of the material. The frequency bands which are not associated with the flexing are identified and classed as indicative bands. These are the first highlighted signs of anomalous zones.

Step 3

- Design and implement a coarse grid matrix enclosing the anomalous zones.
- A one octave analysis is superseded by a one-third octave analysis and a comparison of the bands is made between the two octaves.
- The power spectrum averaged over this coarse grid is executed and mirrored against step 2.
- The preliminary indicative bands noted in step 2 are now confirmed by comparison with the one third octave analysis. A two-dimensional energy flow vector map is created by sampling each of the grid points in two orthogonal directions. The vector map is then processed against the intensity maps.

Step 4

- Identify the following from steps 1, 2, and 3:
  a) Sources and sinks along the structure,
  b) Anomalies and associated frequency bands,
  c) Two- and three-dimensional spatial maps at the indicative frequency bands and at other frequencies not associated with the anomaly such as those related to the natural flexing behaviour of the structure,
  d) Two-dimensional vector directions of the energy flowing in the structure.
- Delineate the targets of interest, define their frequency band and decide on a grid spacing for a more detailed spot investigation.

Step 5

- Establish a finer measurement grid over the anomalous area.
- Optimise the microphone spacing and configuration to the indicative frequency bands from step 4.
- Construct spatial contour maps at these frequencies. Vector plots can be performed at this stage.

- Compare the grid point power spectra with the area averaged power spectrum as obtained over the finer grid.

- Statistically quantify the spatial changes.

Step 6

- Further investigation into the morphology of the crack, including depth, width and shape, can now be initiated using a 1/16 octave examination via a Fast Fourier Transform (FFT) analysis. The logic now retraces steps 3, 4 and 5. This step is a tentative suggestion yet to be validated experimentally.

For each loading state (see section II), sound intensity measurements were taken following the five steps. In the case of the measurements made during cyclic loading, a trigger unit was introduced to ensure that the intensity measurements for each grid location were made at the same point in the loading cycle. The data were subsequently analyzed on a Hewlett-Packard 310 computer using software running under the Basic 4.0 operating system. The five steps were implemented using dedicated software to formulate the interrogation logic of the concept.

Grid Locations on Specimen

The initial scans (step 1) confirmed the location of the defect as identified by the AC field measurement technique. Two measurement grids were then established as described in steps 4 and 5. The first was a 6 by 10 matrix with a grid spacing of 70 mm. This was used for measurements during the two static loading states (3 kN and 315 kN). This grid was centred around the saddle point of the weld with the fatigue crack at the weld toe running across its width (See Figure 3). The second grid was employed for measurements made during the cyclic loading tests executed between 51 kN and 315 kN. A 6 by 8 matrix with a spacing of 50 mm, was selected so that the grid lay above the crown point and contain the fatigue crack running across one half of its width (see Figure 4).

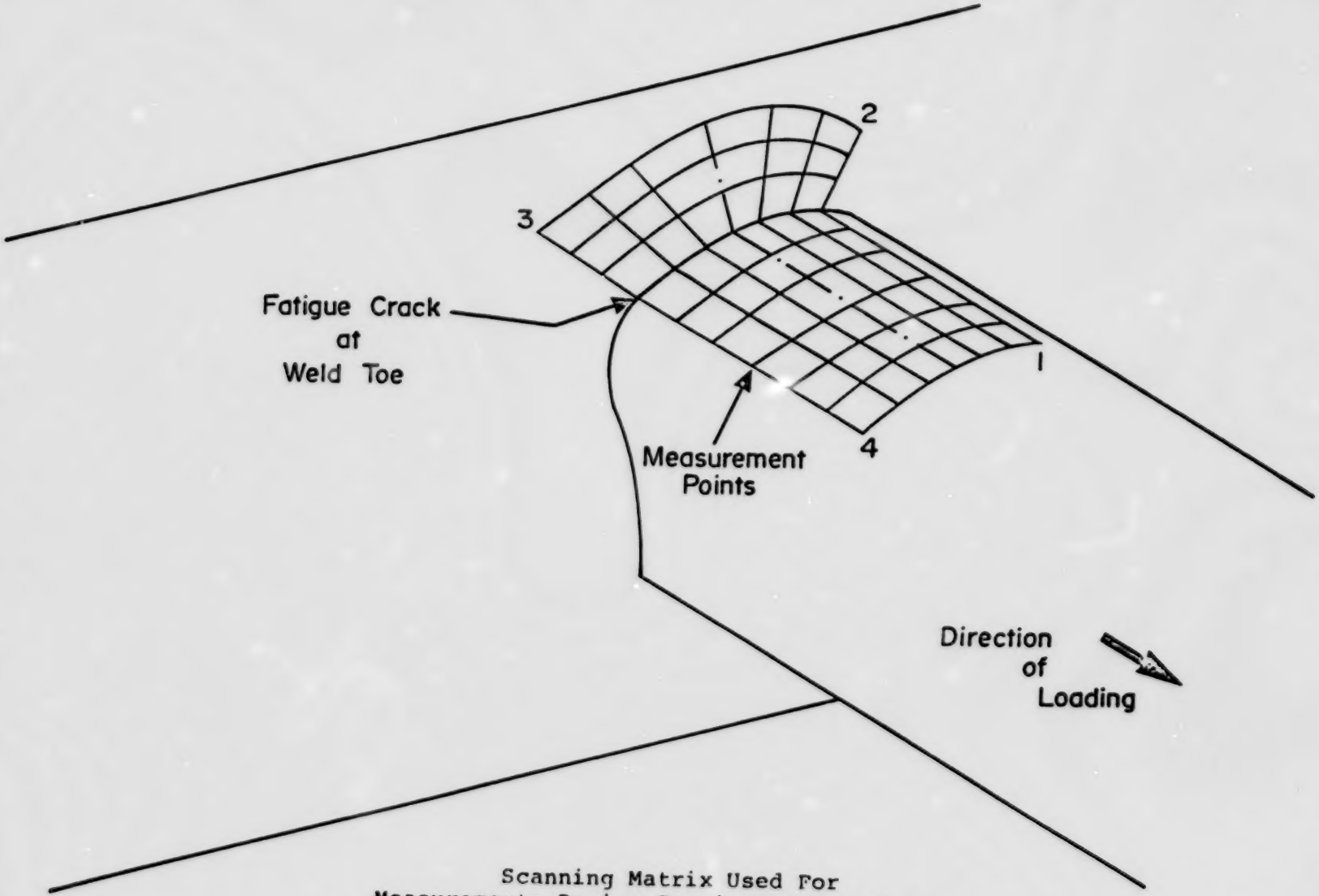

Scanning Matrix Used For
Measurements During Static Loading States

Figure 3

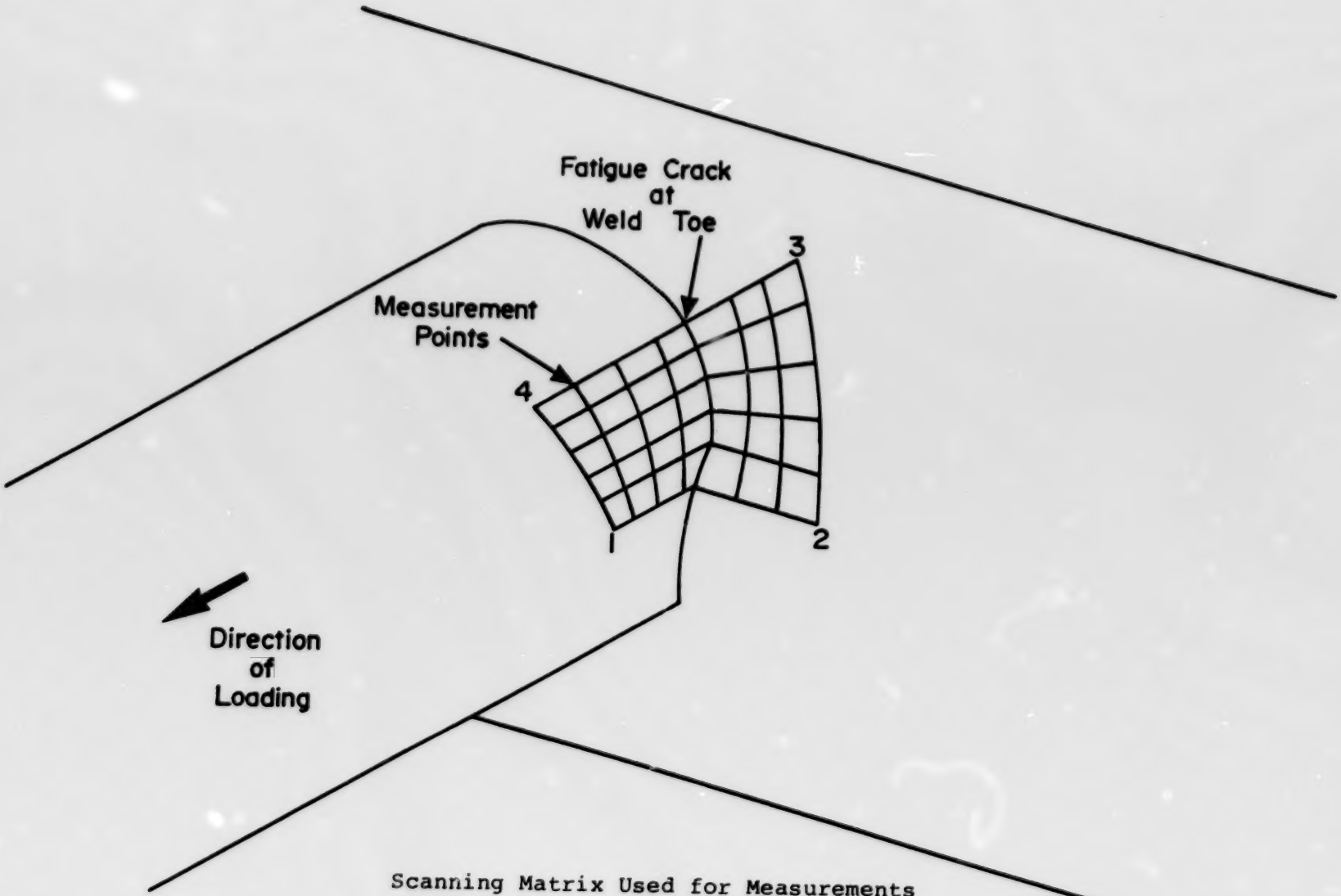

Scanning Matrix Used for Measurements

During Dynamic Loading States

Figure 4

III RESULTS

Fatigue Crack

As stated in section II, an AC field measurement technique monitored the initiation and propagation of the fatigue crack. The technique was calibrated both on small scale test specimens and by 'beachmarking' on the tubular joint. The crack profile at the time of the intensity measurements is shown in Figure 5, along with the position of the grid lines for reference. Photograph 1 shows the specimen at the completion of the failure test and illustrates the final extent of the fatigue cracking.

Intensity Measurements

The sound intensity measurements were made by recording the full intensity spectrum at each grid location. The data were then transferred to the computer and stored on disc. Once the full grid had been scanned, the data were analyzed to produce three-dimensional intensity plots for a single frequency or for an average over selected frequency ranges.

The three-dimensional intensity plots at selected frequencies are shown in Figures 6 to 11. In the translation from the specimen to a planar representation, the scanning matrix is reduced to a rectangular grid so it is not drawn to scale; the ordinate is calibrated to show intensity in units of dB. For each figure; a) shows the positive and b) the negative intensity, where polarity refers to a calibrated directionality. The data plots are produced by carrying out a linear interpo-lation of four steps between the data points; this is cross-checked by carrying out an additional scan between the grid points.

Interpretation

The experiments were confined to the three different loading states described in section II. Figure 12 exhibits the sound power spectra recorded during steps 1 and 2. In the initial interrogation (step 1) the 50 dB level was found to be the cutoff between contributions relating to the

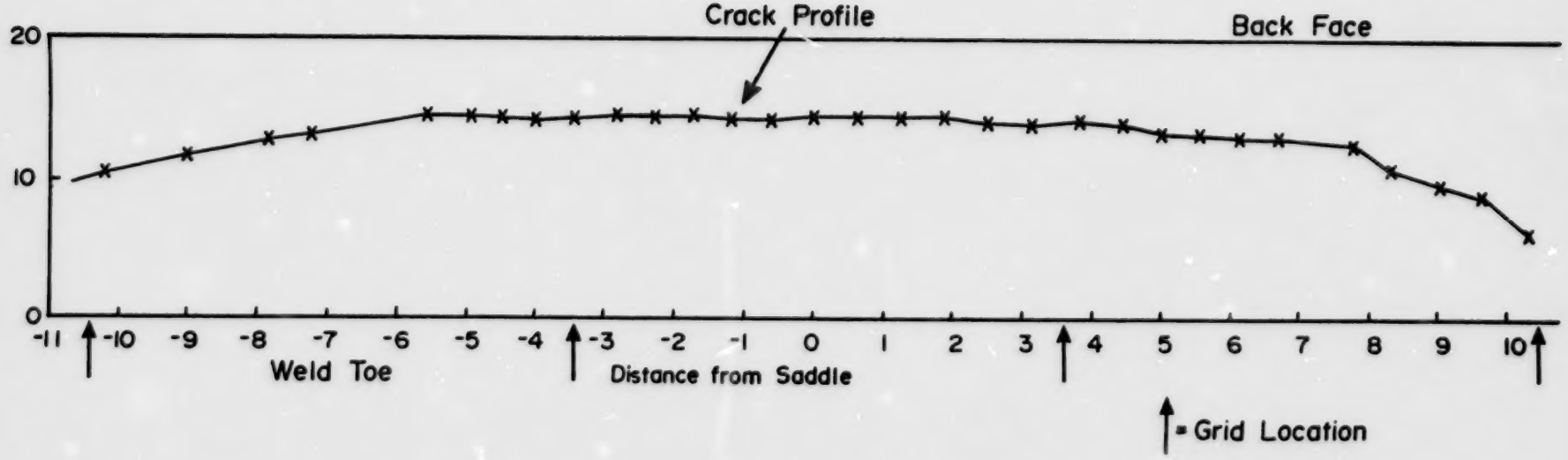

Crack Depth Vs. Position
At Time of Intensity Measurements

Figure 5

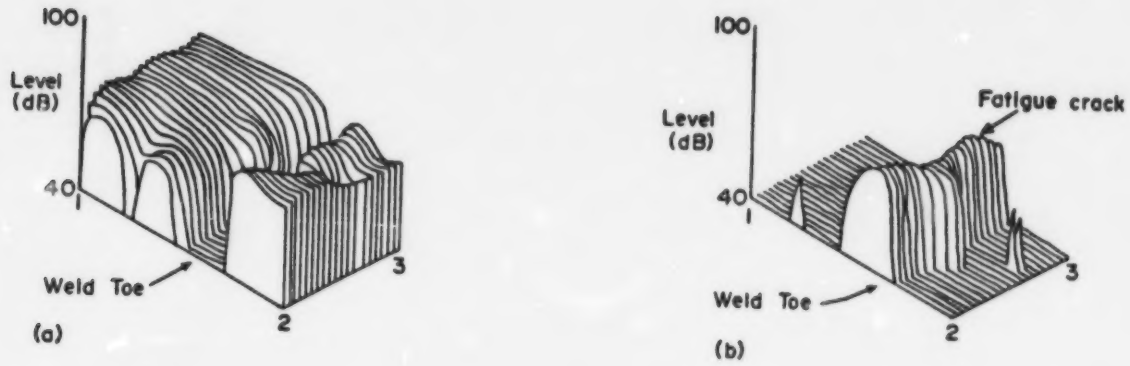

3KN Load, 100 Hz Data
Figure 6

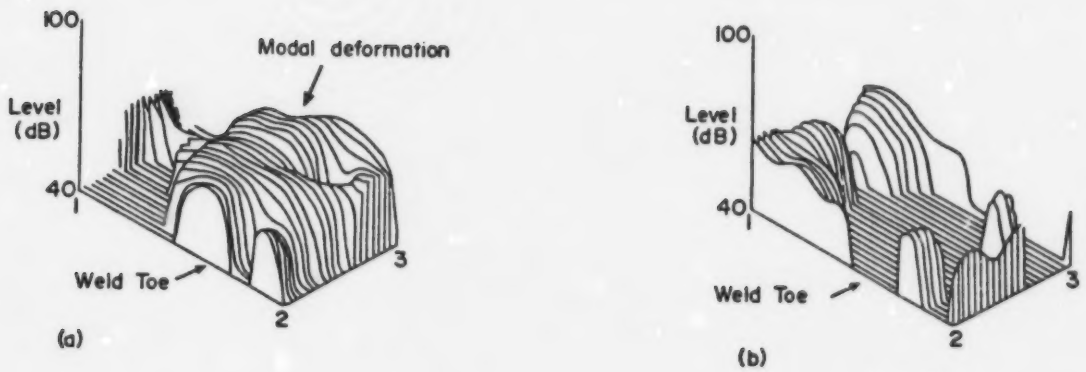

3KN Load, 200 Hz Data
Figure 7

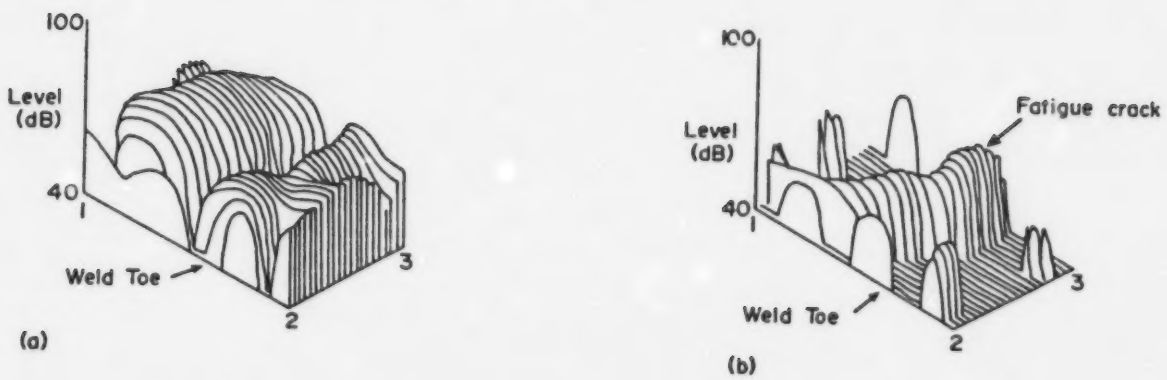

3KN Load, 800 Hz Data

Figure 8

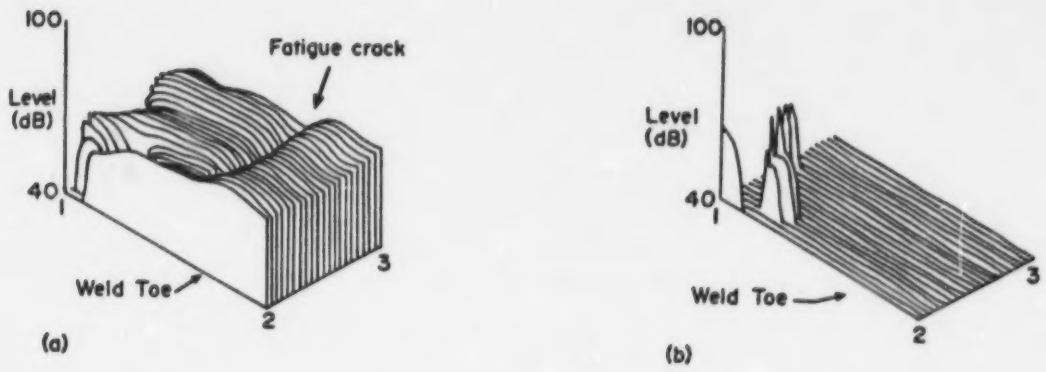

315 KN Load, 100 Hz Data
Figure 9

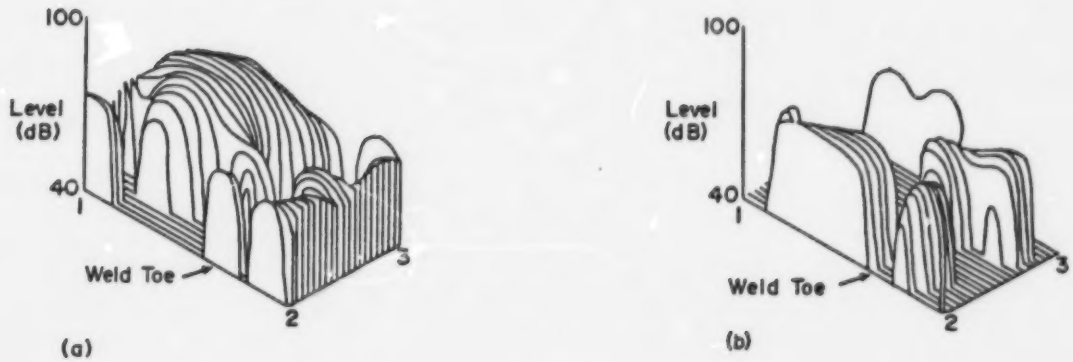

315 KN Load, 800 Hz Data
Figure 10

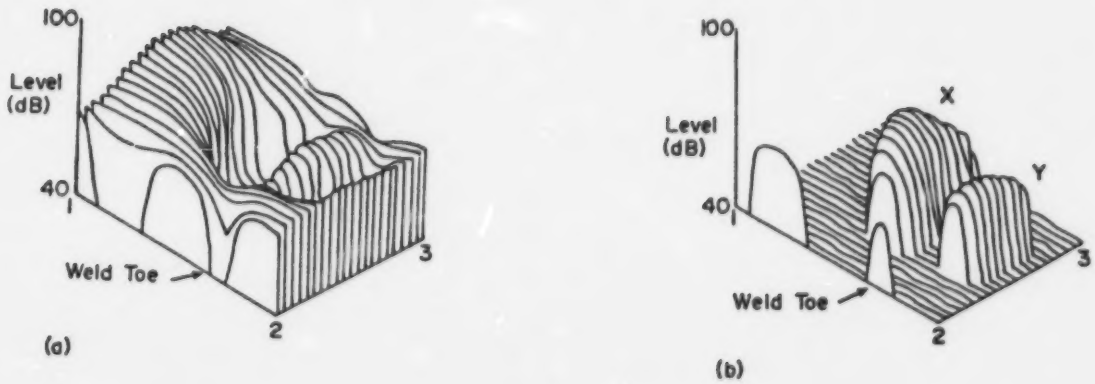

Cyclic Load, 800 Hz Data

Figure 11

energy flowing in the specimen, and those linked to a reactive component (refer to Figure 12a). This reactive component was found to be associated with environmental noise and standing waves. Focusing on frequencies with levels above the 50 dB boundary, three key frequency bands were revealed for each loading state; see Figures 12b, c and d. These are summarised in Figure 12e. During the cyclic loading, the dominant frequency bands were noted to centre on 800 Hz and 630 Hz. In the 3 kN and 315 kN static loading tests, the dominant frequency band was also 800 Hz, with two additional significant bands at 100 Hz and 200 Hz. The reduction in the 100 Hz band for the cyclic test (Figure 12b) was indicative of differences in the source of radiated energy connected with the hydraulic system. The actuator was being cycled at a frequency of 4 Hz during this period.

From the three-dimensional intensity plots that were computed from steps 2, 3 and 4, we can see that the 200 Hz data describes the natural flexing behaviour of the specimen. For example, Figures 7a and 7b highlight this modal deformation during the 3 kN loading. The intensity anomalies affiliated with the 800 Hz data, Figure 8, present details of the crack location, while the 100 Hz data, Figure 6, accentuates the shape of the crack.

In section II the physics of attenuation were introduced. With reference to this, the propagation of the energy through the specimen during the 3 kN and the 315 kN load trials was examined. In theory, the 100 Hz frequency band should have encountered less attenuation than the 800 Hz band. From our three-dimensional intensity plots (step 4 and 5) the 100 Hz band confirmed this and the intensity signature translated into a coherent, strong detection of the sink controlled by the crack (see Figures 6a, 6b, 9a and 9b). In comparison, the 800 Hz band intensity image showed a weaker overall signal due to its greater absorption. At this higher frequency, however, a greater degree of sensitivity to the localised stresses which surrounded the defect was realised through the greater spatial detail of the minor sources and sinks (Figures 8a, 8b, 10a and 10b). Taken together, the two frequency bands yielded information that could not have been obtained through current NDT techniques.

Finally, in the cyclic loading test a finer grid was defined using step 5. The three-dimensional plot for a frequency of 800 Hz is presented in

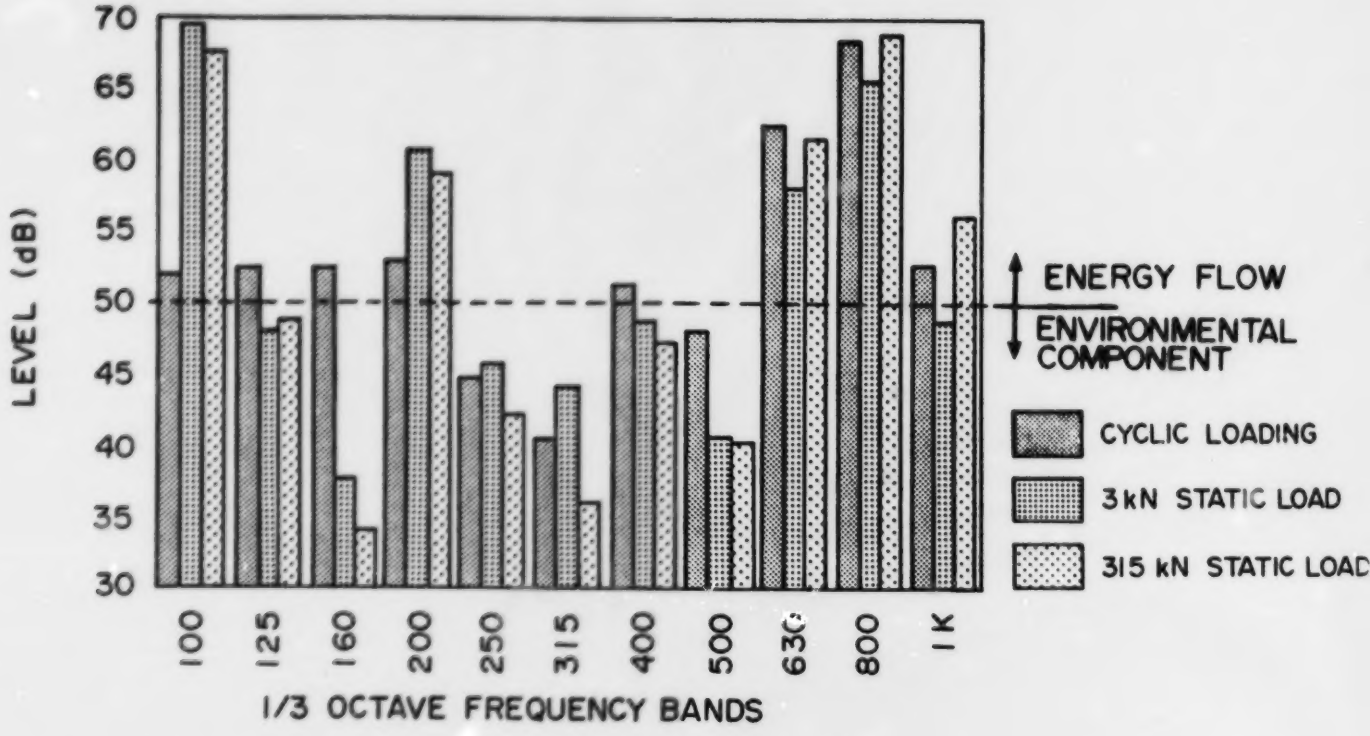

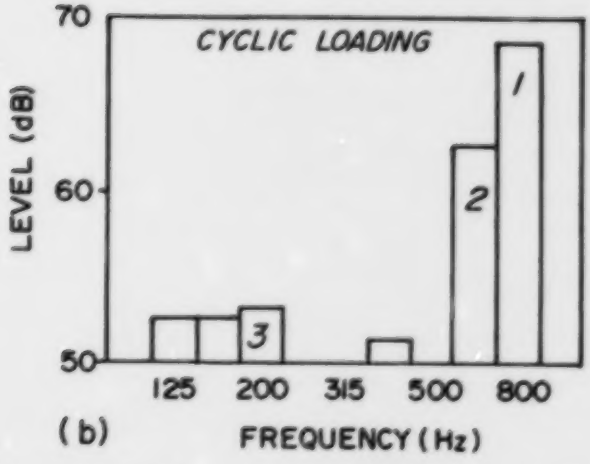

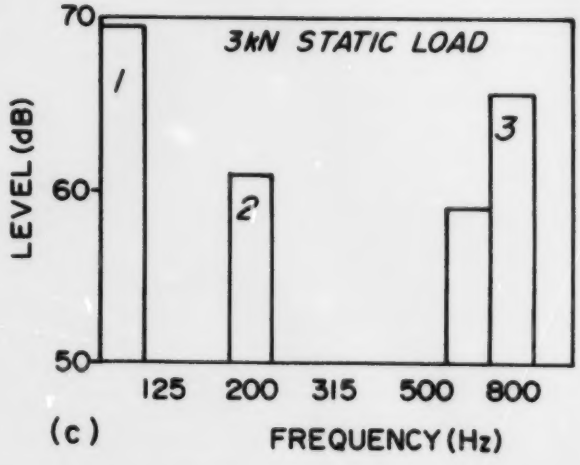

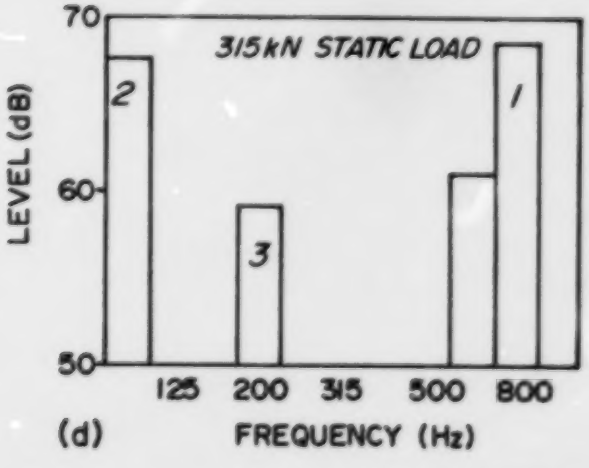

PEAK	CYCLIC		3kN		315kN	
	freq Hz	level dB	freq Hz	level dB	freq Hz	level dB
1	800	68.3	100	69.4	800	68.7
2	630	625	200	60.7	100	67.5
3	200	530	800	655	200	59.1

(e)

Sound Power Spectra
Figure 12.

Figures 11a and 11b. The sink associated with the defect (x) can be seen along with a second sink (y) associated with model deformation around the crack.

IV CONCLUSION

The non-contact sound intensity scanning technique described in this paper has been shown to be a valuable new method for non-destructive testing especially when applied to dynamic interrogation. The spatial plotting of the crack position and shape was coherent and unambiguous. From the cross-referencing of steps 1 to 5, a direct insight was attained of the response of the structure to the loading. On this basis our dynamic acoustic intensity scanning technique can be directed to a wide variety of applications such as:

i) a remote sensing technique on offshore structures to monitor the intensity of welded nodes,

ii) an on-line inspection procedure in metal casting and rolling mills,

iii) a method of monitoring the integrity of pressure vessels, turbine shafts, pipe work and ship hulls without withdrawal from service,

iv) a cost effective system for monitoring concrete structures such as bridges, dams, and concrete gravity based oil platforms.

Further study into the scope of the concept is now underway to establish standards for general applications both in air and in water. Use of an FFT analysis using 1/16 octave bands interfaced with a digital filtering processor is being considered to create step 6.

ACKNOWLEDGEMENTS

Special thanks are due to Mr. Gunnar Rasmussen and Mr. Gary Burns (Brüel & Kjaer Ltd.) for their scientific and technical support of the programme; to Arctec Canada Ltd. and Dr. A. S. J. Swamidas (Memorial University of Newfoundland) for their interest and help in making the tubular T-joint specimen available to test our concept and to Dr. Robert Thompson (CANMET) for his encouragement and advise throughout the work.

REFERENCES

1 Fahy, F. J.
"Measurement of Acoustic Intensity Using the Cross-Spectral Density of Two Microphone Signals." J. Acoust. Soc. Am. 62, pp 1057 - 1059, 1977.

2. Chung, J. Y.
"Cross-Spectral Method of Measuring Acoustic Intensity Without Error Caused by Instrument Phase Mismatch." J. Acoust. Soc. Am. 64, pp 1613 - 1616, 1978.

3. Roth, O.
"A sound Intensity Real-Time Analyzer." Proc. 1st International Congress on Recent Developments in Acoustic Intensity Measurements CETIM, Salis, France pp 69 - 74, 1981.

4. Guigné, J. Y.
"The Concept, Design and Experimental Evaluation of an Acoustic Sub-Seabed Interrogator." Ph. D. Thesis, University of Bath, Published in the Bedford Institute Open File Library, 1986.

5 Forssen, B. & Crocker, M. J.
"Estimation of Acoustic Velocity and Radiation Efficiency by use of the Two-Microphone Technique." J. Acoust. Soc. Am. 73, pp 1047 - 1052, 1983.

6. Rasmussen, G.
"Measuring Intensity", Intensity Measurements, G Rasmussen (ed.), Brüel & Kjaer No. BA 7196 - 11, A1 - A10, 1985.

7. Watkinson, P. S.
"Calibration and Inherent Errors of a Two Hydrophone Sound Intensity Measurement System." Proc. Inst. Acoustics Vol. 6, Pt. 5, 1984.

8. Thompson, J. K. & Tree, D. R.
"Finite Difference Approximation Errors in Acoustic Intensity Measurements." J. Sound & Vibration 75, pp 229 - 238, 1981.

9. Gade, S.
"The Validity of Intensity Measurements." Brüel & Kjaer Technical Review 4, pp 3 - 31, 1985.

10. Rasmussen, P.
Intensity Measurements, Brüel & Kjaer, No. BA 7196 - 11, B1 - D5, 1985.

11. Swamidas, A. S. J., Munaswamy, K. & Williams, P. G.
"Progress Report on Fatigue Test of Tubular Joint 1." AMCA-DSS Report (Unpublished), 1987. In collaboration with Arctec Canada Ltd.

Submitted to Marine Technology/Meerestechnik (Germany)
Published December 1987 Vol. 18 No. 4

ANALYSIS OF THE DEFORMATION IN A PARTIALLY CRACKED WELDED T-PLATE

BY

J. Y. Guigné[+*], P. G. Williams, and V. H. Chin[+]

Centre for Cold Ocean Resources Engineering,
Memorial University of Newfoundland,
St. John's, A1B 3X5

+ C-CORE, Memorial University of Newfoundland,
St. John's, Newfoundland.

* NORDCO LTD., St. John's, Newfoundland.

ABSTRACT

An innovative Dynamic Acoustic Intensity Scanning (DAIS) technique was applied to the analysis of a partially cracked welded T-plate specimen. Through its unique analysis of the sound intensity distributions the position and shape of a fatigue crack was revealed. In addition, direct insight into the modal response of a structure was obtained.

The primary objective was to compare the response of the cracked side with that of the non-cracked side as disclosed by the DAIS' interrogation logic. The results showed that the fatigue crack could be clearly identified by the manner in which the energy propagated through the plate and that the modal deformation was exposed with perspicacity. In addition, DAIS detected anomalies in the intensity distribution which appear to be linked to small fatigue cracks. It is believed that this phenomenon cannot be detected by current non-destructive testing methods.

INTRODUCTION

The use of an innovative Dynamic Acoustic Intensity Scanning technique (DAIS) to detect fatigue cracking in a large scale welded tubular node has been introduced by the authors [1]. A methodology for the approach has been described and it was shown that the position and shape of cracks could be revealed coherently and unambiguously from an analysis of the sound intensity distribution. In addition, the cross-referencing routines of the interrogation logic yielded a direct insight into the transfer functions of the structure [1].

As a continuation of this work a study was carried out into the application of this methodology to the analysis of a partially cracked welded T-plate specimen. The primary objective of this paper is to present a comparison of the response of the cracked side with that of the non-cracked side as illustrated by the technique's interrogation logic.

I SETTING

Specimen

As part of the ongoing research into fatigue at Memorial University of Newfoundland, a number of welded T-plate specimens were tested. The dimensions of the specimens are shown in Figure 1. Each end of the specimen was clamped between two roller bearings and the vertical section attached to the hydraulic actuator. The specimen was then subjected to tension-tension loading in the range 20 kN to 140 kN. Fatigue cracks initiated at a number of sites along the weld toe. These small cracks (X) grow and coalesce (Y) to form a crack growing across the full width of the plate (Z) (refer to Figure 2). This crack will then propagate through the thickness of the plate until failure is complete.

When this investigation took place, the specimen had cracking across the full width of the weld on one side of the vertical section (V) but had no visible cracking on the other side (W); see Figure 1. This provided an ideal opportunity to verify the ability of the DAIS to capture the signatures of the cracked and non-cracked sides.

The welds were independently monitored using an AC field measurement method [2] and its instrumentation is illustrated in Plate 1.

Scanning Technique

The logic utilised in the intensity mapping and interrogations, including continuous error assessment, has been described [1] and involves a collective learning feedback [3]. The collective learning feedback process refers to the assimilation and processing of newly acquired information for subsequent iterations.

The measurements were made using a Brüel & Kjaer type 3360 Sound Intensity Analysing System, with two 1/4" microphones (ANSI S1.12 1967 Type M) and a reference pistonphone for calibration. The data were subsequently analyzed on a Hewlett-Packard 310 computer system running dedicated software to implement the DAIS.

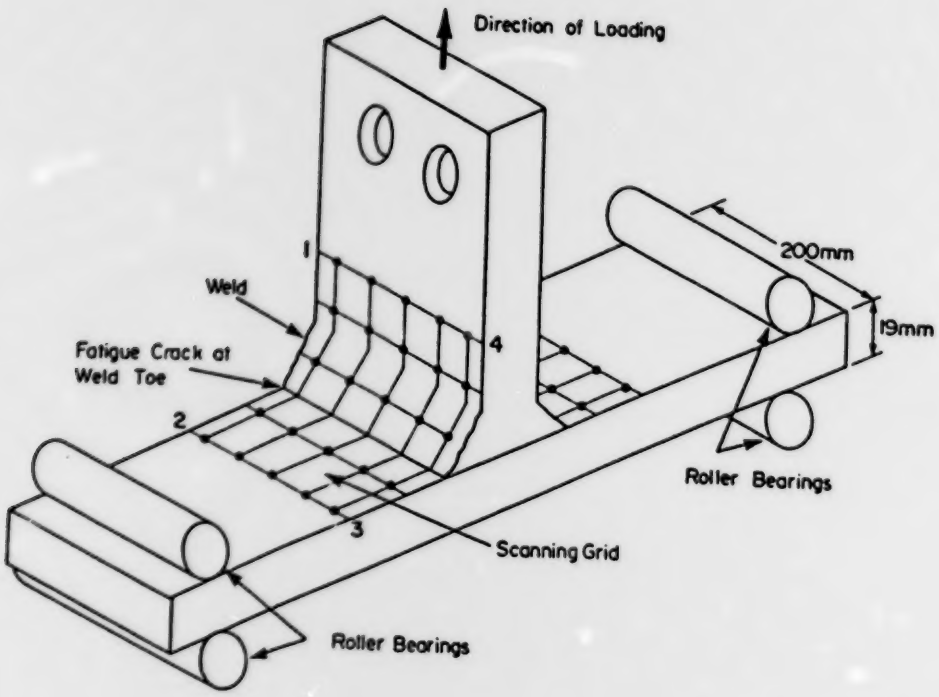

Welded T-Plate Specimen

Figure 1

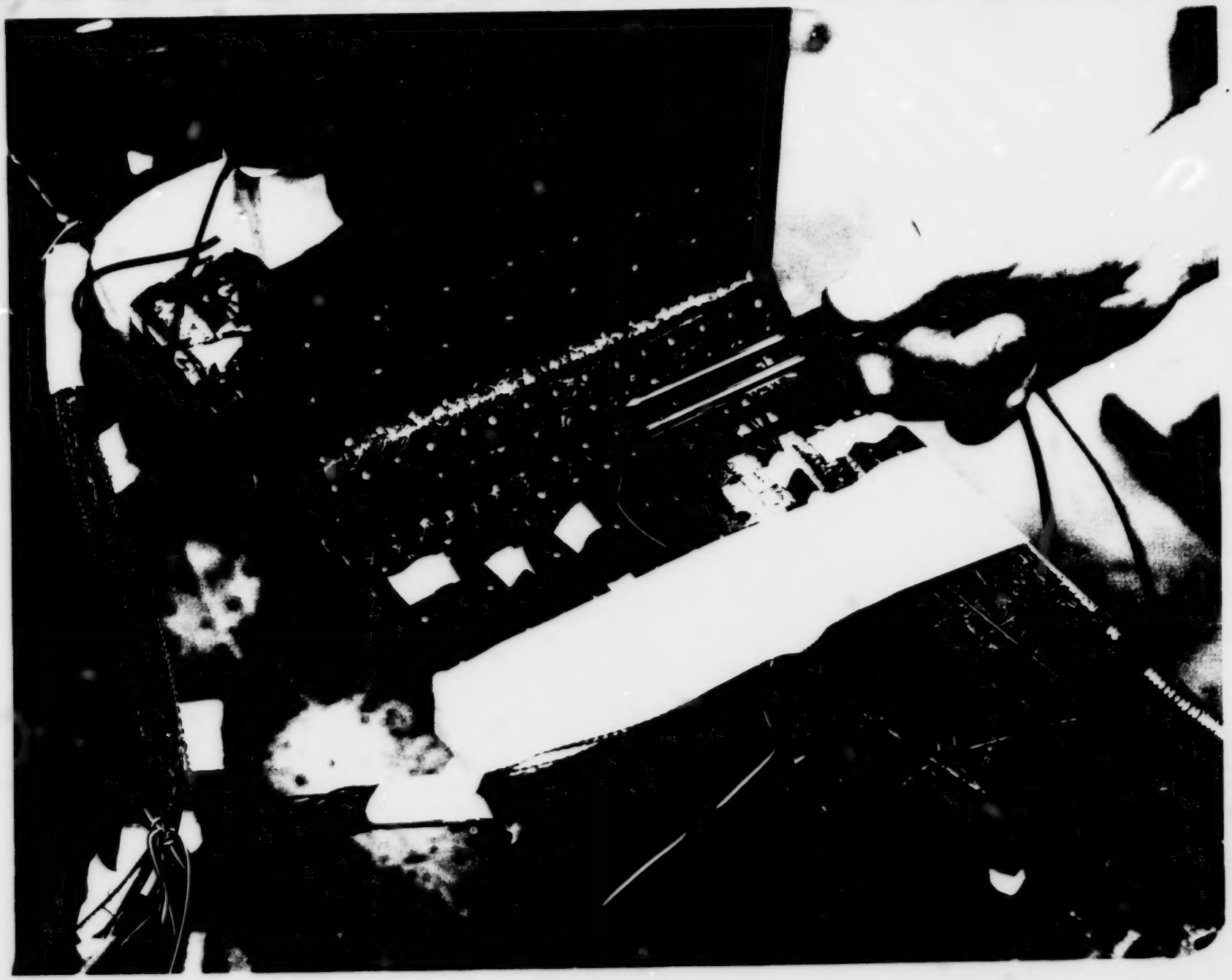

Grid Location

The AC field measurement technique confirmed the location of the cracked side and the defect character. Two identical grids were then established with a 5 by 5 matrix and a spacing of 35 mm. The grids were selected so that they had the weld toe/defect running across the centre of the grid (see Figure 2).

II RESULTS

DAIS Analysis

DAIS measurements were made by capturing an intensity spectrum for each grid location on each side of the T-plate at a set static load. Once stored on disc, an analysis was executed to produce two- and three-dimensional intensity plots at selected frequencies and averaged over a particular frequency range. The translation from the specimen to the planar representation required that the scanning matrix be reduced to a flat display, not true to scale. However, the ordinate is calibrated in units of dB with polarity referring to direction of flow (Figure 3). Error calculations were made in real time and the microphone size and spacing optimised accordingly.

Sound power spectra were derived by integrating the resultant sound intensity over the grid. The abscissae is logarithmic showing frequency in one-third octave bands; the ordinate shows sound level in dB (refer to Figures 4 and 5).

Interpretation

The interpretation of both the cracked and non-cracked sides demonstrated that while the energy level flowing in the specimen was low, direct information relating to the structure could still be extracted even in the presence of high environmental noise (see Figure 3). The DAIS captures vector quantities and is therefore able to target discrete energy sources. This allows the noise contribution to be identified through the

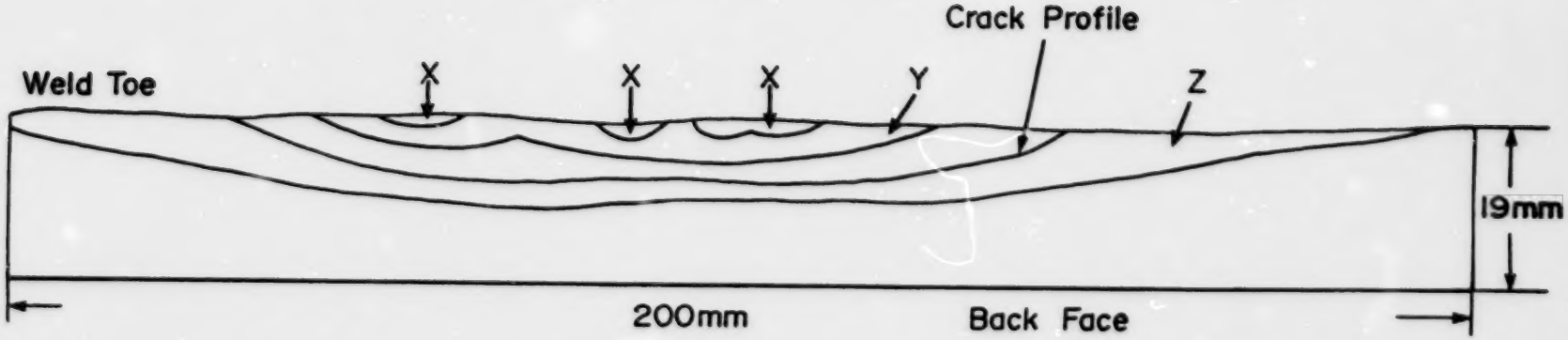

Fatigue Crack Propagation Through
a Welded T-Plate

Figure 2

SOUND POWER

FREQUENCY Hz	LEVEL CRACKED SIDE dB	LEVEL NON-CRACKED SIDE dB
100	20.8	16.3
127	27.2	22.7
160	17.6	9.2
200	17.3	21.1
250	26.2	18.0
315	23.4	19.7
400	21.0	20.4
500	17.0	18.2
630	21.0	21.1
800	23.5	24.0
1000	18.6	18.0
1250	16.4	25.4
1600	13.7	21.7
2000	16.9	16.5
2500	14.4	14.6
3150	15.3	16.0
4000	19.7	24.6
5000	15.2	16.0
6300	13.7	16.2

(a)

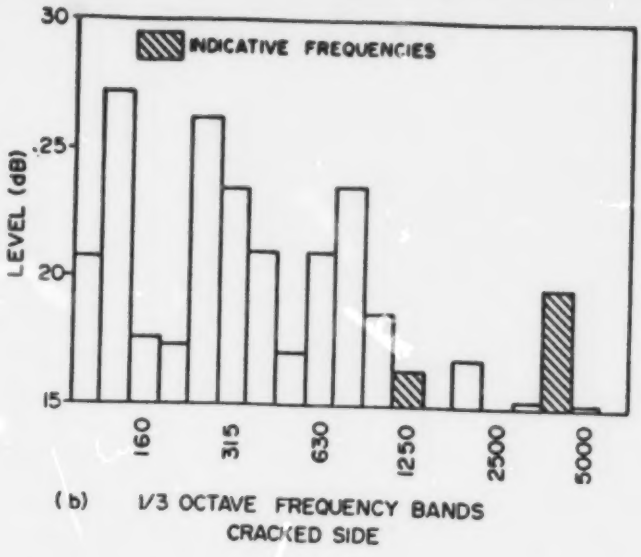

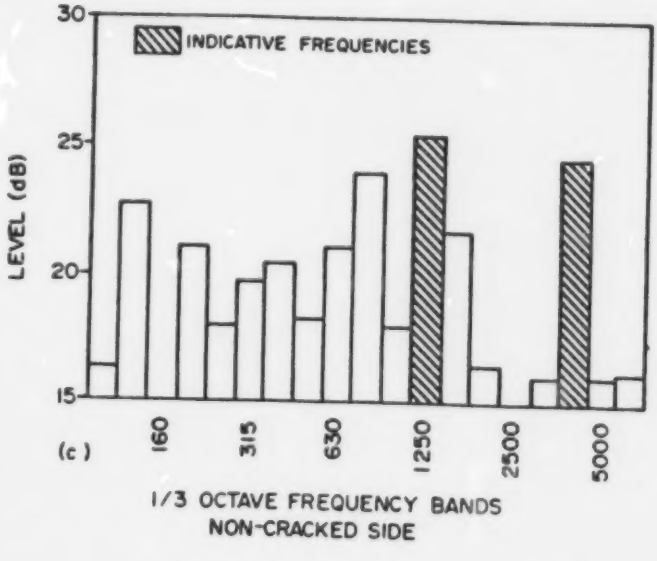

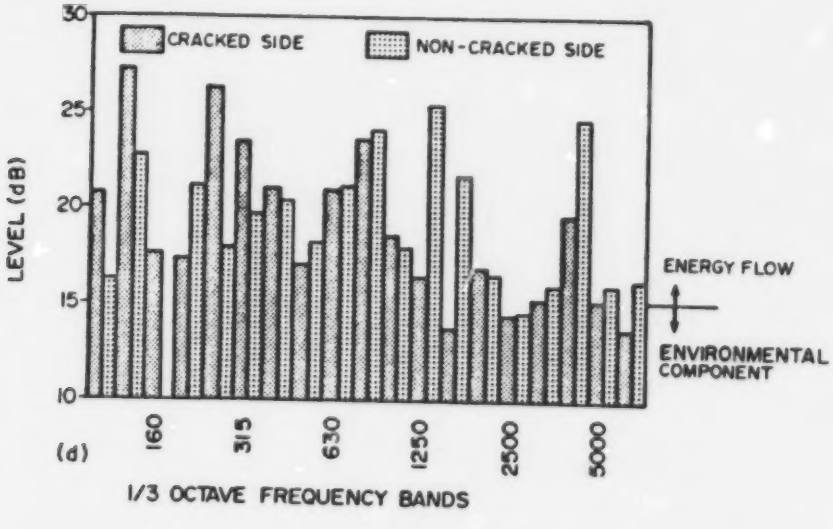

Sound Power Spectra

Figure 3

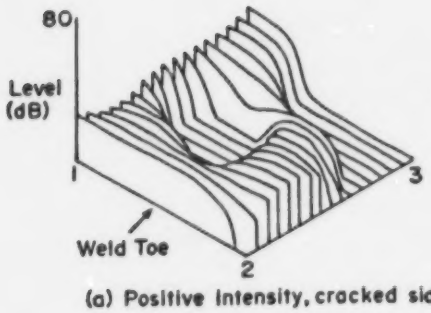

(a) Positive intensity, cracked side

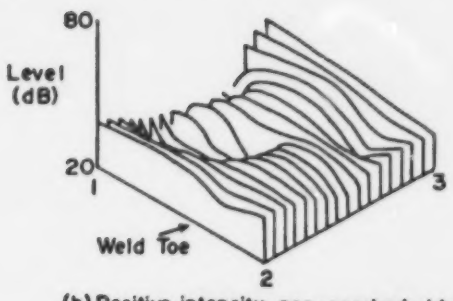

(b) Positive intensity, non-cracked side

● dB level at grid location

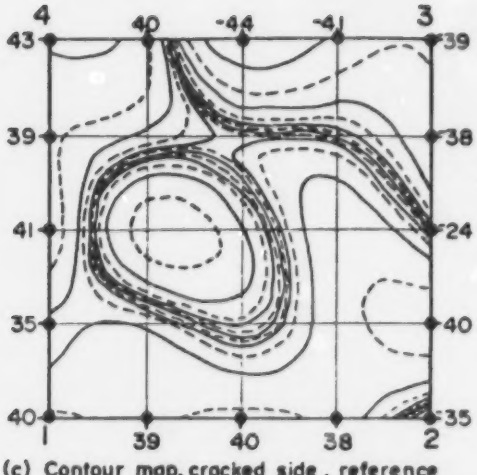

(c) Contour map, cracked side, reference level 20 dB, 3dB steps between contours

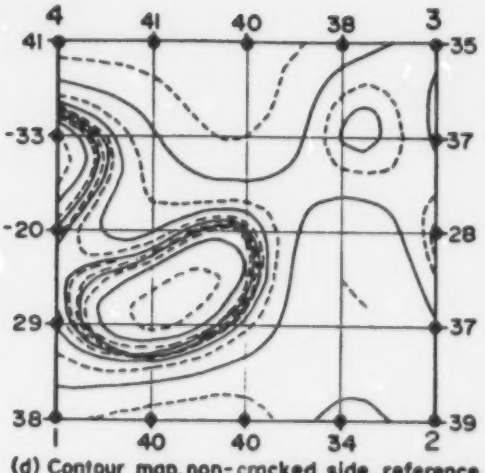

(d) Contour map, non-cracked side, reference level 20 dB, 3dB steps between contours

Intensity Distibution in the
4000 Hz. Frequency Band

Figure 4

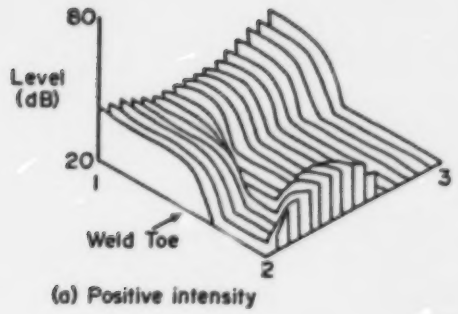

(a) Positive intensity

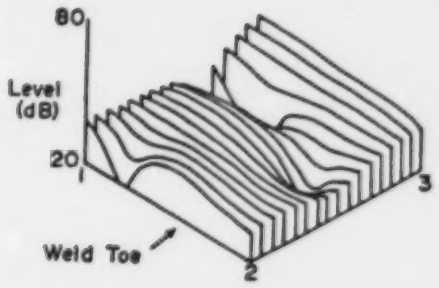

(b) Positive intensity

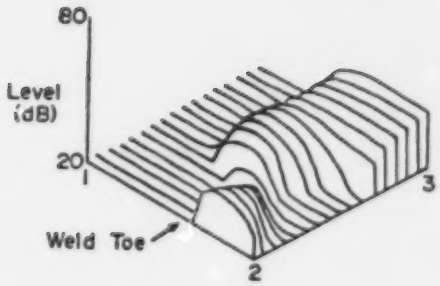

(c) Negative intensity

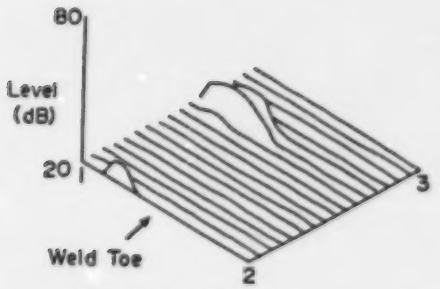

(d) Negative intensity

Intensity Distribution in the
1250 Hz Frequency Band

Figure 5

DAIS logic. Conventional acoustics measure scalar quantities and are therefore affected and limited by ambient conditions.

Two key frequency bands (4000 Hz and 1250 Hz) were revealed as illustrated in Figure 3d. At these two frequencies, a definite reduction is apparent in the positive intensity values for the cracked sides, clearly indicative of the greater attenuation (negative intensity) associated with the defect. The analysis was therefore made to concentrate on these indicative frequency bands. At 4000 Hz the flexing of the plate is exposed by the periodic patterning of sources and sinks associated with the energy flow. These are exhibited by Figure 4 which compares the intensity flow on either side of the weld at this frequency. Whilst the intensity values and patterning are not absolute, the same modal characteristics appear (see the isoline representation in Figures 4c and 4d). The localised discrepancies are due to the natural influence the crack has on the flexing of the plate.

Using the 1250 Hz data, the three-dimensional intensity plots (Figures 5a and 5c) disclose the location of the defect on the cracked side in a coherent manner. On the non-cracked side the spatial distribution of the intensity levels is seen to be nearly homogeneous (Figure 5b). This is theoretically concordant with the anticipated vector distribution of the near field flow since energy should be radiating outward from the plate in a uniform manner. The small sinks seen in the positive intensity plots are linked to natural but very minor plate movement, possibly due to the effect of the roller bearings. However, a distinct anomalous zone is highlighted and predicted from the patterning of the negative intensity plot, seen in Figure 6d. The significance of the detection of this anomaly in the 'non-cracked' side is that the information was imparted using a non-contact, remote scanning technique. This zone was not detected by either the AC or the visual inspection methods. A more in-depth verification is however required before the full extent of the DAIS sensitivity can be ascertained with complete confidence for this application.

III CONCLUSION

The results presented in this paper demonstrate that the DAIS approach is able to provide reliable and detailed information on defects even in a

high noise environment where other acoustic techniques would have failed. The technique therefore shows great promise as a remote, non-contact method for the very early detection of fatigue damage in a structure. It is possible that this dynamic intensity approach is more sensitive than current visual and electrical inspection technologies. Further study into this phenomenon of early warning is required to quantify the sensitivity and confidence to be placed on data collected by the DAIS. Such work is currently in progress through a collaboration between the Centre for Cold Ocean Resource Engineering (C-CORE) at Memorial University of Newfoundland, and the Canada Centre for Mineral and Energy Technology (CANMET)in Ottawa.

ACKNOWLEDGEMENTS

Special thanks are due to Mr. Gunnar Rasmussen and Mr. Gary Burns (Brüel & Kjaer Ltd.) for their scientific support of the programme; to Arctec Canada Ltd. and Dr. A. S. J. Swamidas (Memorial University of Newfoundland) for their interest and help in making the welded T-plate specimen available and to Dr. Robert Thompson (CANMET) for his encouragement and advice throughout the work.

REFERENCES

1. Guigné, J. Y., Williams, P. G., and Chin, V. H., "An Innovative Dynamic Acoustic Intensity Scanning Approach for the Detection of Fatigue Cracks." Marine Technology/Meerestechnik (Submitted for publication Sept 1987).

2. Swamidas, A. S. J., Munaswamy, K. and Williams, P. G., "Progress Report on Fatigue Test of Tubular Joint 1." AMCA-DSS Report (unpublished). In collaboration with Arctec Canada Ltd.

3. Guigné, J. Y., "The Concept, Design, and Experimental Validation of and 'Acoustic Sub-Seabed Interrogator'" Ph. d. Thesis, Univ. of Bath (1986), Published in the Bedford Institute Open File Series.

Submitted to Brüel & Kjaer Ltd. (Denmark)
Under review for publication as a Monograph.

AN INTRODUCTION TO THE APPLICATION OF DYNAMIC ACOUSTIC INTENSITY SCANNING FOR NON-CONTACT DETECTION OF FATIGUE CRACKS

BY

J. Y. Guigné[+*], P. G. Williams, and V. H. Chin[+]

Centre for Cold Ocean Resources Engineering,
Memorial University of Newfoundland,
St. John's, A1B 3X5

+ C-CORE, Memorial University of Newfoundland,
St. John's, Newfoundland.

* NORDCO LTD., St. John's, Newfoundland.

FOREWORD

This monograph introduces an innovative acoustic intensity scanning approach to detect fatigue cracking in welded structures. In essence the energy flow in a structure, as radiated by ambient vibration and measured as intensity, is utilized to provide an early indication of fatigue cracking. Most current non-destructive testing (NDT) techniques, such as ultrasound or magnetic particle inspection, rely on the defect to produce measurable perturbations of an introduced pulse or field within finite spatial and temporal resolution limits. In contrast, the concept described here measures the spatial flow of energy over the entire area of the structure. A dynamic intensity analysis of the structure differentiates between its modal behaviour and anomalous characteristics. The anomalies highlight and correspond to discrete sources and sinks in the energy field. The location of a defect is revealed after the energy spectra have been processed and the resultant acoustic signatures have been exhibited in the context of the natural flexing mode of the structure.

With the advent of sophisticated real-time analyzers for digital filtering and Fourier analysis, the practical measurement of intensity is now possible [1],[2],[3]. Dedicated computer processors and the use of self-calibrating acoustic manipulations [4] allow for the structure to be interrogated.

A significant aspect of this passive approach is that the receivers can be microphones, hydrophones or accelerometers. Since measurements can be made without surface contact and in most fluid media, the method is not affected by surface finish or environment and yet it is highly sensitive.

It is envisioned that the concept of Dynamic Acoustic Intensity Scanning (DAIS) could lead to an early predictive monitoring NDT tool which would help direct more effective usage of other NDT techniques and result in substantial cost saving.

1.0 PHYSICS OF INTENSITY

1.1 Definition

The classic definition for sound intensity is a vector quantity that describes the net amount and direction of flow of acoustic power at a given point in space (where intensity is in W/m^2 and the intensity level is in dB re $1pW/m^2$). It is well established and stated in physics that if the intensity vector $\vec{I}$ (the energy flow vector) is the net rate of flow of energy per unit area at the given position, then the acoustic power, W, passing through a surface, S is:

$$W = \int_S \vec{I}.\, d\vec{S} \qquad (1)$$

$$W = \int_S I_n.\, dS \qquad (2)$$

where I_n is the vector component normal to the surface. In a medium without flow or bulk movement, the intensity vector $\vec{I}$ is equal to the time averaged product of the instantaneous pressure p(t) and the corresponding particle velocity $\vec{V}(t)$ at the same point. This is expressed mathematically as:

$$\vec{I} = \lim_{T\to\infty} \frac{1}{T} \int_{-T/2}^{+T/2} p(t).\vec{v}(t)dt \qquad (3)$$

Hence the intensity vector component in a given direction I_r is:

$$I_n = \lim_{T\to\infty} \frac{1}{T} \int_{-T/2}^{+T/2} p(t).v_r(t)dt \qquad (4)$$

It should be noted that DAIS incorporates these fundamentals. The application of expression (4) is described in the following section.

1.2 Measurement of Intensity

From Eulers equation we know that, for a sound field propagating in a fluid, the particle acceleration A is given by the ratio of the pressure gradient to the fluid density ρ :

$$A = \frac{1}{\rho} \frac{\partial p}{\partial r} \qquad \text{(Eulers equation)} \qquad (5)$$

The particle velocity can thus be obtained by integrating the particle acceleration:

$$V = \frac{1}{\rho} \int \frac{\partial p}{\partial r} \, dt \qquad (6)$$

The pressure gradient is a continuous function which for two closely spaced microphones can be approximated using a finite difference method [5],[6] :

$$\frac{\partial p}{\partial r} = \frac{P_b - P_a}{\Delta r} \qquad (7)$$

where P_a and P_b are the pressures measured at the two microphones, and Δr is the receiver spacing; see Figure 1.

This gives an approximation for the pressure gradient at the centre of the microphone pair. The pressure at this point is derived from the average pressure of the two microphones:

$$P = \frac{P_a + P_b}{2} \qquad (8)$$

Substituting expressions (6), (7) and (8) into (4) we find that intensity can in practice be computed from:

$$I = \frac{P_a + P_b}{2\rho\Delta r} \int (P_b - P_a)\, dt \qquad (9)$$

Our dynamic intensity scanning approach uses sophisticated electronic equipment which applies Eulers equation and the supporting theory directly through the use of digital filtering and integration. The operations are executed in real time as shown in Figure 1.

1.3 Limitations

There are inherent limitations in measuring intensity using two closely spaced microphones and a finite pressure difference approximation for the derivation of the particle velocity [7]. The use of this technique in the measurement of sound intensity introduces a number of errors which limit the useful frequency range of the system. These errors have been well studied [8],[9],[10], and can be synthesised into the following categories:

i) a finite difference approximation error at high frequencies,

ii) an error due to the phase mismatch when the phase difference between the two element positions is small,

iii) a random error.

Errors can be minimized by optimising the receiver array and its configuration, and by having high transducer performance in accordance with IEC, ISO and ANSI standards (e.g. ANSI S1.12 1967 type XL, M). Signal averaging, as dictated by the ambient back-ground conditions, will substantially reduce the random error. For the detection of fatigue cracks, the application of a continuous calibration and a collective learning feedback diminishes the effect of errors and meets operational

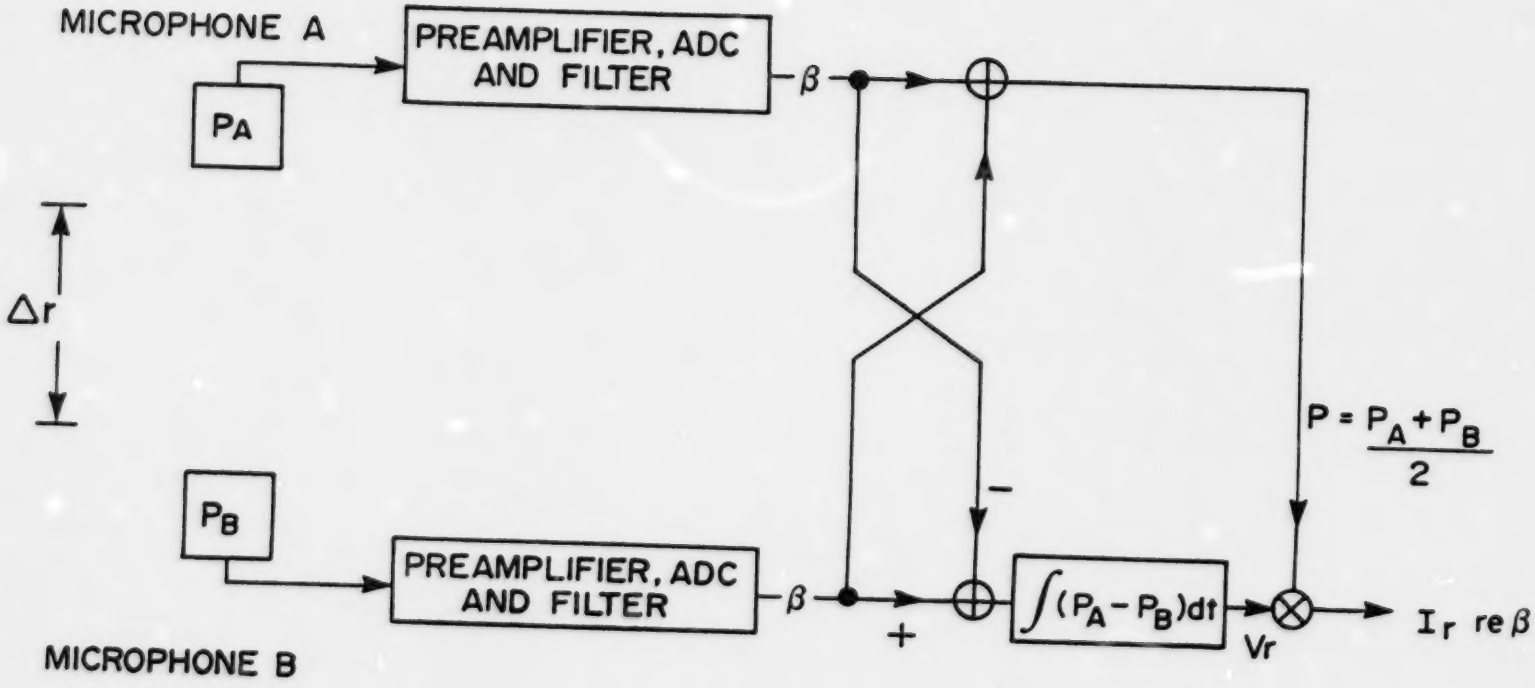

β Referenced to a Selected Frequency Band

Block Diagram for Real Time Intensity Measurements

Figure 1

specifications and standards [4]. Continuous optimization of the measurement system yields high levels of precision.

1.4 Attenuation of Intensity

As energy propagates through a medium it can be redistributed as reflections, back-scatter and attenuation. The flexing of the specimen is displayed by the first two redistribution modes while the fatigue cracking of the node is revealed by the absorption that occurs. Changes in the mediums shear viscosity and bond relaxation, will cause an energy conversion into heat. The resultant intensity will be a negative direction seen as a sink. For instance, if we examine the intensity of a plane wave passing through an homogeneous steel plate, then we can express the absorption component classically by:

$$\frac{dI}{I} = -n\ dx \qquad (10)$$

where I is the intensity at some distance having a range R_1; dI is the loss of intensity in travelling a small distance, dx, having a range R_2; n is a proportional constant with a minus sign to indicate a negative change of intensity at dI. Upon integration between the two ranges, we find that the relationship between the two intensities is simply:

$$I_2 = I_1 \exp(-n(R_2 - R_1)) \qquad (11)$$

Expressed in dB, equation (11) becomes:

$$10 \log_{10} (I_2) - 10 \log_{10} (I_1) = - 10\ n(R_2 - R_1) \log_{10} (e) \qquad (12)$$

If we substitute $\alpha = 10\ n \log_{10}(e)$ we can now obtain a change of intensity level between R_2 and R_1 as:

$$10 \log_{10} (I_2) - 10 \log_{10} (I_2) = -\alpha(R_2 - R_1) \qquad (13)$$

or in other words:

$$\alpha = \frac{10 \log_{10} (I_1) - 10 \log_{10} (I_2)}{R_2 - R_1} \qquad (14)$$

Therefore expression (14) establishes the logarithmic absorption coefficient in decibels per metre (dB/m). For each metre travelled the intensity is diminished through absorption by α dB. The absorption is frequency dependant. Extensive studies and investigations into sound attenuation in fluids and sedimentary media have been widely reported and acknowledged in the literature [4]. This frequency factor is important and is exploited during our intensity interrogations of a specimen.

2.0 LABORATORY INVESTIGATION

2.1 Laboratory Test Specimen

The application of the DAIS concept can be illustrated by the following two case histories:

i) Tubular T-joint

A welded tubular T-joint was mounted in a test frame and subjected to a cyclic, tension-tension loading in the axial direction using an MTS 600 kip servo-hydraulic actuator (refer to Figure 2 for dimensions). Fatigue cracking started at the weld toe in the region of the saddle point and the crack grew around the weld toe and through the thickness of the chord until near-complete failure had occurred [11]. The crack growth was monitored using an AC field measurement technique as part of the ongoing base research. This provided an opportunity to have a reliable and calibrated baseline to evaluate the sensitivity and performance of the logic inherent in the DAIS.

ii) T-plate

A welded T-plate specimen was also tested. The dimensions of the specimens are shown in Figure 3. Each end of the specimen was clamped between two roller bearings and the vertical section attached to the hydraulic actuator. Fatigue cracks initiated at a number of sites along the weld toe. These small cracks (X) grow and coalesce (Y) to form a crack growing across the full width of the plate (Z) (refer to Figure 4). This crack will then propagate through the thickness of the plate until failure is complete.

When this investigation took place, the specimen had cracking across the full width of the weld on one side of the vertical section (V) but had no visible cracking on the other side (W); see Figure 3. This verified the ability of the DAIS to capture signatures of the cracked and non-cracked sides and allowed for direct comparisons to be made. Its instrumentation

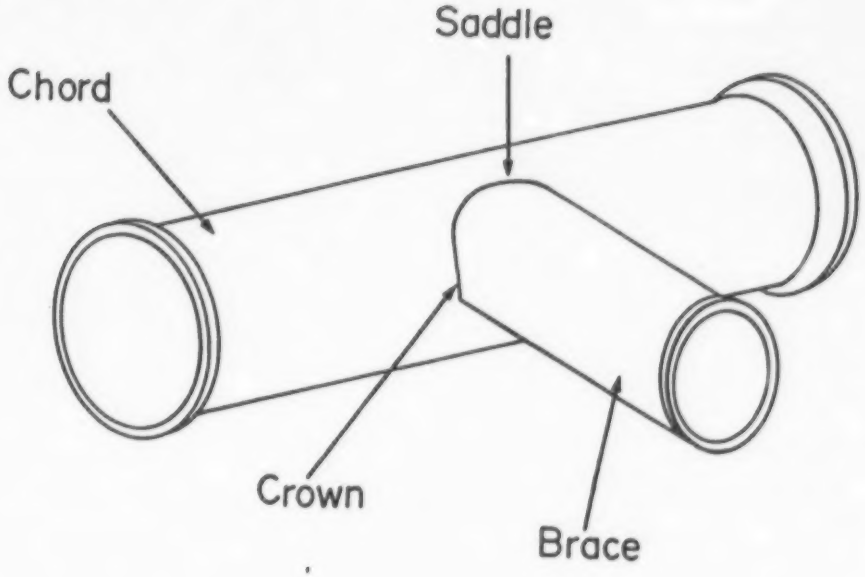

Chord diameter	= 914 mm
Brace diameter	= 457 mm
Plate thickness	= 19 mm
Chord length	= 2896 ± 5mm

Dimensions of Welded
Tubular T-Joints

Figure 2

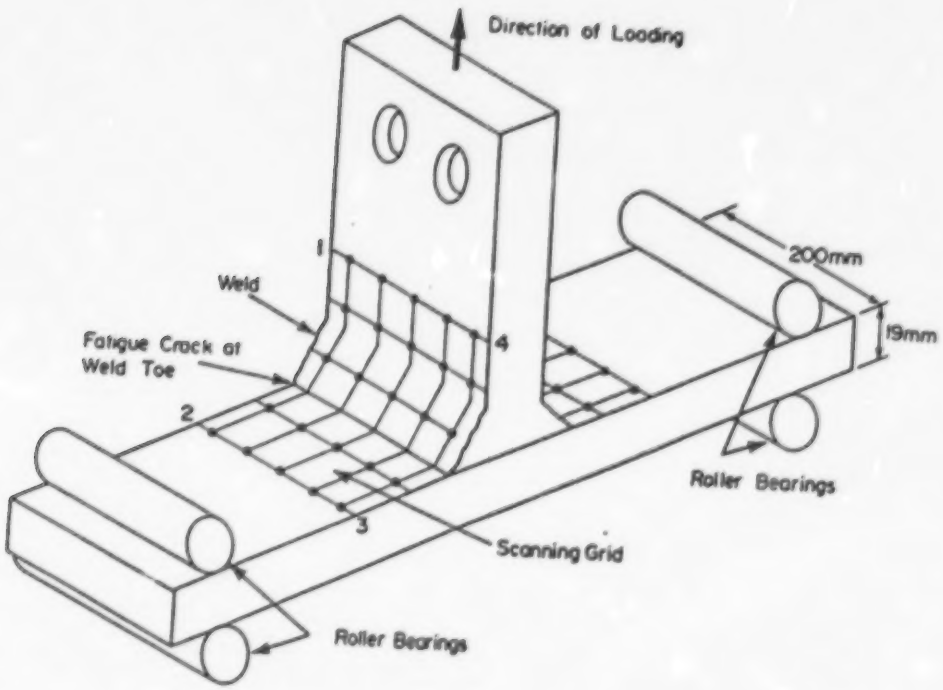

Dimensions of Welded
T-Plate Specimen

Figure 3

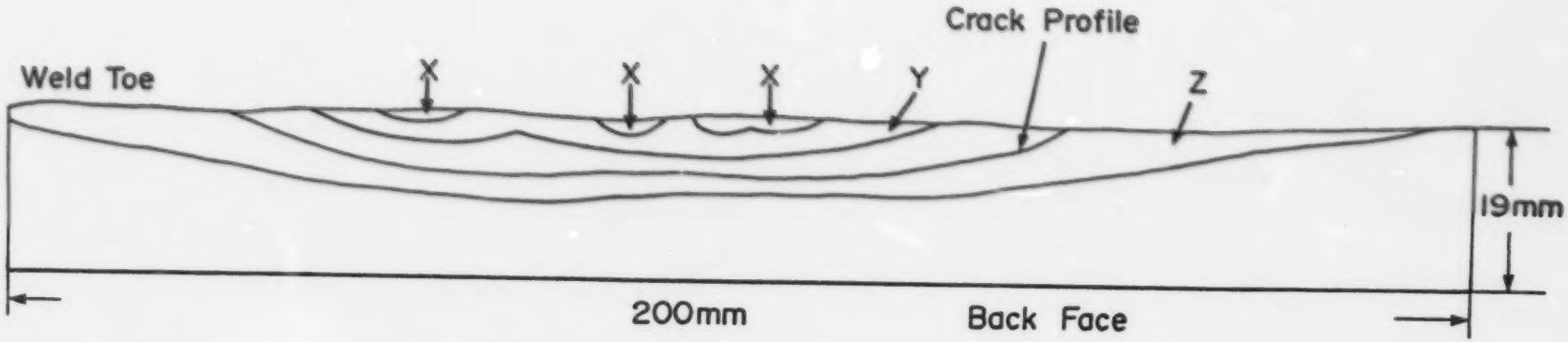

Fatigue Crack Propagation Through
a Welded T-Plate

Figure 4

is illustrated in Plate 1.

2.2 Experimental Setting

The MTS system, and in particular the hydraulic power supply and servo-valve, were employed as a source of energy. This energy propagated through the actuator and linkage to the specimen. It is this energy, freely flowing through the structure, that was targeted by our intensity scans.

Measurements for the Tubular T-joint were taken for three different loading states:

i) a static load of 3 kN (nominally zero),

ii) a static load of 315 kN (maximum test load),

iii) a cyclic load between 51 kN and 315 kN at a frequency of 4 Hz.

The T-plate was subjected to tension-tension loading in the range 20 kN to 140 kN.

The intensity measurements were made using the Brüel and Kjaer type 3360 sound intensity analyzing system using two 1/2" microphones (ANSI S1.12 1967 type XL) and a reference pistonphone for calibration.

2.3 Scanning Methodology

The interrogation logic utilised in the dynamic intensity scans, including continuous error analysis, is described by the following steps:

Step 1

- Obtain the intensity at a point to isolate the maximum and minimum energy directions and the corresponding spectra.
- Define the measurement parameters from this initial step, e.g. the trigger cycle and signal averaging. This information can also be used to select an appropriate gated trigger for the measurements and to acquire an estimate of the number of samples and their duration required for the trigger gate.

Step 2

- Perform a continuous scan over the surface using a one octave analysis to produce a power spectrum averaged over an area.
- Compare the frequency bands of the spectrum obtained from step 1 with

the area averaged spectrum. This produces a first look at the natural flexing of the material. The
frequency bands which are not associated with the flexing are identified and classed as indicative bands. These are the first highlighted signs of anomalous zones.

Step 3

- Design and implement a coarse grid matrix enclosing the anomalous zones.

- A one octave analysis is superseded by a one-third octave analysis and a comparison of the bands is made between the two octaves.

- The power spectrum averaged over this coarse grid is executed and mirrored against step 2.

- The preliminary indicative bands noted in step 2 are now confirmed by comparison with the one third octave analysis. A two-dimensional energy flow vector map is created by sampling each of the grid points in two orthogonal directions. The vector map is then processed against the intensity maps.

Step 4

- Identify the following from steps 1, 2, and 3:

  a) Sources and sinks along the structure,

  b) Anomalies and associated frequency bands,

  c) Two- and three-dimensional spatial maps at the indicative frequency bands and at other frequencies not associated with the anomaly such as those related to the natural flexing behaviour of the structure,

  d) Two-dimensional vector directions of the energy flowing in the structure.

- Delineate the targets of interest, define their frequency band and decide on a grid spacing for a more detailed spot investigation.

Step 5

- Establish a finer measurement grid over the anomalous area.

- Optimise the microphone spacing and configuration to the indicative frequency bands from step 4.

- Construct spatial contour maps at these frequencies. Vector plots can

be performed at this stage.

- Compare the grid point power spectra with the area averaged power spectrum as obtained over the finer grid.

- Statistically quantify the spatial changes.

Step 6

- Further investigation into the morphology of the crack, including depth, width and shape, can now be initiated using a 1/16 octave examination via a Fast Fourier Transform (FFT) analysis. The logic now retraces steps 3, 4 and 5. This step is a tentative suggestion yet to be validated experimentally.

For each loading state (see section 2.2), sound intensity measurements were made following the five steps of the interrogation logic. In the case of the measurements taken during cyclic loading, a trigger unit was introduced to ensure that the intensity measurements for each grid location were made at the same point in the loading cycle. The data were subsequently analyzed on a Hewlett-Packard 310 computer using software running under the Basic 4.0 operating system. The five steps were implemented using dedicated software to formulate the interrogation logic of the concept.

2.4 Grid Locations

The initial scans (step 1) on the Tubular T-joint confirmed the location of the defect as identified by the AC field measurement technique. Two measurement grids were then established as described in steps 4 and 5. The first was a 6 by 10 matrix with a grid spacing of 70 mm. This was used for measurements during the two static loading states (3 kN and 315 kN) and was centred around the saddle point of the weld with the fatigue crack at the weld toe running across its width (See Figure 5). The second grid was employed for measurements made during the cyclic loading tests executed between 51 kN and 315 kN. A 6 by 8 matrix with a spacing of 50 mm, was selected so that the grid lay above the crown point and contained the fatigue crack running across one half of its width (see Figure 6).

On the T-plate the AC field measurement technique confirmed the

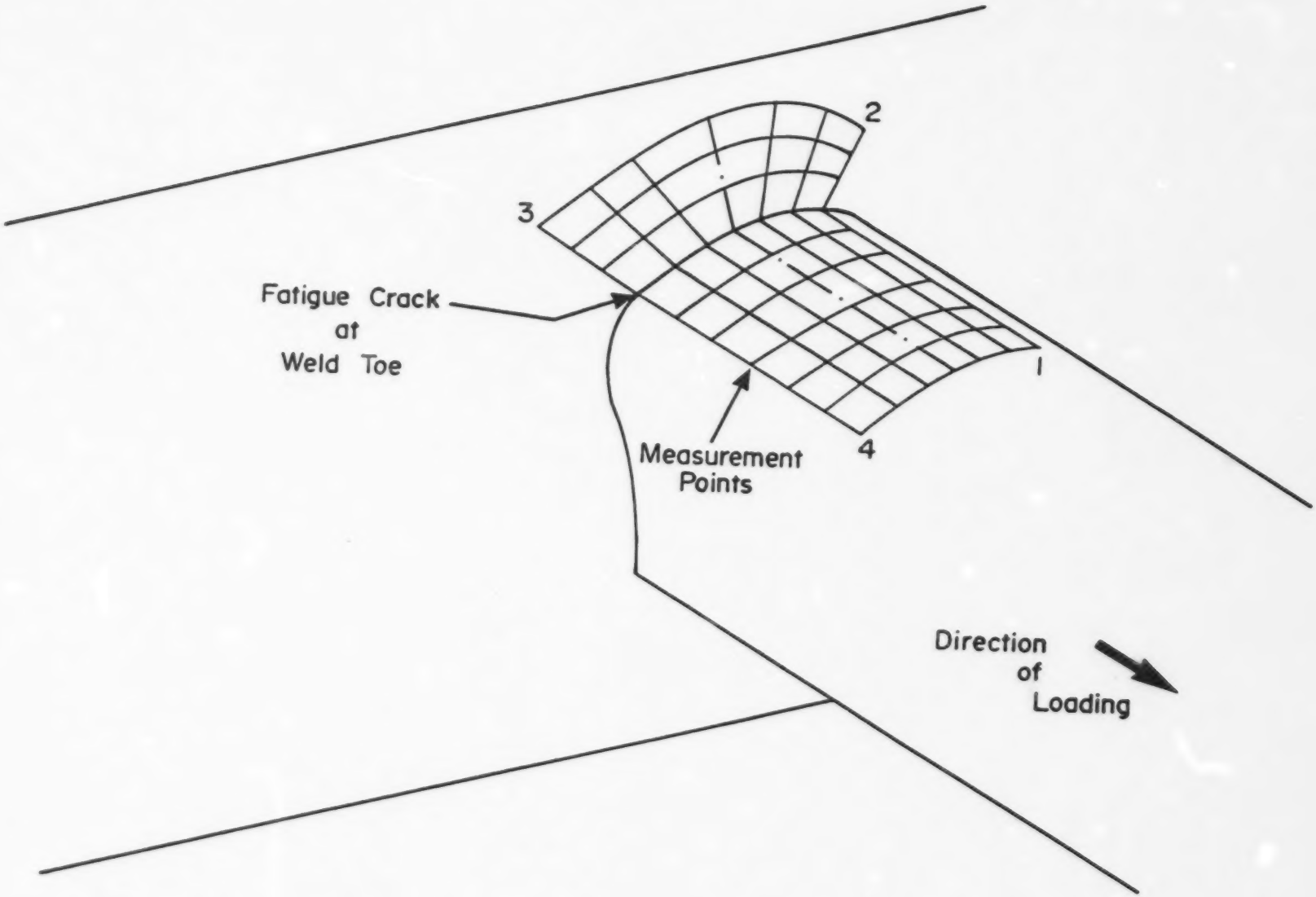

Scanning Matrix Used for
Measurements During Static Loading

Figure 5

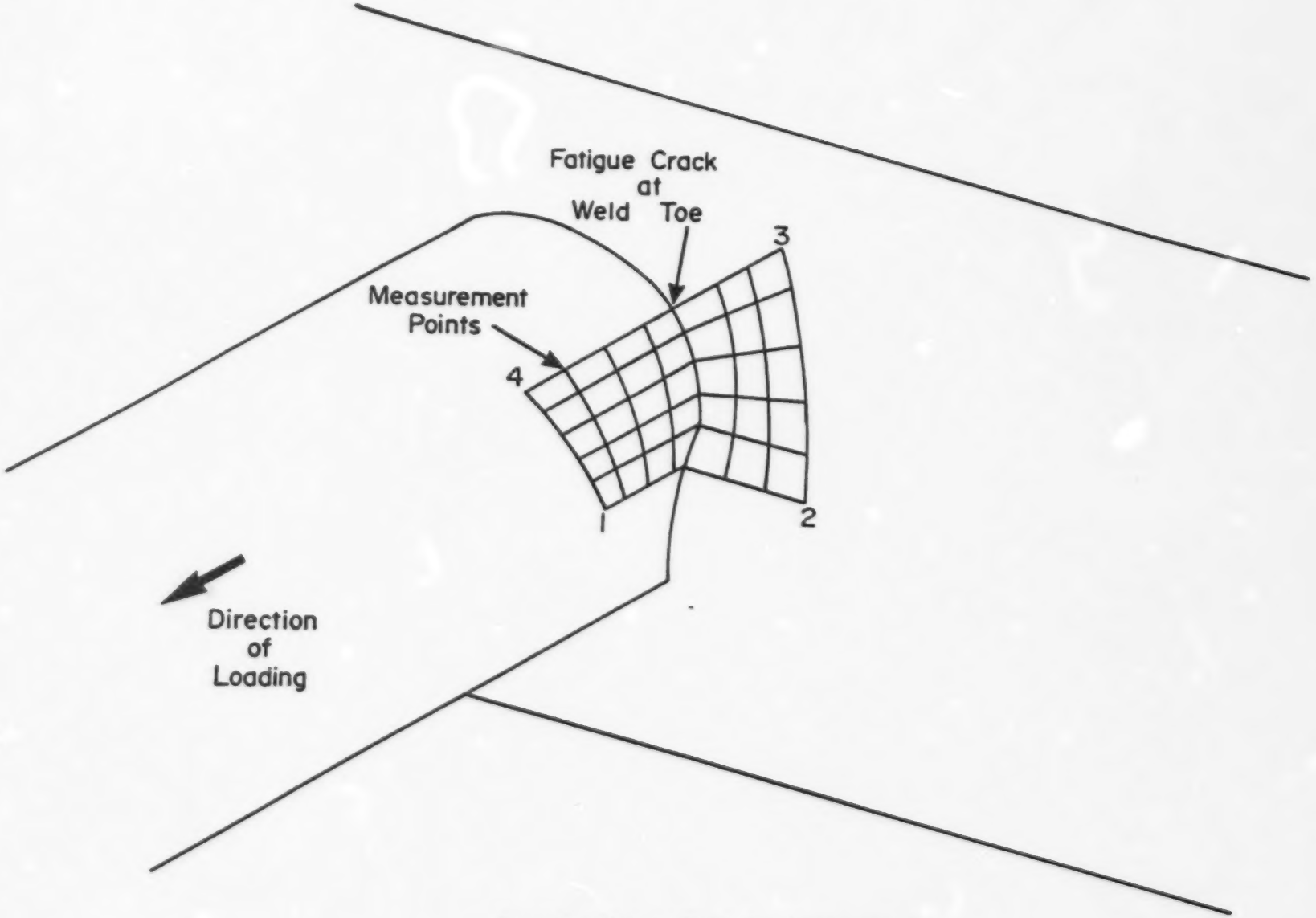

Scanning Matrix Used for Measurements
During Dynamic Loading

Figure 6

location of the cracked side and the defect character. Two identical grids were then established with a 5 by 5 matrix and a spacing of 35 mm. The grids were selected so that they had the weld toe/defect running across the centre of the grid (see Figure 3).

3.0 RESULTS

3.1 Sound Intensity and Sound Power Measurements

The acoustic intensity measurements were made by recording the full intensity spectrum at each grid location. The data were then transferred to the computer and stored on disc. Once the full grid had been scanned, the data were analyzed to produce three-dimensional intensity plots for a single frequency or for an average over selected frequency ranges. In the translation from the specimen to a planar representation, the scanning matrix is reduced to a rectangular grid so it is not drawn to scale; the ordinate is calibrated to show intensity in units of dB. For each figure; a) shows the positive and b) the negative intensity, where polarity refers to a calibrated directionality. The data plots are produced by carrying out a linear interpolation of four steps between the data points; this is cross-checked by carrying out an additional scan between the grid points. Error calculations were made in real time and the microphone size and spacing optimised accordingly.

Sound power spectra were derived by integrating the resultant sound intensity over the grid. The abscissae is logarithmic showing frequency in one-third octave bands; the ordinate shows sound level in dB (refer to Figures 4 and 5).

3.2 Tubular T-joint Results and Interpretation

As stated in section 2.1, an AC field measurement technique monitored the initiation and propagation of the fatigue crack. The technique was calibrated both on small scale test specimens and by 'beachmarking' on the tubular joint. The crack profile at the time of the intensity measurements is shown in Figure 7, along with the position of the grid lines for

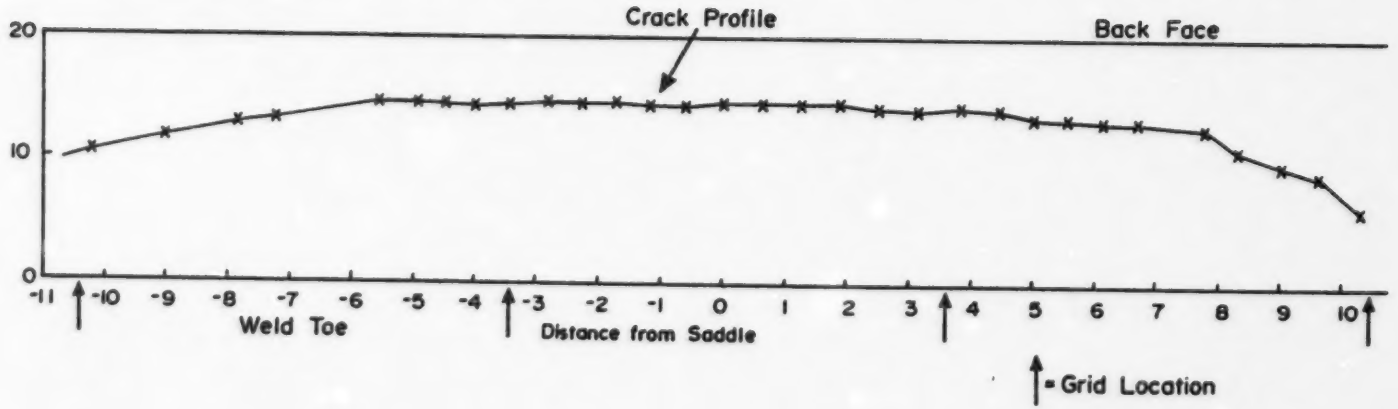

Crack Depth vs. Position for Tubular
T-joint at Time of Intensity Measurements

Figure 7

reference. Plate 2 shows the specimen at the completion of the failure test and illustrates the final extent of the fatigue cracking.

The acoustic measurements were confined to the three different loading states described in section 2.2. Figure 8 exhibits the sound power spectra recorded during steps 1 and 2. In the initial interrogation (step 1) the 50 dB level was found to be the cutoff between contributions relating to the energy flowing in the specimen, and those linked to a reactive component (refer to Figure 8a). This reactive component was found to be associated with environmental noise and standing waves. Focusing on frequencies with levels above the 50 dB boundary, three key frequency bands were revealed for each loading state; see Figures 8b, c and d. These are summarised in Figure 8e. During the cyclic loading, the dominant frequency bands were noted to centre on 800 Hz and 630 Hz. In the 3 kN and 315 kN static loading tests, the dominant frequency band was also 800 Hz, with two additional significant bands at 100 Hz and 200 Hz. The reduction in the 100 Hz band for the cyclic test (Figure 8b) was indicative of differences in the source of radiated energy connected with the hydraulic system. The actuator was being cycled at a frequency of 4 Hz during this period.

From the three-dimensional intensity plots that were computed from steps 2, 3 and 4, we can see that the 200 Hz data describes the natural flexing behaviour of the specimen. For example, Figures 10a and 10b highlight this modal deformation during the 3 kN loading. The intensity anomalies affiliated with the 800 Hz data, Figure 11, present details of the crack location, while the 100 Hz data, Figure 9, accentuates the shape of the crack.

In section II the physics of attenuation were introduced. With reference to this, the propagation of the energy through the specimen during the 3 kN and the 315 kN load trials was examined. In theory, the 100 Hz frequency band should have encountered less attenuation than the 800 Hz band. From our three-dimensional intensity plots (step 4 and 5) the 100 Hz band confirmed this and the intensity signature translated into a coherent, strong detection of the sink controlled by the crack (see Figures 9a, 9b, 12a and 12b). In comparison, the 800 Hz band intensity image showed a weaker overall signal due to its greater absorption. At this higher frequency, however, a greater degree of sensitivity to the localised

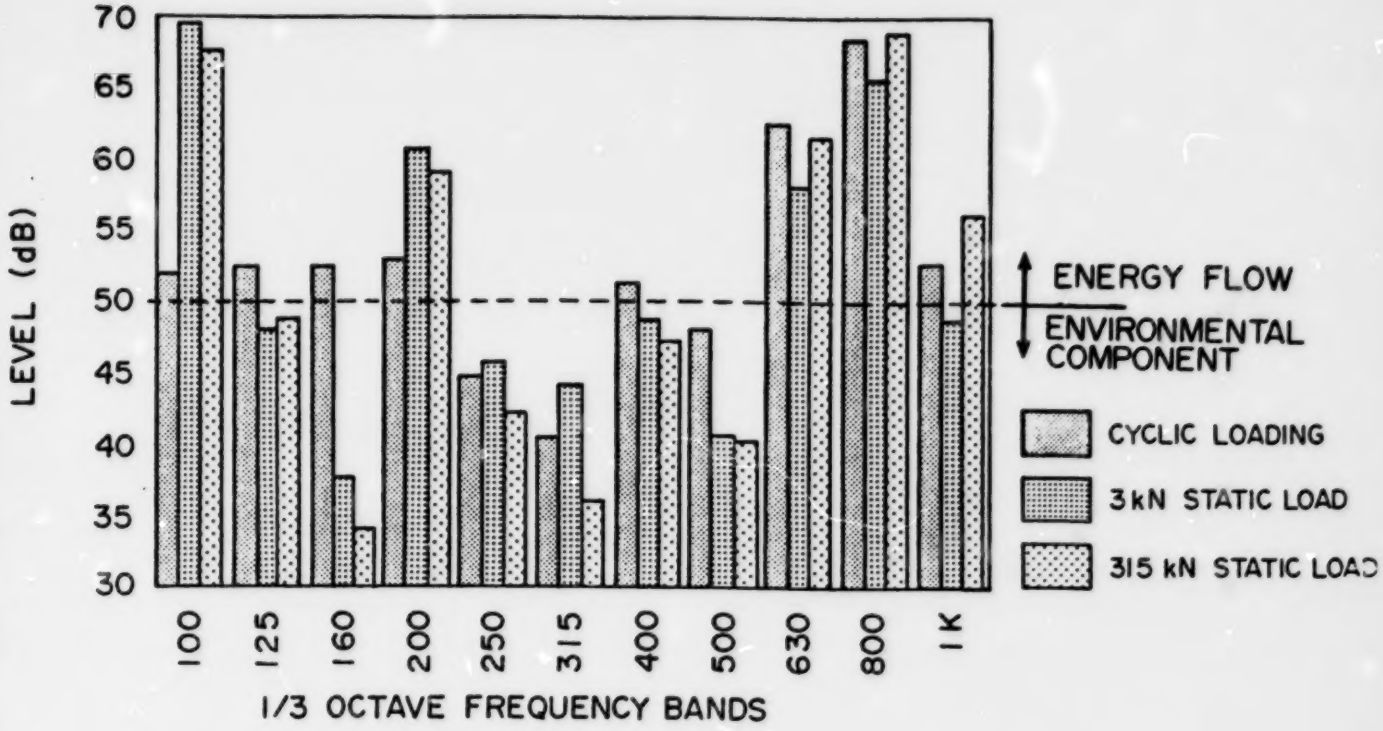

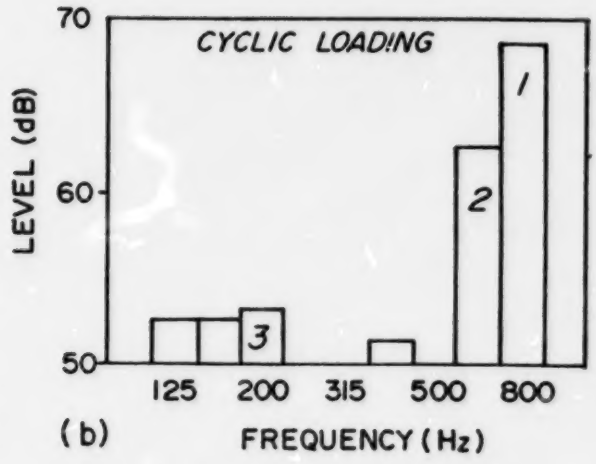

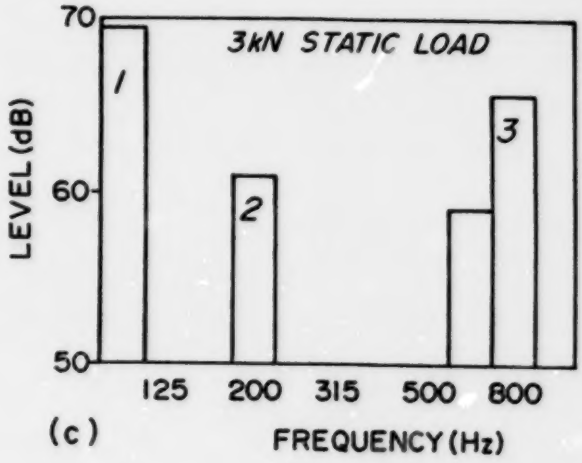

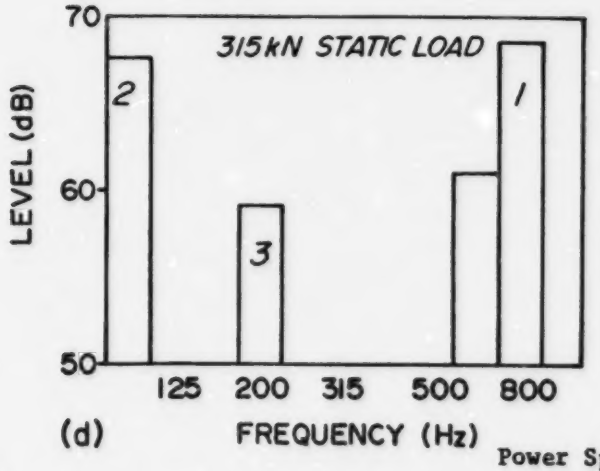

PEAK	CYCLIC		3kN		315kN	
	freq Hz	level dB	freq Hz	level dB	freq Hz	level dB
1	800	68.3	100	69.4	800	68.7
2	630	62.5	200	60.7	100	67.5
3	200	53.0	800	65.5	200	59.1

(e)

Power Spectra
Figure 8

1971

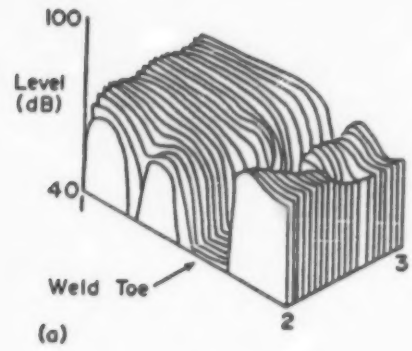

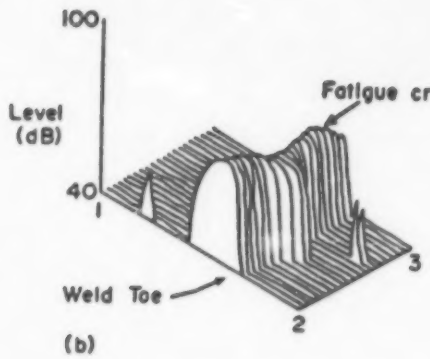

3KN Load, 100Hz Data
Figure 9

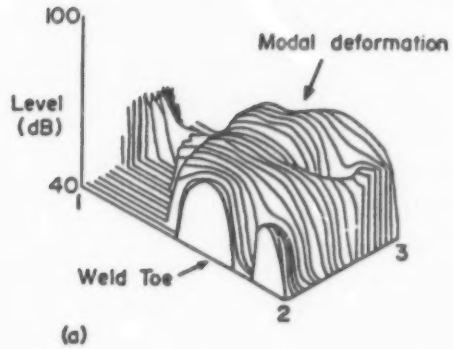

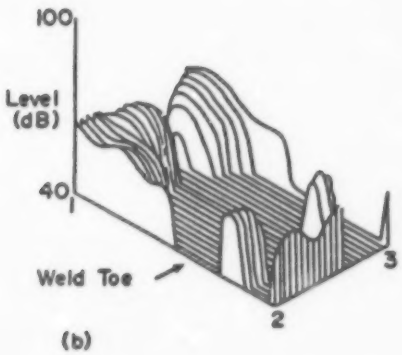

3KN Load, 200Hz Data
Figure 10

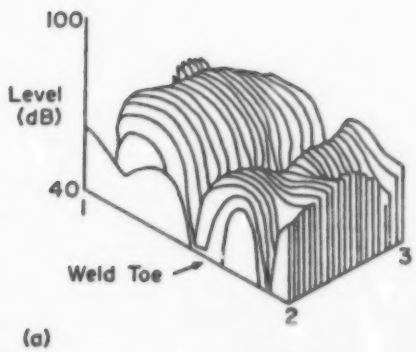

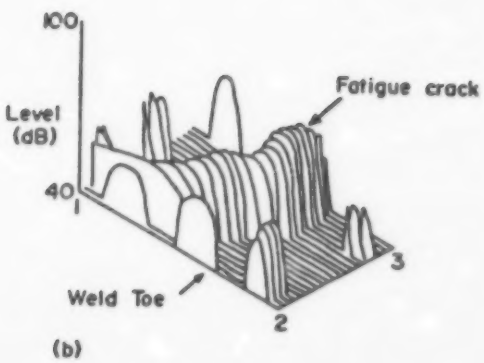

3KN Load, 800Hz Data
Figure 11

stresses which surrounded the defect was realised through the greater spatial detail of the minor sources and sinks (Figures 11a, 11b, 13a and 13b). Taken together, the two frequency bands yielded information that could not have been obtained through current NDT techniques.

Finally, in the cyclic loading test a finer grid was defined using step 5. The three-dimensional plot for a frequency of 800 Hz is presented in Figures 14a and 14b. The sink associated with the defect (x) can be seen along with a second sink (y) associated with model deformation around the crack.

3.3 T-plate Results and Interpretation

The interpretation of both the cracked and non-cracked sides demonstrated that while the energy level flowing in the specimen was low, direct information relating to the structure could still be extracted even in the presence of high environmental noise (see Figure 15). The DAIS captures vector quantities and is therefore able to target discrete energy sources. This allows the noise contribution to be identified through the DAIS logic. Conventional acoustics measure scalar quantities and are therefore affected and limited by ambient conditions.

Two key frequency bands (4000 Hz and 1250 Hz) were revealed as illustrated in Figure 15d. At these two frequencies, a definite reduction is apparent in the positive intensity values for the cracked sides, clearly indicative of the greater attenuation (negative intensity) associated with the defect. The analysis was therefore made to concentrate on these indicative frequency bands. At 4000 Hz the flexing of the plate is exposed by the periodic patterning of sources and sinks associated with the energy flow. These are exhibited by Figure 16 which compares the intensity flow on either side of the weld at this frequency. Whilst the intensity values and patterning are not absolute, the same modal characteristics appear (see the isoline representation in Figures 16c and 16d). The localised discrepancies are due to the natural influence the crack has on the flexing of the plate.

Using the 1250 Hz data, the three-dimensional intensity plots (Figures 17a and 17b) disclose the location of the defect on the cracked side in a coherent manner. On the non-cracked side the spatial distribution of the

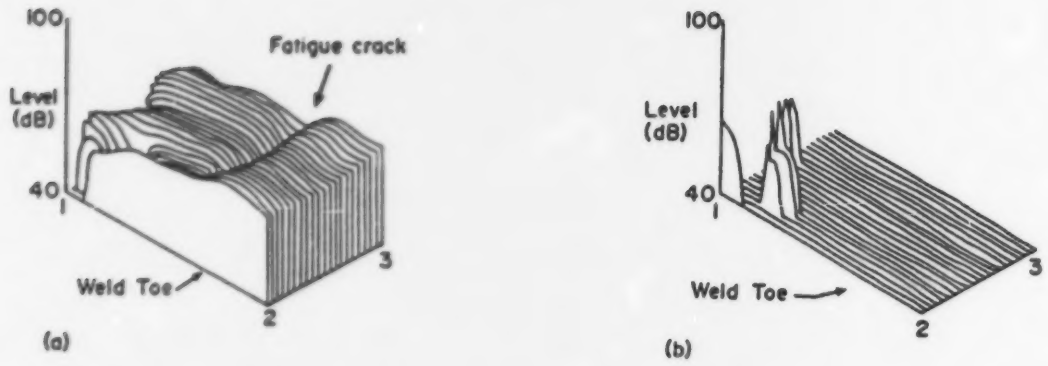

315KN Load, 100Hz Data
Figure 12

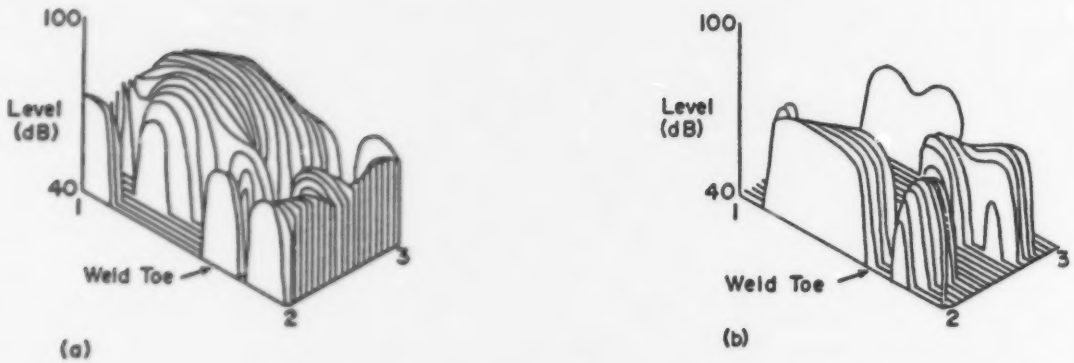

315KN Load, 800Hz Data
Figure 13

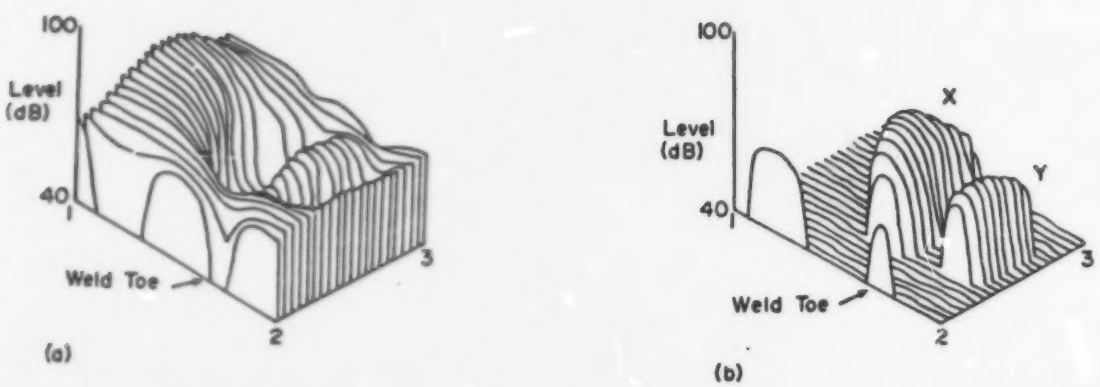

Cyclic Load, 800Hz Data
Figure 14

SOUND POWER

FREQUENCY Hz	LEVEL CRACKED SIDE dB	LEVEL NON-CRACKED SIDE dB
100	20.8	16.3
127	27.2	22.7
160	17.6	9.2
200	17.3	21.1
250	26.2	18.0
315	23.4	19.7
400	21.0	20.4
500	17.0	18.2
630	21.0	21.1
800	23.5	24.0
1000	18.6	18.0
1250	16.4	25.4
1600	13.7	21.7
2000	16.9	16.5
2500	14.4	14.6
3150	15.3	16.0
4000	19.7	24.6
5000	15.2	16.0
6300	13.7	16.2

(a)

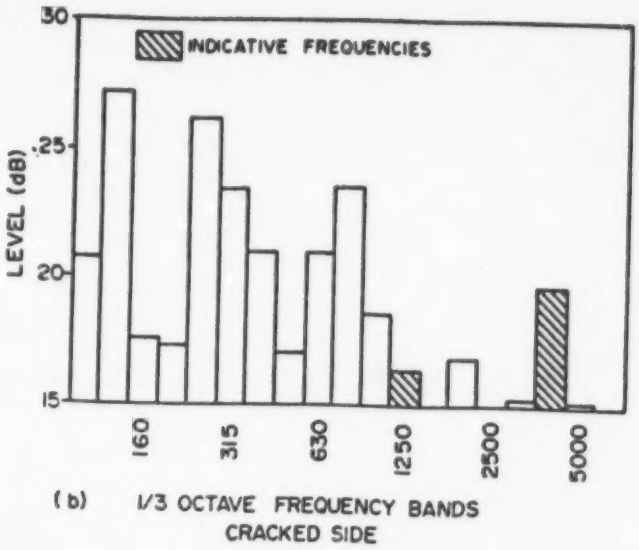

(b) 1/3 OCTAVE FREQUENCY BANDS
CRACKED SIDE

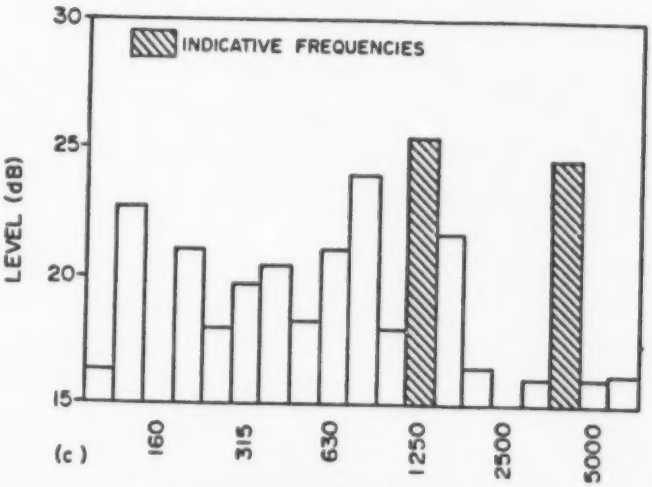

(c) 1/3 OCTAVE FREQUENCY BANDS
NON-CRACKED SIDE

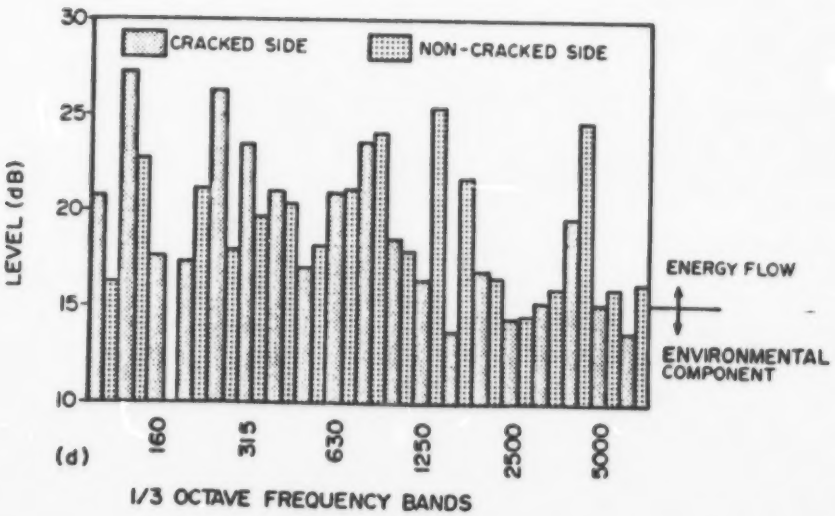

(d) 1/3 OCTAVE FREQUENCY BANDS

Sound Power Spectra
Figure 15

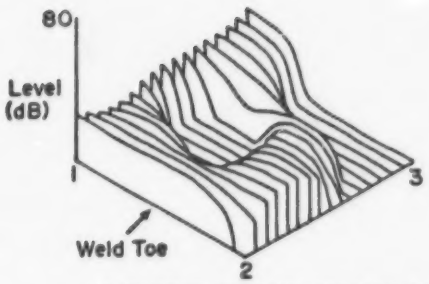

(a) Positive intensity, cracked side

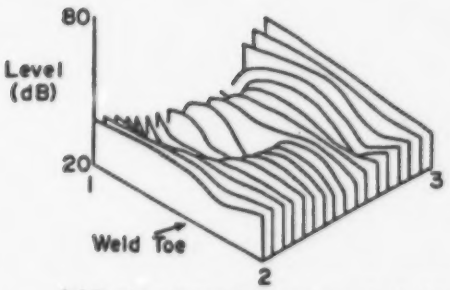

(b) Positive intensity, non-cracked side

• dB level at grid location

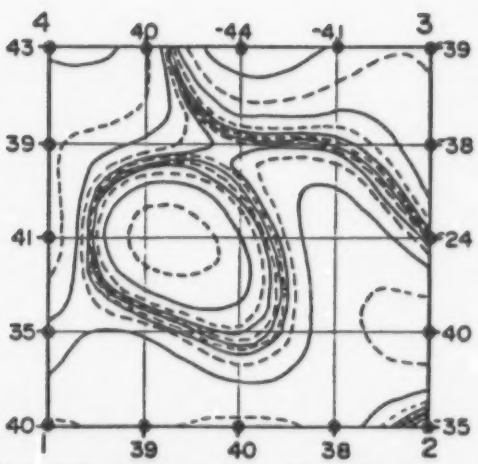

(c) Contour map, cracked side, reference level 20 dB, 3dB steps between contours.

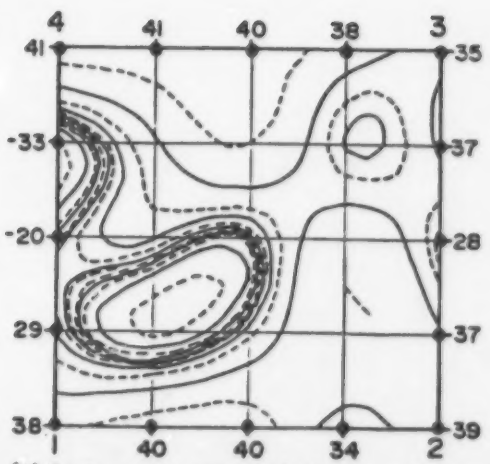

(d) Contour map, non-cracked side, reference level 20 dB, 3dB steps between contours.

Intensity Distribution in the
4000Hz Frequency Band

Figure 16

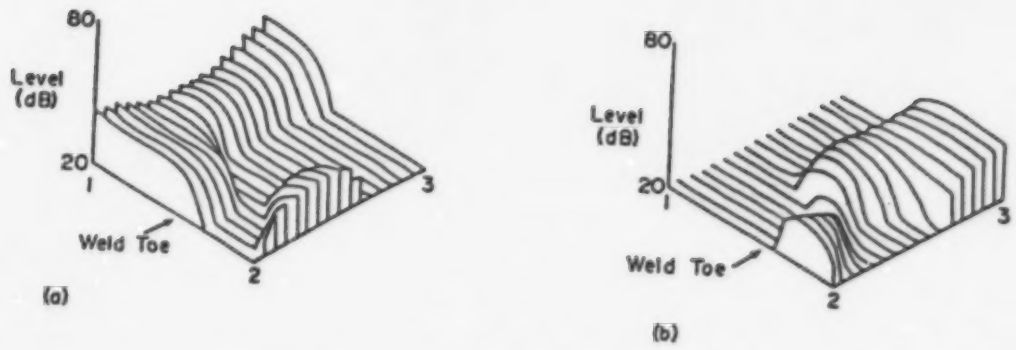

Cracked Side, 1250Hz
Figure 17

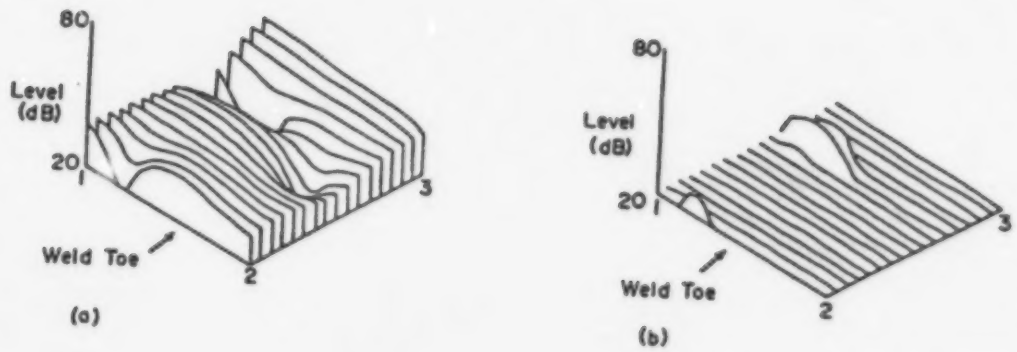

Non-Cracked Side, 1250Hz
Figure 18

intensity levels is seen to be nearly homogeneous (Figure 18a). This is theoretically concordant with the anticipated vector distribution of the near field flow since energy should be radiating outward from the plate in a uniform manner. The small sinks seen in the positive intensity plots are linked to natural but very minor plate movement, possibly due to the effect of the roller bearings. However, a distinct anomalous zone is highlighted and predicted from the patterning of the negative intensity plot, seen in Figure 18b. The significance of the detection of this anomaly in the 'non-cracked' side is that the information was imparted using a non-contact, remote scanning technique. This zone was not detected by either the AC or the visual inspection methods. A more in-depth verification is however required before the full extent of the DAIS sensitivity can be ascertained with complete confidence for this application.

4.0 CONCLUSION

The non-contact sound intensity scanning technique described in this paper has been shown to be a valuable new method for non-destructive testing especially when applied to dynamic interrogation. The spatial plotting of the crack positions and shapes were coherent and unambiguous for both specimens tested. From the cross-referencing of steps 1 to 5, a direct insight was attained of the response of the structure to the loading. On this premise, dynamic acoustic intensity scanning can be directed to a wide variety of applications such as:

i) a remote sensing technique on offshore structures to monitor the intensity of welded nodes,

ii) an on-line inspection procedure in metal casting and rolling mills,

iii) a method of monitoring the integrity of pressure vessels, turbine shafts, pipe work and ship hulls without withdrawal from service,

iv) a cost effective system for monitoring concrete structures such as bridges, dams, and concrete gravity based oil platforms.

Further study into the scope of the concept is now underway to establish standards for general applications both in air and in water. Use

of an FFT analysis using 1/16 octave bands interfaced with a digital filtering processor is being considered to create step 6.

ACKNOWLEDGEMENTS

Special thanks are due to Mr. Gunnar Rasmussen and Mr. Gary Burns (Brüel & Kjaer Ltd.) for their scientific and technical support of the programme; to Arctec Canada Ltd. and Dr. A. S. J. Swamidas (Memorial University of Newfoundland) for their interest and help in making the tubular T-joint and T-plate specimens available to test our concept and to Dr. Robert Thompson (CANMET) for his encouragement and advise throughout the work.

REFERENCES

1 Fahy, F. J.
"Measurement of Acoustic Intensity Using the Cross-Spectral Density of Two Microphone Signals." J. Acoust. Soc. Am. 62, pp 1057 - 1059, 1977.

2. Chung, J. Y.
"Cross-Spectral Method of Measuring Acoustic Intensity Without Error Caused by Instrument Phase Mismatch." J. Acoust. Soc. Am. 64, pp 1613 - 1616, 1978.

3. Roth, O.
"A sound Intensity Real-Time Analyzer." Proc. 1st International Congress on Recent Developments in Acoustic Intensity Measurements CETIM, Salis, France pp 69 - 74, 1981.

4. Guigné, J. Y.
"The Concept, Design and Experimental Evaluation of an Acoustic Sub-Seabed Interrogator." Ph. D. Thesis, University of Bath, Published in the Bedford Institute Open File Library, 1986.

5 Forssen, B. & Crocker, M. J.
"Estimation of Acoustic Velocity and Radiation Efficiency by use of the Two-Microphone Technique." J. Acoust. Soc. Am. 73, pp 1047 - 1052, 1983.

6. Rasmussen, G.
"Measuring Intensity", Intensity Measurements, G Rasmussen (ed.), Brüel & Kjaer No. BA 7196 - 11, A1 - A10, 1985.

7. Watkinson, P. S.
"Calibration and Inherent Errors of a Two Hydrophone Sound Intensity Measurement System." Proc. Inst. Acoustics Vol. 6, Pt. 5, 1984.

8. Thompson, J. K. & Tree, D. R.
"Finite Difference Approximation Errors in Acoustic Intensity Measurements." J. Sound & Vibration 75, pp 229 - 238, 1981.

9. Gade, S.
"The Validity of Intensity Measurements." Brüel & Kjaer Technical Review 4, pp 3 - 31, 1985.

10. Rasmussen, P.
Intensity Measurements, Brüel & Kjaer, No. BA 7196 - 11, B1 - D5, 1985.

11. Swamidas, A. S. J., Munaswamy, K. & Williams, P. G.
"Progress Report on Fatigue Test of Tubular Joint 1." AMCA-DSS Report (Unpublished), 1987. In conjunction with Arctec Canada Ltd.

Presented at Acoustic Imaging 88, Sendai, Japan.
Conference Proceedings Published by Plenum.

ACOUSTICAL IMAGING USING A DAIS TECHNIQUE FOR NON-DESTRUCTIVE TESTING

BY

J. Y. Guigné, P. G. Williams, and D.K.Mak*

Centre for Cold Ocean Resources Engineering,
Memorial University of Newfoundland,
St. John's, A1B 3X5

* Physical Metallurgy Research Laboratories,
Centre for Mineral and Energy Technology
Ottawa

INTRODUCTION

The extraction of oil from offshore sites off the East Coast of Canada will probably be achieved using steel and concrete platforms comparable to those used in the North Sea. The welded steel nodes of these structures are susceptible to fatigue damage which occurs because of dynamic loading under the wave action and stress concentrations at the weld [1]. This fatigue damage leads to surface breaking cracks which propagate through the chord wall and cause a rapid decrease in stiffness. It is therefore important that these surface cracks be detected through inspection at the earliest opportunity after crack initiation. Fracture mechanics based models can then be used to assess the fatigue crack growth rate and the remaining life of the joint. Repairs can thus be effectively conducted as necessary. Laboratory studies [2,3] of such nodes have shown that the time period between initiation and breakthrough of such a crack is of the order of one to six months and this is extended for the in-service situation.

A technique known as Dynamic Acoustic Intensity Scanning (DAIS) has been developed which makes use of the energy flow in a structure to provide an early indication of fatigue cracking [4,5]. Most current non-destructive testing (NDT) techniques such as ultrasound or magnetic particle inspection, rely on the defect to reflect an introduced pulse or field within finite spatial and temporal resolution limits. Acoustic Emission is also limited as an NDT technique as it relies on the continuous monitoring of the transmission emanating from the defect and on the sensitivity in tuning the receiving instrumentation to the transmitted frequency.

In contrast DAIS captures the flow of acoustic energy in the near field of a steel structure, mapping sources and sinks which relate directly to the work taking place. Intensity vectors are measured using phase matched microphones, and the resulting energy flow patterns are dynamically displayed using a combination of vector plots and contour plots. From these, a unique Residual Factor (R_f) is calculated which expresses the perturbation in energy flow as a response to the changes which occur in the structure as a function of time. It is this change in energy flow, as quantified by the acoustic images, which identifies clearly the behaviour and location of the defect.

A significant aspect of this passive approach is that the receivers can be microphones, hydrophones or accelerometers. Since measurements can be made without surface contact and in most fluid media, the method is not affected by surface finish or environment, and yet it is highly sensitive [4]. This technique has been verified on large scale welded tubular T-joint and T-plate specimens [4]. This paper presents the results of experiments using the DAIS technique on flat steel plates with weld beads and machined notches.

INTENSITY AND DAIS

Intensity

The classic definition for sound intensity is a vector quantity which describes the net amount, and direction of flow, of acoustic power at a given point in space [4], and has units W/m^2. In a medium without bulk movement or flow, the intensity vector can be written simply as the time-averaged product of the instantaneous pressure and the corresponding particle velocity:

$$\vec{I} = \lim_{T\to\infty} \frac{1}{T} \int_{-T/2}^{+T/2} p(t).\vec{v}(t)dt$$

and hence the intensity vector component in a given direction I_r is:

$$I_r = \lim_{T\to\infty} \frac{1}{T} \int_{-T/2}^{+T/2} p(t).v_r(t)dt$$

In practice, intensity can be measured using two closely spaced phase matched microphones by applying Eulers equation and a finite difference approximation to obtain the particle velocity [3].

$$I = \overline{\frac{P_a + P_b}{2\rho\Delta r} \int (P_b - P_a)\, dt}$$

where ρ is the density of the propagation medium, Δr is the microphone spacing, and P_a and P_b are the pressures measured at the two transducers. The bar denotes time averaging. This technique allows for the measurement of the projection of the intensity vector along the line of the receivers, which provides sufficient information for sound power and source location calculations.

Dynamic Acoustic Intensity Scanning

It is necessary to measure the intensity vector by simultaneously acquiring its three spatial components if a complex sound field is to be defined. For stationary or periodic fields such as those seen over vibrating structures this instantaneous time restriction is relaxed. The DAIS logic [4,5] is designed to collect and analyse sound fields by measuring the three spatial components of the intensity vector. The use of real time digital filtering along with phase matched microphone pairs and expert software allows a dynamic interrogation of the energy flow to be performed.

A combination of a vector map for the z-plane component, and a contour map for the z-direction (Fig. 3(a)) illustrates the data in the three spatial dimensions. Alternatively, the three directional components making up the energy flow can be displayed separately as contour maps (Fig. 4(a)), where the dashed lines represent 'negative' flow and the solid lines 'positive' flow relative to the probe orientation.

The Residual Factor (R_f) is the relative difference between the magnitude of the intensity levels (in dB) measured over the same area. This 'energy difference' is then displayed as a contour map for each component, as shown by Figure 6. The R_f processing and data display are carried out through software.

LABORATORY INVESTIGATION

Objective

A laboratory investigation has been undertaken to validate the use of the DAIS Residual Factor (R_f) processing. This has been performed on flat steel specimens with machined notches and weld beads introduced into the specimens and referenced against the no-defect situation.

Test Specimens

The specimens were cut from 19mm thickness 1024 steel plate, and had dimensions of 100mm x 600mm (Fig. 1). A triangular extension was left at one end to provide a location for an accelerometer. Three specimens were fabricated with notches or weld beads as follows:

- Plate 1: No defect
- Plate 2: 10mm wide weld bead run across width of plate, 25mm from centre line (see Fig. 1)
- Plate 3: 1.6mm wide X 6.25mm deep notch machined across width of plate at centre line (see Fig. 1)

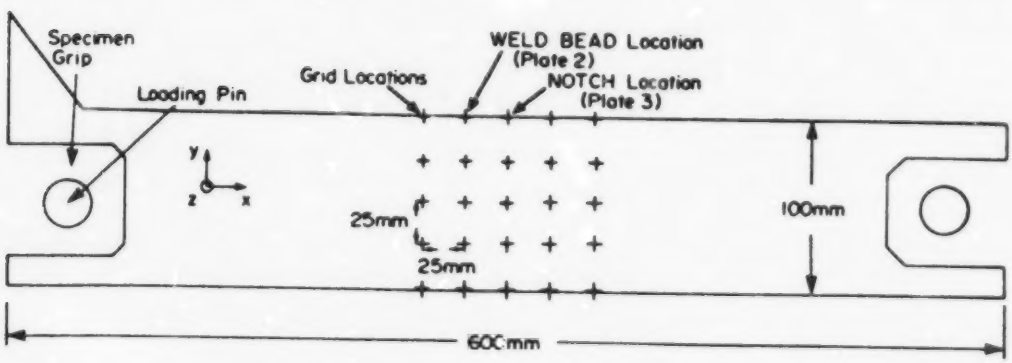

Fig. 1 Steel Test Specimen Dimensions.

The specimens were placed in a servo-hydraulic test frame (see photograph 1) and loaded in tension to a static load of 75 KN. On top of

this static load, a dynamic loading with a maximum amplitude of 0.25 KN was applied using a pseudo-random noise source. The pseudo-random noise had a bandwidth of 10 kHz and a sequence length of 32767 events. This provided a stationary acoustic energy source for the plate.

Photograph 1 Specimen Mounted in Test-Frame.

Measurement Technique

The acoustic intensity measurements were made using a 1/3 octave sound intensity analyzer. A bank of digital filters measures the intensity spectrum in real time and all measurements were made using linear averaging over a period of 1 second. A single pair of phase-matched microphones, held manually and rotated to the three required orientations was effectively employed since the stationary nature of the vibrations allowed the finite

time between measurements to be ignored during reconstruction of the data. Figure 2 illustrates the flow of the logic used in the experiment.

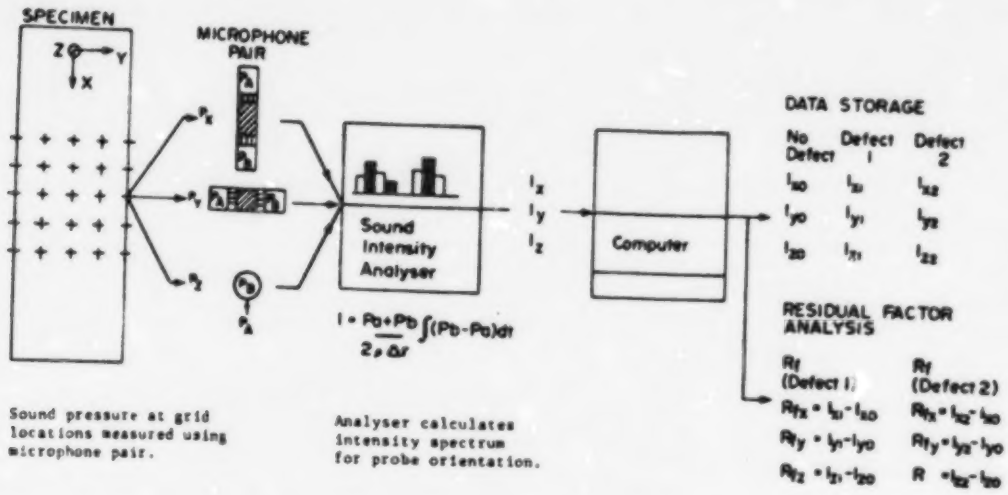

Fig. 2 Flow Logic of DAIS.

Photograph 2 Intensity Spectrum Measurement (x-component).

An imaginary grid was established on each specimen and the intensity spectrum for the three directions was measured at each grid intersection (Photograph 2). The spectra were transferred to a desk top computer for processing. Two sets of data were taken for each specimen configuration in order to provide a control for the validation of the data.

RESULTS

Intensity Measurements

The results of the experimentation on the three control plates are synthesized in Figures 3 to 5. The pertinent frequencies were detected by the DAIS as being 1000 Hz and 10000 Hz and these are presented here. Figures 3(a), (b) and (c) show the combined vector and contour map plots for specimen configurations 1, 2 and 3 respectively (see section "Test Specimens" for defect dimensions). Figures 4 and 5 represent the same data displayed for 1000 Hz and 10000 Hz respectively using separate contour maps for the x, y and z directions.

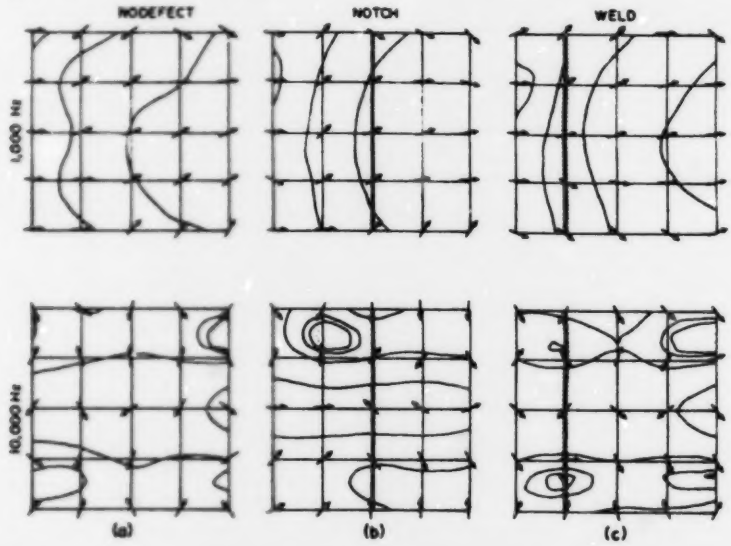

Fig. 3 Combined Vector and Contour Plots 1000 Hz and 10000 Hz Intensity Measurements.

Residual Factor Analysis

The Residual Factor (R_f) was calculated at 1000 Hz and at 10000 Hz for specimens 2 and 3 with respect to the no defect condition represented by specimen 1. Figures 6(a) and 6(c) show the R_f between specimens 1 (no defect) and 2 (notch) at 1000 Hz and at 10000 Hz respectively. The data are exhibited by contour maps for the x, y and z directions. Figures 6(b) and 6(d) are of the R_f between specimens 1 (no defect) and 3 (weld), again at 1000 Hz and 10000 Hz respectively.

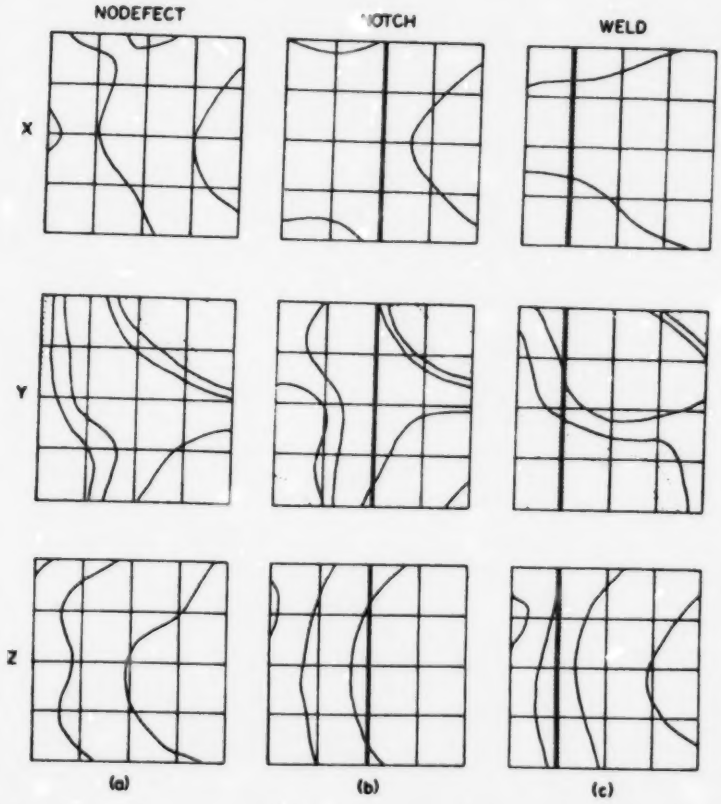

Fig. 4 Contour plots of x,y and z Components of Intensity Measurements at 1000 Hz. 6 dB between Contours.

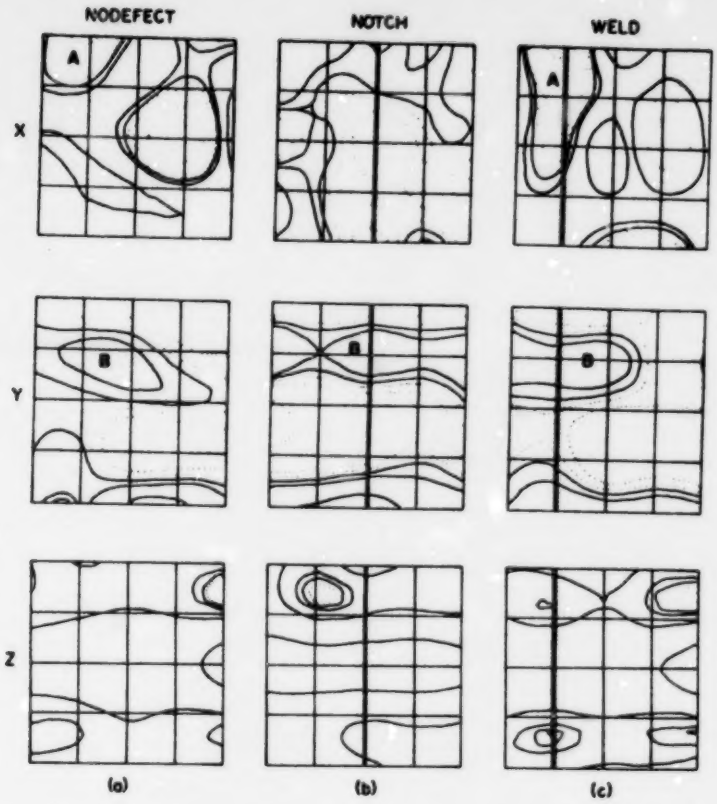

Fig. 5 Contour plots of x,y and z Components of Intensity Measurements at 1000 Hz. 6 dB between Contours.

INTERPRETATION

From inspection of the data presented in Figure 3, where the z-plane component of the vector is plotted over the z-direction contours, we can see that the energy flow patterns for the no defect, notch and weld specimens at the 1000 Hz frequency are similar and that information pertaining to the defect is not revealed explicitly. This holds true for the 10000 Hz frequency data base although anomalies are noted. The reason for the subdued exhibition of differences in the plot is that the vector descriptors mask the information held in the x and y spatial components.

By separating the vectors into isoline representations of their three spatial components (Figures 4 and 5), it becomes clearer that they demonstrate distinct flows of energy, associated with the unique defects in each of the specimens. In particular the 10000 Hz frequency reveals dominant trends of change.

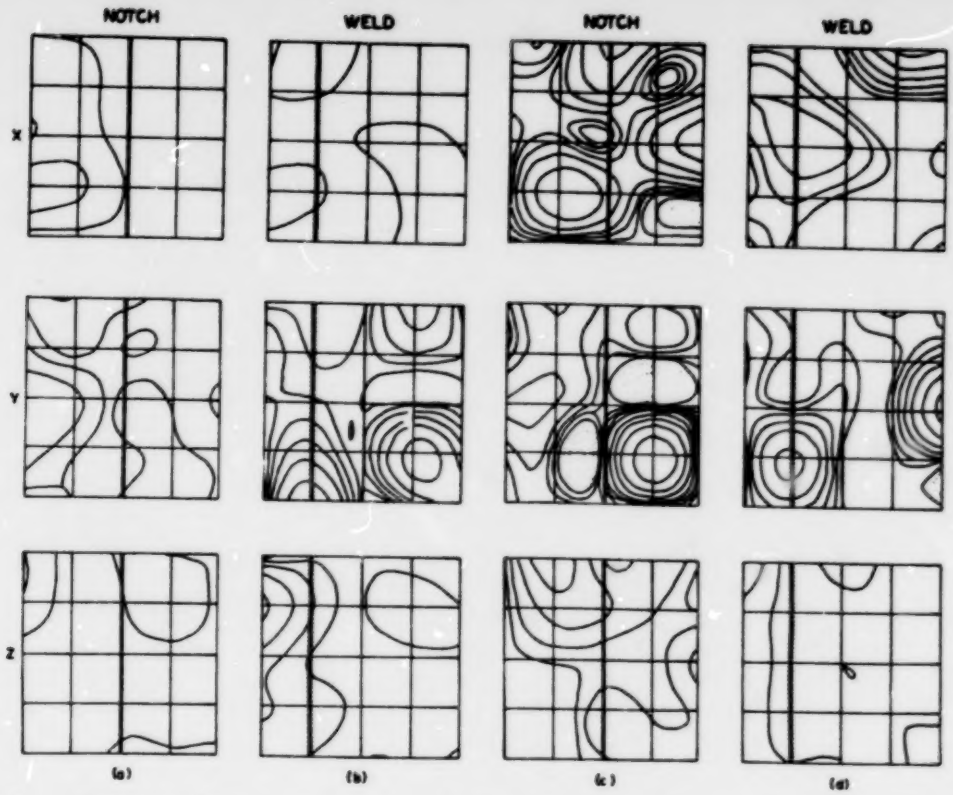

Fig. 6 Contour Plots of x,y and z Components of Residual Factor (a), (b) at 1000 Hz & (c), (d) at 10000 Hz. 2dB Between Contours.

The A zone in the x-isoline plot for the no defect specimen (Fig. 5(a)) is transformed into an elongated feature along the weld bead (Fig. 5(c)). The damping effect that the weld has on the plate is thus highlighted. In contrast, the notched specimen (Fig. 5(b)) redistributes the energy flow in the x-direction in a more symmetrical pattern along both sides of the notch. This reflects the behaviour of minor standing waves in the plate as caused by the notch.

In the y-isoline plots the B zone in all three specimens is indicative of the physics attributed to the plates. For example, where the weld dampens the plate the B zone is foreshortened towards the weld (Fig. 5(c)) compared to the no defect pattern (Fig. 5(a)). In comparison, the notch (Fig. 5(b)) extends the zone B to again give a symmetrical pattern on either side of the notch.

The z-direction represents the energy component radiating normal to the plate and this is less affected by the weld bead damping or by the reverberation at the notch. Minor pattern changes are, however, still to be observed, and these are indicative of the sensitivity of the technique.

The residual factors are noted in Figure 6. The isolines represent the relative difference between the magnitude of the intensity levels. The energy flow differences for the notch and for the weld are contrasted by their x and y component isoline representations, especially at 10000 Hz (Fig. 6(b) & (d)). At 1000 Hz, the distinctions between the two specimens are found mainly in the y-isoline representation of the R_f. The Residual Factor approach therefore directly illustrates the effect of defects, related to damping (Fig. 6(a) & (b)) and reverberation (Fig. 6(c) & (d)), on the flow of energy. These patterns could thus be used for image processing in non-destructive testing applications.

CONCLUSIONS

The flow of acoustic energy in the near field of three steel plates, was captured using the DAIS technique. Two of the three specimens contained calibrated defects. The resultant intensity vectors were differentiated into their orthogonal components. This approach characterized the perturbation of the energy flow by the defects in a definitive manner which cannot be obtained directly from the vector images.

The Residual Factor (R_f) process further removed ambiguities associated with the defect free plate. The final R_f images exhibited damping and reverberation flow patterns in concordance with the weld and notch defect.

These R_f patterns are ideally suited to robotic pattern matching techniques. An attempt is now in place to store and retrieve the R_f information using a neural network architecture. This should provide the DAIS with an ability to handle problematic patterns, similar to the type of analysis executed in a biological brain. Matching complex and "blurry" images would be feasible using the Neural Network's adaptive rules, complementing and extending the DAIS' already broad dynamic range for non-destructive testing as seen in this paper.

ACKNOWLEDGEMENTS

Thanks are due to C-CORE for supporting this research, to NORDCO Ltd. and Dr. A.S.J. Swamidas (Memorial University of Newfoundland) for their interest, and to Dr. Robert Thompson and CANMET for encouragement and financial backing of the program. Thanks are also due to Desiree King for the diagrams and Norma Matthews for typing the paper.

REFERENCES

1. W.D. Dover and L.J. Bond. Weld Crack Characterization on Offshore Structures Using AC Potential Difference and Ultrasonics. NDT International Vol. 19, No. 4, (1986).

2. A.A. Laurenssen and O.O. Dijkstra. Fatigue Tests on Large Post-Weld Heat Treated and as Welded Tubular T-Joints. 14th Annual Offshore Technology Conference, Houston, (1982).

3. M. Hara, Y. Kawai, A. Narumoto and S. Matsumoto. Corrosion Fatigue Strength of 490 MPa Class High Strength Steels Produced by the Thermo-Mechanical Control Process. 18th Annual Offshore Technology Conference, Houston (1986).

4. J.Y. Guigné, P.G. Williams and V. Chin. A Concept for the Detection of Fatigue Cracks in Welded Steel Nodes, Marine Technology, Vol. 18, No. 4, (1987).

5. J.Y. Guigné, P.G. Williams and V. Chin. Analysis of the Deformation in a Partially Cracked Welded T-Plate, Marine Technology, Vol. 18, No. 4, (1987).

6. P. Rasmussen. Intensity Vector Measurements, ICA Toronto, (1986).

Submitted to Journal of the Acoustical Society
of America. Under review.

STATIONARITY OF ACOUSTIC INTENSITY MEASUREMENTS ON STEEL PLATES

BY

J. Y. Guigné, P. G. Williams, and J. G. Adams

Centre for Cold Ocean Resources Engineering,
Memorial University of Newfoundland,
St. John's, A1B 3X5

Introduction

A Dynamic Acoustical Intensity Scanning concept (DAIS) has been proposed and verified for the detection of fatigue cracks in offshore structures [1,2]. In this non-destructive testing technique, the measurement of sound intensity allows the mapping of the flow of acoustic energy through a structure. The energy flow patterns produced respond to the changes which occur in the structure over time. The resultant changes in the energy flow at indicative frequency bands clearly identify the presence of defects in the structure.

In previous work on the DAIS concept, the selection of the indicative frequency bands was based on the level (in dB) of the acoustic power spectrum which was calculated by integrating the intensity over the surface area of the grid at each frequency. Frequency bands showing levels higher than a determined cutoff, below which represents a pseudo-reactive or environmental component, were chosen. Figure 1, which was reproduced from Guigné et al, 1987 [1] illustrates this logic. In this example, 50 dB was chosen as the cutoff value.

This selection process, however, is insufficient because of the non-stationarity in certain frequency bands. This has been observed from inspection of experimental data which show that some frequency bands exhibit significant changes over time even when structural properties are held constant. It is therefore essential that frequency bands be chosen in which the energy flow patterns are repeatable and hence give consistent results under constant conditions. Subsequent changes in these patterns can then be confidently attributed to structural defects rather than random fluctuations.

Although visual inspection can be used to identify stationary frequency bands, this method is time consuming and is limited by inherent subjectivity and a lack of quantitative results. This paper introduces two identification methods: a residual factor and an intensity time variation. These are evaluated along with power spectra as alternatives to the visual inspection approach.

Experimental Methods

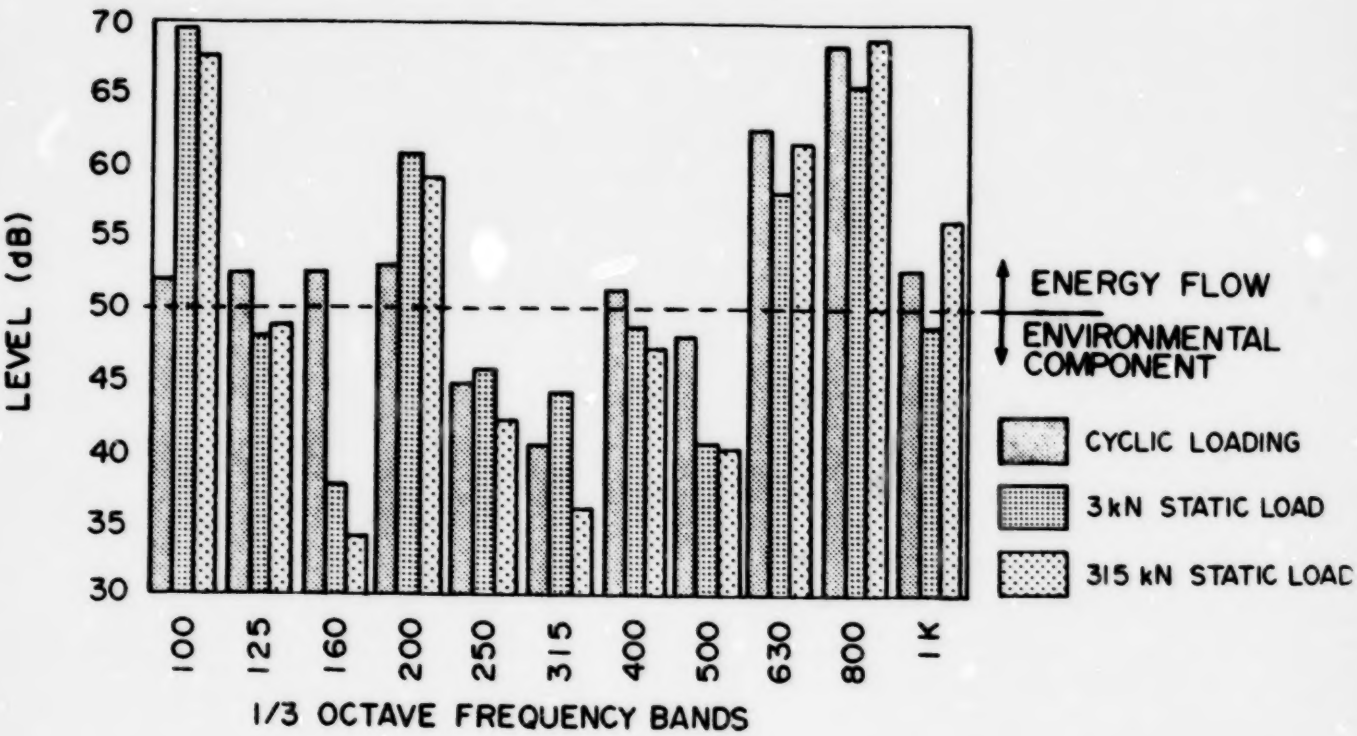
70
65
60
55
50
45
40
35
30
LEVEL (dB)
100
125
160
200
250
315
400
500
630
800
1K
1/3 OCTAVE FREQUENCY BANDS
ENERGY FLOW
ENVIRONMENTAL COMPONENT
CYCLIC LOADING
3kN STATIC LOAD
315 kN STATIC LOAD

Figure 1

Specimen:

The specimen used was a plate fabricated from 1024 structural steel. This plate had a 4 mm. wide, 12.5 mm. deep notch machined into it. The notch served as a calibrated defect. A scanning grid of six columns and four rows was marked on the specimen. The grid and plate dimensions are shown in Figure 2.

Instrumentation:

A servo-hydraulic test system was used to apply an axial static tensile load of 75 kN to the specimen. The specimen was then subjected to an additional pseudo random load oscillating with a band width of 10 kHz. Although this oscillating load was small (0.25 kN), acoustic energy was produced from the vibrations. This energy propagated through the actuator and linkage to the specimen where it became the target of the intensity mapping.

The instrumentation setup is illustrated in Figure 3. Microphone responses were referenced to a pistonphone producing a calibrated sound pressure of 124 dB at 100 Hz.

Measurement Technique

At each grid location, a 1/3 octave band intensity spectrum over the frequency range 100 Hz to 4000 Hz was captured by the analyzer. The microphone probe was held in the Z orientation, 5 mm from the surface of the plate (see Figure 2) and a stand was employed to ensure consistent positioning and reproducible reflection characteristics. This mapping was carried out three times.

In addition to the mapping, intensity versus time data was also collected. Twenty intensity spectra were recorded at intervals of approximately two seconds with a linear averaging time of two seconds. These readings were taken before each mapping.

The data were transferred to the computer for storage and processing.

Data Processing

The data are presented as three-dimensional surface maps, for each frequency in the measured range, formed by interpolating the intensity

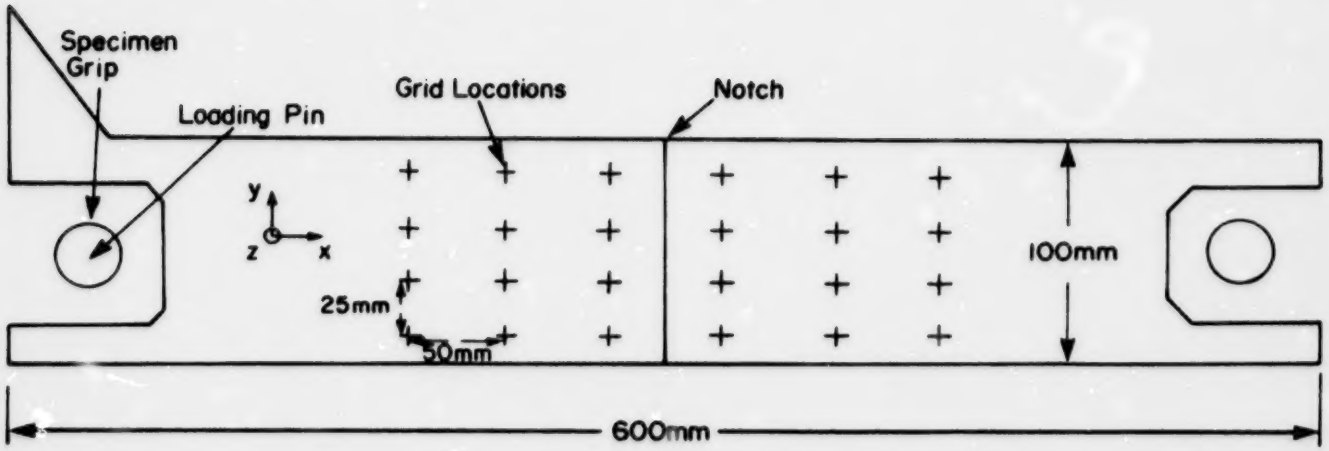

Specimen
Figure 2

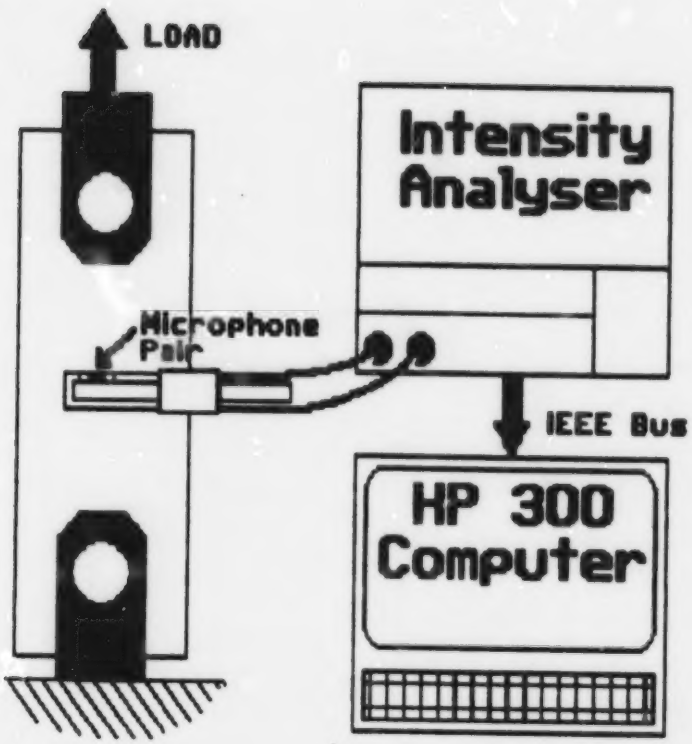

Figure 3. Measurement Setup

levels between grid locations. These surface maps facilitate the easy visual comparison of data between trials (for example, see Figures 5, 6 and 7). In addition, the contour map for each frequency is plotted over the measurement grid, and the intensity levels at the grid locations displayed. Intensity levels having a magnitude less than the 40 dB base level were omitted from these plots (treated as zero).

Four methods of identifying stationary frequency bands were examined as follows:

i) Power Spectra

The sound power spectra was calculated for each mapping of the plate. This was achieved by integrating the intensity over the grid area. A single level representing the sound power at each frequency for the entire grid resulted. The power spectra for three mappings are displayed in Figure 4.

ii) Visual Inspection

This correlation method involved a visual comparison between the graphical plots at each frequency band from two mappings. Three classifications were used: Coherent, Partial Coherence, and No Coherence. An example of each is shown in Figures 5, 6 and 7.

iii) Residual Factor

In an attempt to quantify the visual inspection technique, the residual factor was applied. The residual factor is the relative difference between the magnitudes of the intensity levels (in dB) measured over the same area. This energy difference was displayed as a data map showing the residual factors at each grid location. Figure 8 shows the residual factor data maps for the same data that was compared visually in Figures 5, 6 and 7. Note that the locations marked with a "*" are ignored because at these locations at least one of the intensity levels used to calculate the residual fell below the 40 dB base level and hence was not statistically acceptable.

iv) Intensity Versus Time

As an alternative to the above methods, the more direct approach of examining intensity versus time data was applied to find frequency bands

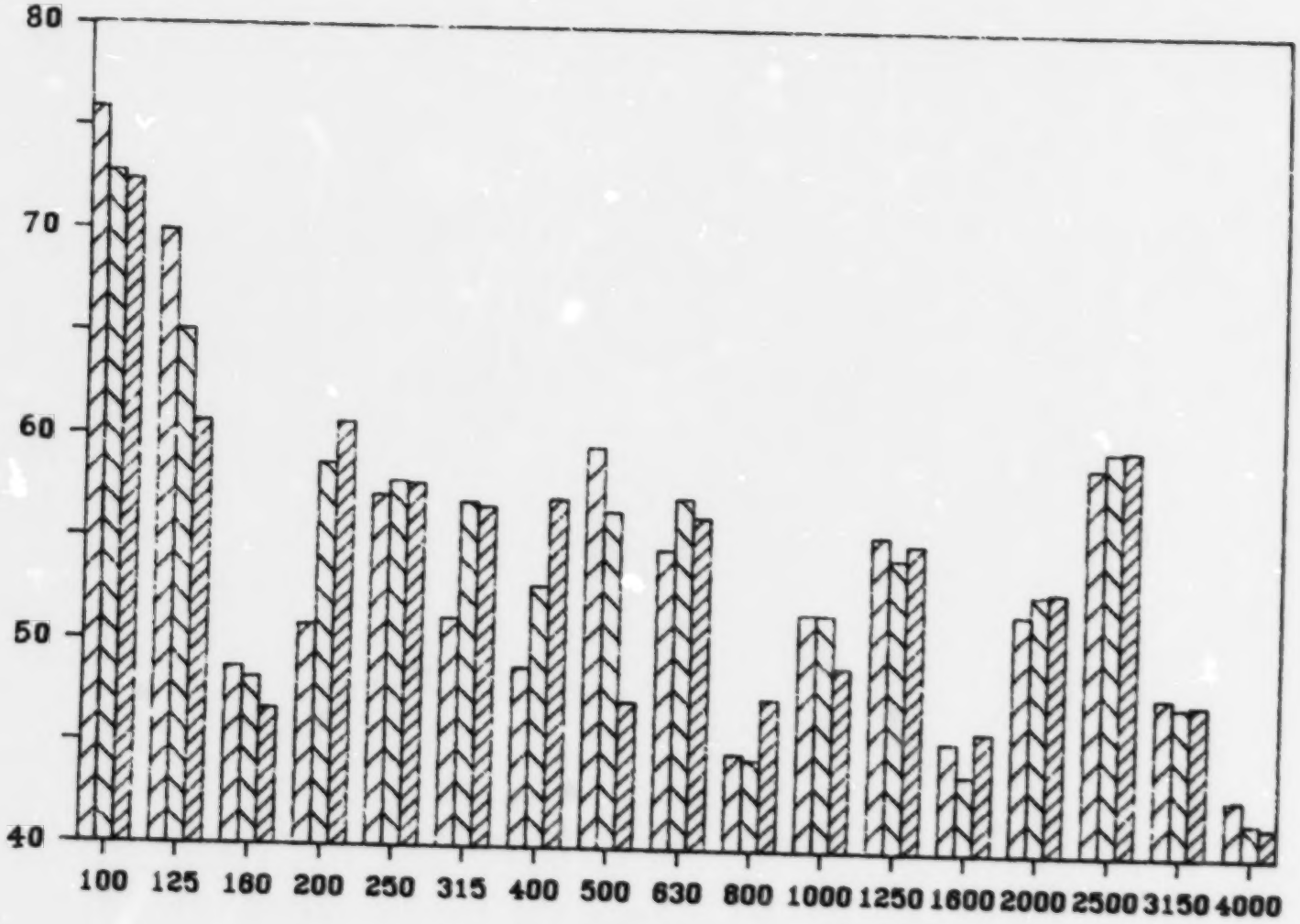

Sound Power Spectra
Figure 4

Contour Map

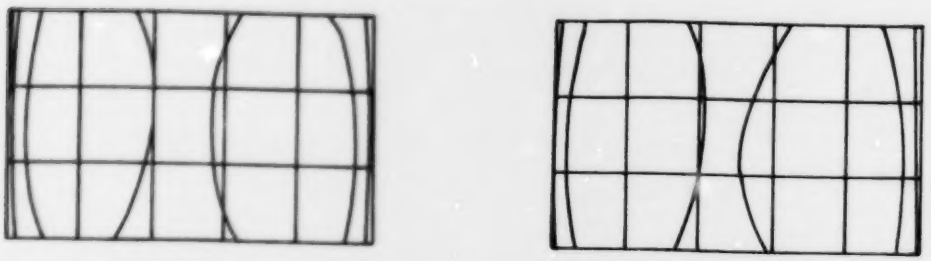

Scan 1 Scan 2

Negative Intensity

Scan 1 Scan 2

Positive Intensity

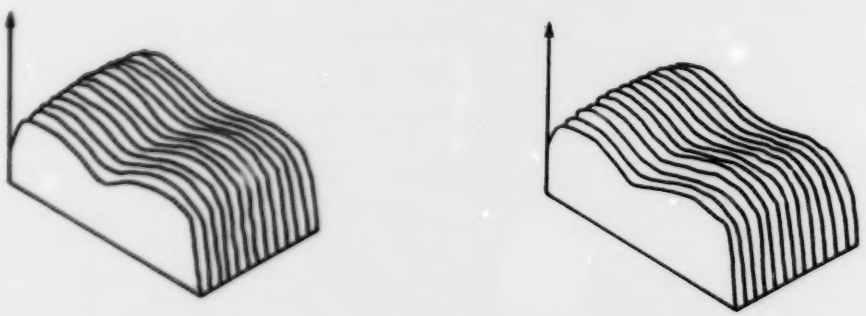

Scan 1 Scan 2

Coherent
(trials 1 & 2 @ 2500 Hz)
Figure 5

Contour Map

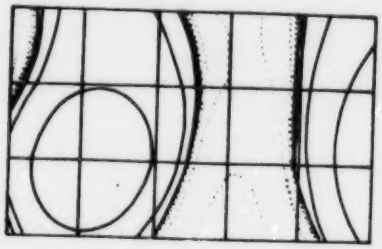

Scan 1

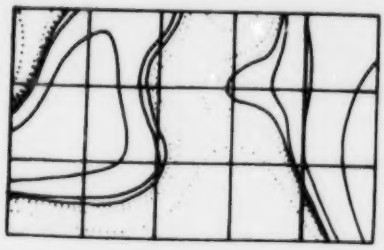

Scan 2

Negative Intensity

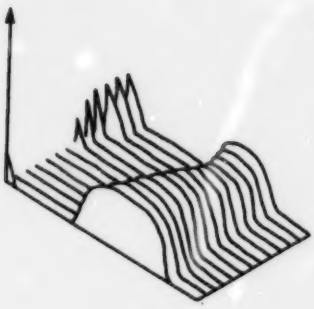

Scan 1

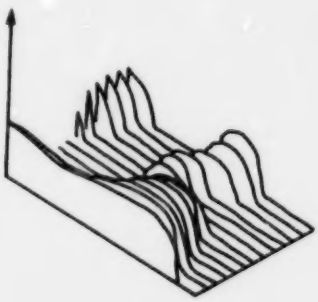

Scan 2

Positive Intensity

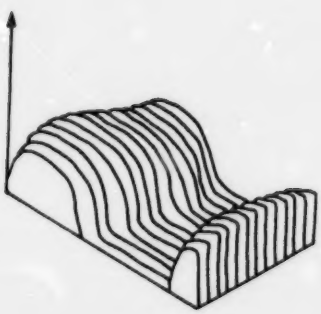

Scan 1

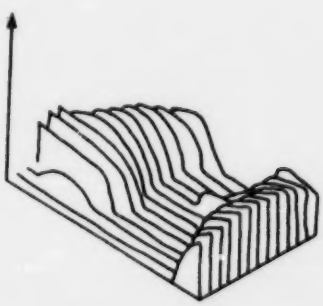

Scan 2

Partial Coherence
(trials 1 & 2 @ 800 Hz)
Figure 6

Contour Map

Scan 1

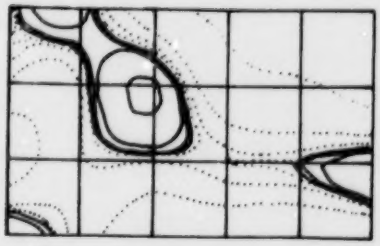

Scan 2

Negative Intensity

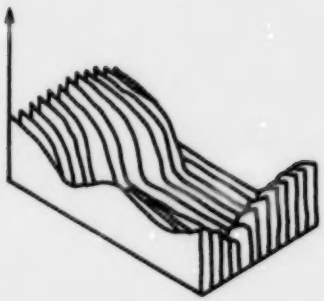

Scan 1

Scan 2

Positive Intensity

Scan 1

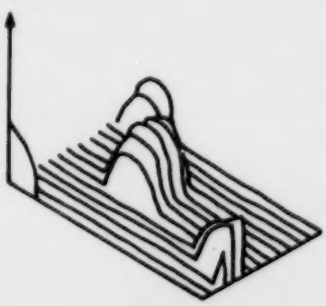

Scan 2

No Coherence
(trials 1 & 2 @ 400 Hz)
Figure 7

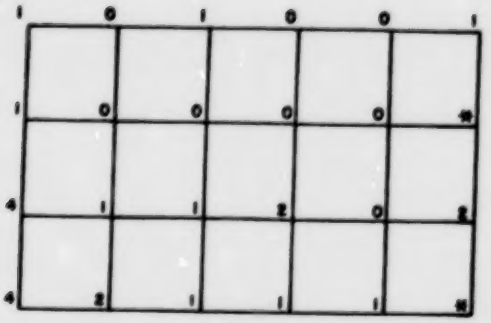

a) Coherent

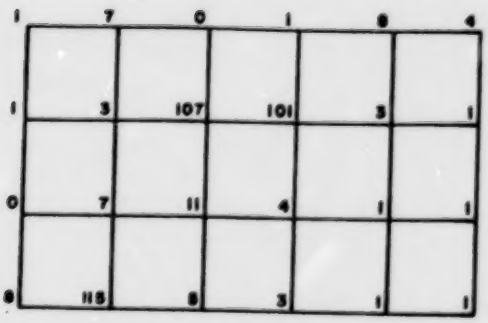

b) Partial Coherence

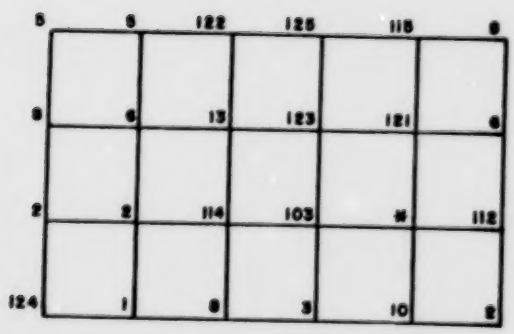

c) No Coherence

Residual Factors
Figure 8

displaying constant intensity levels.

For each frequency band, the mean and standard deviations of the 20 recorded points were calculated. The standard deviation was used as an indicator of the scatter of the points about the mean. Example plots are displayed in Figure 9.

Results and Interpretation

Table 2 shows the results from the visual inspection analysis performed between mappings 1 and 2, 1 and 3, and 2 and 3. These results served as a reference for all other methods. Note that C stands for coherent correlation, P for partial, and N for no coherence.

Examination of the power spectra (Figure 4) shows that in every frequency band the sound power emitted from the plate was deterministic and repeatable between all three scans. This is indicative of the stationarity of the noise source used, but intensity variations are not revealed.

The intensity versus time analysis however is more sensitive to these changes. This analysis produced a mean and standard deviation for each frequency band (see Table 1). The results (see Table 2) indicate that a standard deviation of less than one implies visual correlation. In only 12% of the frequency bands did this criteria fail to produce the correct results. Figure 9 verifies that a standard deviation of less than one does indicate a stationary frequency band.

Analysis of the residual factor data, while more complex, yielded equally precise results. It was found, in a preliminary method used, that the average of the residual factor over the grid, was not a good indicator of correlation. Slight shifts between two intensity patterns in an area of steep contours resulted in very large residual factors even though visually the patterns were very similar. Figures 10 and 11 highlight this point. Figures 10(a), 10(b) and 10(c) are the contour maps and positive and negative 3D plots of two trials of the same measurement performed at 400 Hz. Visually the patterns are similar, however the data map of the residual factors, Figure 11, reveals large values where the energy field has shifted slightly.

For this reason, the percentage of points in the residual factor above

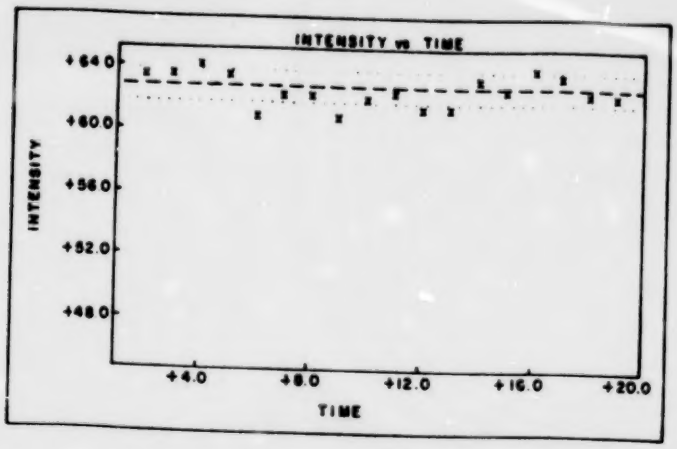

a) Standard Deviation = 1.00

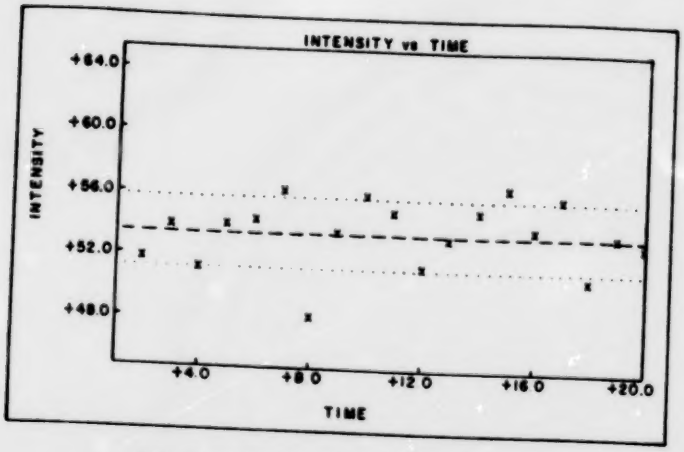

b) Standard Deviation = 2.38

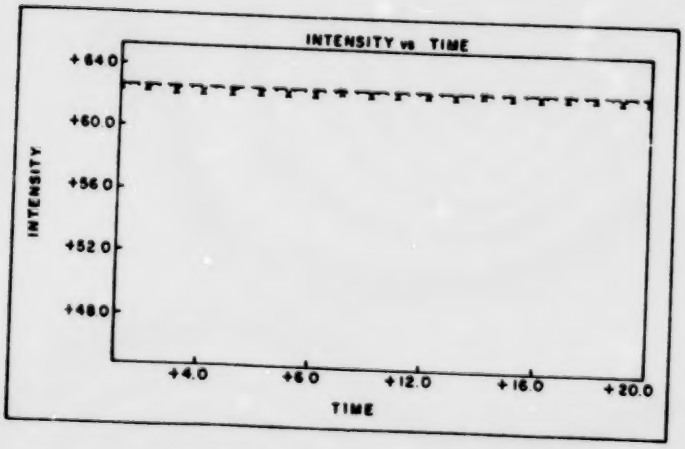

c) Standard Deviation = 0.07

Sample Plots of Intensity vs. Time Data
Figure 9

Freq. (Hz)	Standard Deviation			Mean		
	Trial 1	Trial 2	Trial 3	Trial 1	Trial 2	Trial3
100	0.39	0.81	0.21	73.09	-73.71	-78.97
125	0.54	0.31	1.37	-78.12	-73.66	-69.83
160	39.29	49.26	38.11	-17.65	37.94	33.46
200	1.05	50.32	1.37	-40.78	-69.73	-70.88
250	0.74	0.63	1.00	64.97	63.73	62.80
315	0.64	1.31	0.21	-61.64	-62.69	-67.43
400	2.39	49.23	1.18	-16.98	59.83	-60.73
500	0.35	0.42	0.60	-62.96	-66.24	62.03
630	1.42	1.54	0.91	63.46	63.90	64.09
800	43.82	2.38	2.28	54.82	26.31	53.45
1000	0.20	0.28	0.30	-65.00	-64.33	-63.88
1250	0.24	0.20	0.18	62.73	61.76	61.62
1600	0.41	0.38	0.47	56.23	56.43	57.19
2000	0.10	0.09	0.07	62.03	62.20	62.61
2500	0.06	0.10	0.11	68.87	68.98	69.40
3150	0.18	0.15	0.19	53.08	52.92	52.70
4000	0.15	0.25	0.29	46.88	45.90	45.22

Table 2. Standard Deviation and Mean for Intensity vs. Time Data

Freq. (Hz)	Average Standard Deviation	Visual Inspection Between 1 & 2	Visual Inspection Between 1 & 3	Visual Inspection Between 2 & 3
100	0.47	C	C	C
125	0.74	N	N	N
160	42.22	C	P	P
200	17.58	P	P	N
250	0.79	C	C	C
315	0.72	N	N	C
400	17.60	N	N	N
500	0.46	N	N	P
630	1.29	P	P	P
800	16.16	P	P	P
1000	0.26	C	C	C
1250	0.21	C	C	C
1600	0.42	C	C	C
2000	0.09	C	C	C
2500	0.09	C	C	C
3150	0.17	C	C	C
4000	0.23	C	C	C

Table 2. Average Standard Deviation vs. Visual Inspection

Contour Map

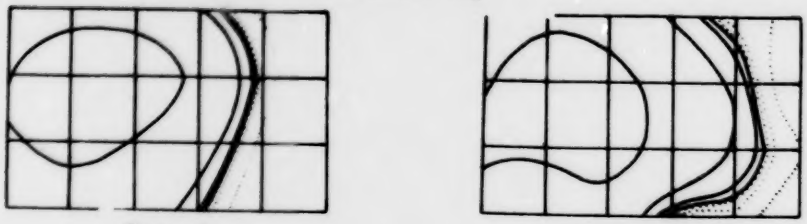

Scan 1 Scan 2

Negative Intensity

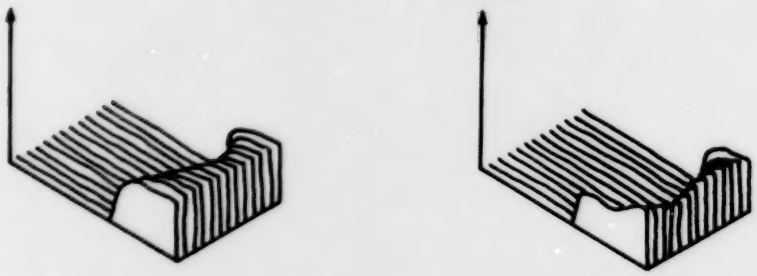

Scan 1 Scan 2

Positive Intensity

Scan 1 Scan 2

Coherent
Figure 10

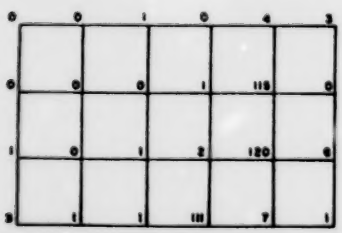

Data Map Showing Result
of Energy Shift
Figure 11

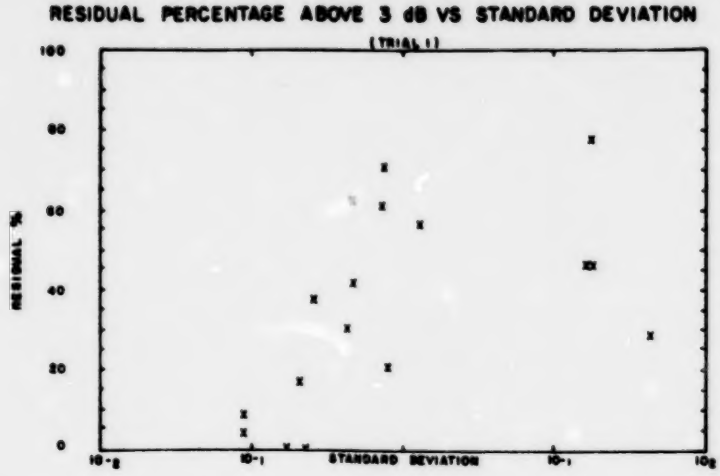
RESIDUAL PERCENTAGE ABOVE 3 dB VS STANDARD DEVIATION
(TRIAL 1)
RESIDUAL %
STANDARD DEVIATION

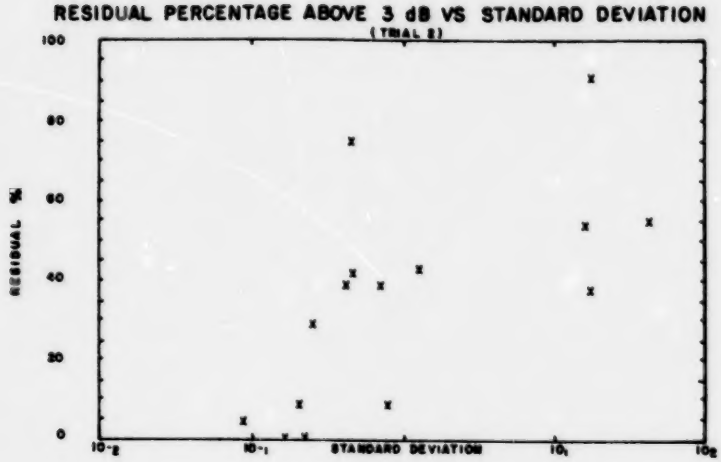
RESIDUAL PERCENTAGE ABOVE 3 dB VS STANDARD DEVIATION
(TRIAL 2)
RESIDUAL %
STANDARD DEVIATION

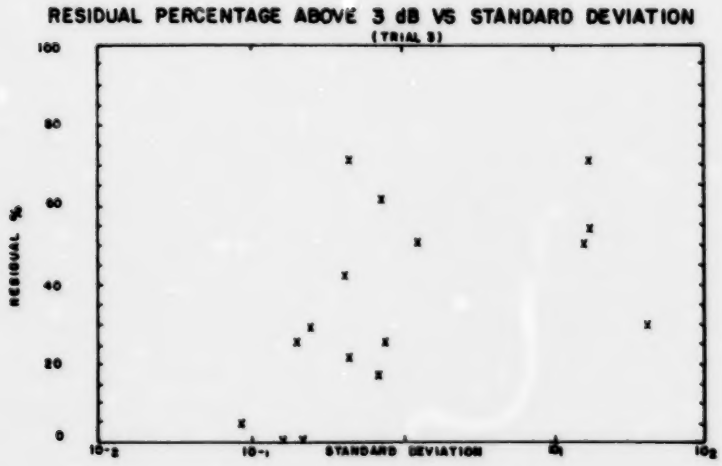
RESIDUAL PERCENTAGE ABOVE 3 dB VS STANDARD DEVIATION
(TRIAL 3)
RESIDUAL %
STANDARD DEVIATION

Figure 12

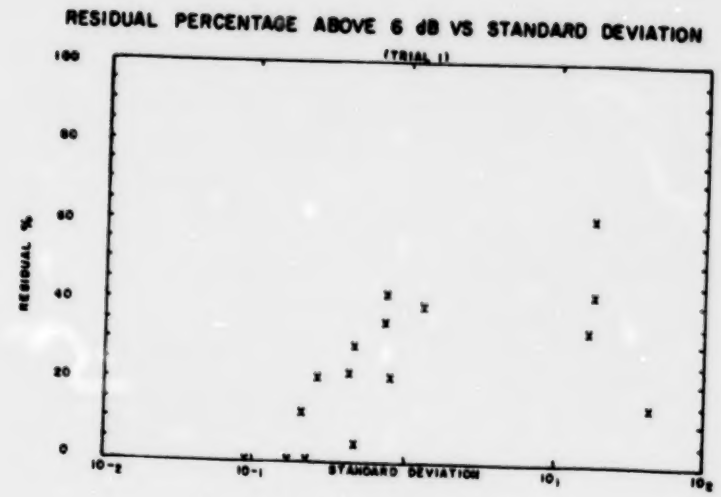
RESIDUAL PERCENTAGE ABOVE 6 dB VS STANDARD DEVIATION
(TRIAL 1)
RESIDUAL %
100
80
60
40
20
0
10-2
10-1
STANDARD DEVIATION
10₁
10₂

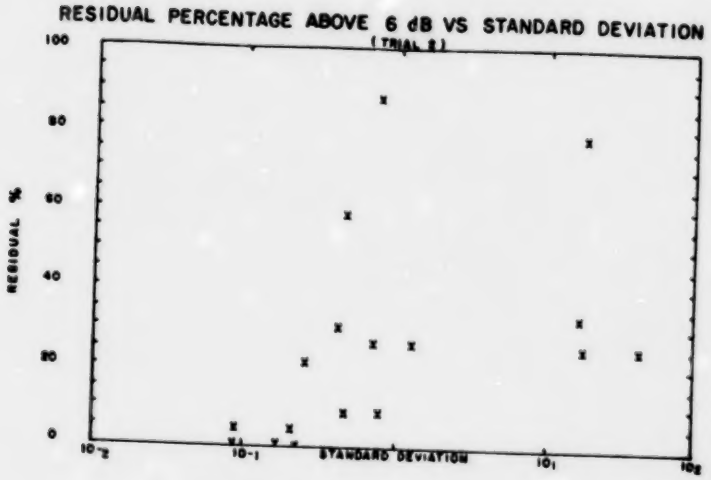
RESIDUAL PERCENTAGE ABOVE 6 dB VS STANDARD DEVIATION
(TRIAL 2)
RESIDUAL %
100
80
60
40
20
0
10-2
10-1
STANDARD DEVIATION
10₁
10₂

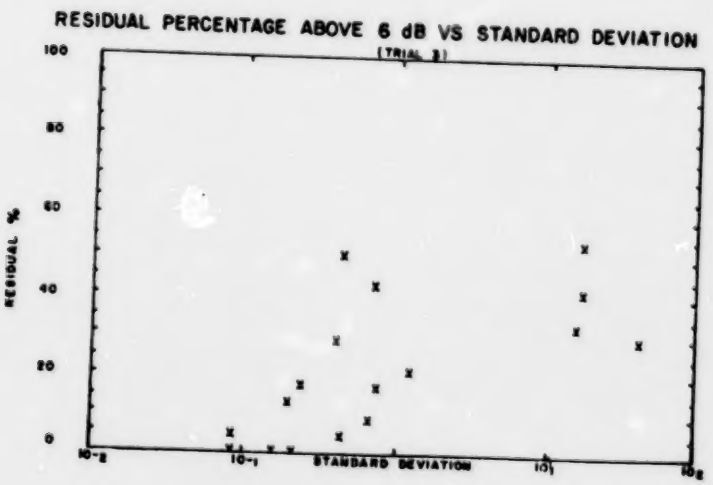
RESIDUAL PERCENTAGE ABOVE 6 dB VS STANDARD DEVIATION
(TRIAL 3)
RESIDUAL %
100
80
60
40
20
0
10-2
10-1
STANDARD DEVIATION
10₁
10₂

Figure 13

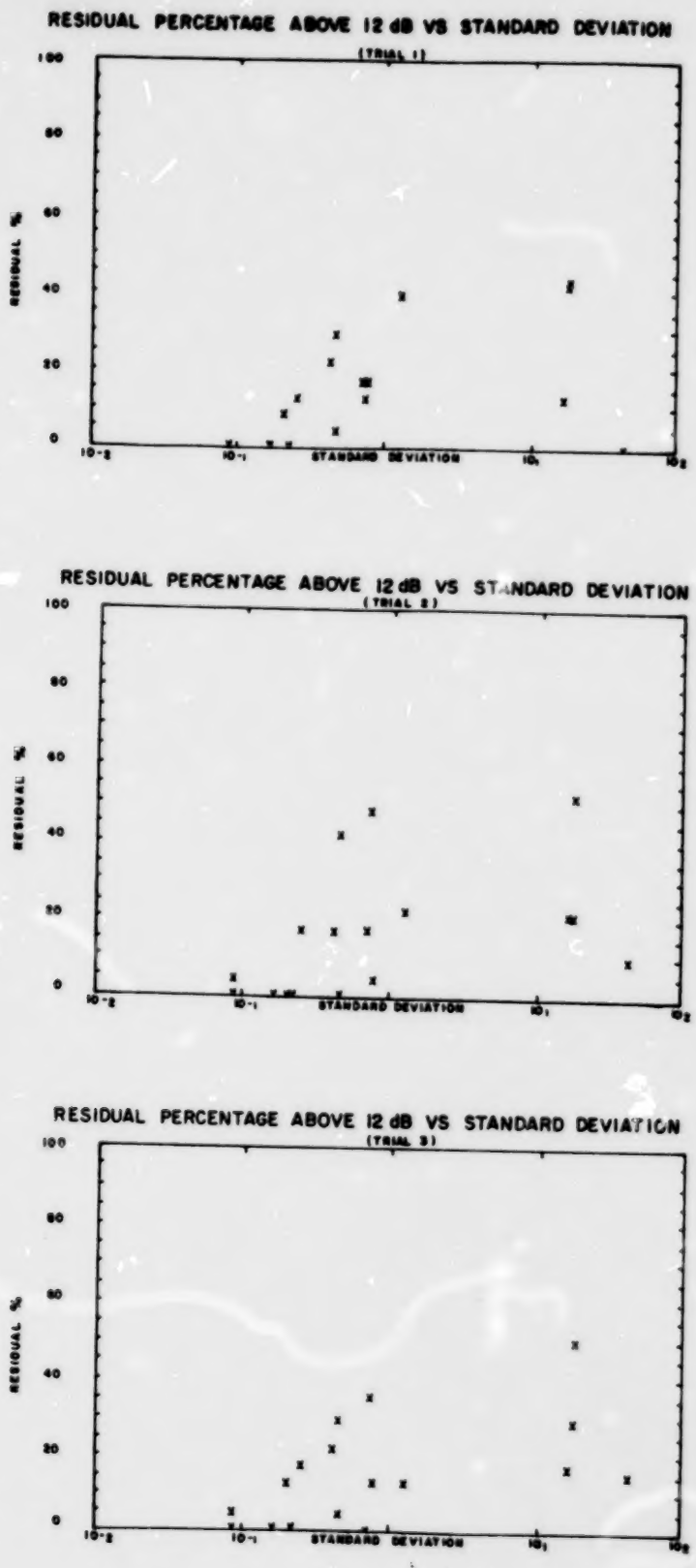
RESIDUAL PERCENTAGE ABOVE 12 dB VS STANDARD DEVIATION
(TRIAL 1)
RESIDUAL %
STANDARD DEVIATION
RESIDUAL PERCENTAGE ABOVE 12 dB VS STANDARD DEVIATION
(TRIAL 2)
RESIDUAL %
STANDARD DEVIATION
RESIDUAL PERCENTAGE ABOVE 12 dB VS STANDARD DEVIATION
(TRIAL 3)
RESIDUAL %
STANDARD DEVIATION

Figure 14

certain values: 3, 6 and 12 dB, were considered as an indicator. Figures 12, 13, and 14 represent the percentage of points above 3, 6 and 12 dB respectively compared with the previously calculated standard deviation value on the log scale (one plot per figure for each comparison). Circled points indicate definite visual correlation, boxed points indicate possible visual correlation and no correlation is represented by the point enclosed in a triangle.

The standard deviation criteria can be verified by drawing a vertical line through one. Points on the left of this line correlate and those on the right do not. On the 3 dB graphs, if a horizontal line is drawn through 45% then correlation is represented almost exclusively below this line. The same is true for a line through 30% on the 6 dB graphs. Such a cutoff however does not exist in the 12 dB plot.

Note that the best results are realized when both residual factor and time variation of intensity data are applied simultaneously forming an envelope bounded by a standard deviation of one and the appropriate percentage (45% or 30%).

Conclusions

Consistent mappings of acoustic intensity for the specimen have been obtained. For the most part mappings are repeatable in the high (1000 to 4000 Hz) frequency ranges and also at 125, 400 and 500 Hz.

It has been shown that power spectra is not a suitable means of identifying indicative frequency bands. However, both intensity versus time and residual factors have been shown to be adept in this identification. For the purpose of stationary band detection in the DAIS system, the time variation of intensity method is easier to implement. One number eventuates from this type of measurement which characterizes the repeatability of the frequency band. By recording intensity versus time data before scanning a plate, unwanted frequency bands can be automatically ignored in the scan. Residual factor requires at least two scans of the plate and a critical comparison of the data sets before any conclusions can be made.

However, the residual factor method, while more complex to execute, is very effective in its comparison between data sets [3]. This type of evaluation can lead to pattern recognitions performed by a neural networking

computer [4].

Ultimately, the use of the residual factor and time variation of intensity methods serve to eliminate the subjectivity of visual inspection.

Acknowledgements

Thanks are due to C-CORE for supporting this research, to NORDCO Ltd. and Dr. A.S.J. Swamidas (Memorial University of Newfoundland) for their interest, and to Dr. Robert Thompson and CANMET for encouragement and financial back[illegible] of the program. Thanks are also due to Desiree King for the diagrams.

References

1. J.Y. Guigné, P.G. Williams, and V. Chin. A Concept for the Detection of Fatigue Cracks in Welded Steel Nodes, Marine Technology, Vol. 18, No. 4, (1987).

2. J.Y. Guigné, P.G. WIlliams, and V. Chin. Analysis of the Deformation in a Partially Cracked Welded T-Plate, Marine Technology, Vol. 18, No. 4, (1987).

3. J.Y. Guigné, P.G. Williams, and D.K. Mak. Acoustical Imaging Using a DAIS Technique for Non-Destructive Testing, Conference Proceedings of Acoustical Imaging, Tokyo, (1988).

4. V.H. Chin, and J.Y. Guigné. Heuristic Information Processing, C-CORE News, Vol. 13, No. 2, (1988).

Submitted to NORDCO Ltd., St.John's
Propriety Technical Report

HYDROPHONE PHASE MATCHING FOR UNDERWATER INTENSITY MEASUREMENTS

BY

J. Y. Guigné and P. G. Williams

Centre for Cold Ocean Resources Engineering,
Memorial University of Newfoundland,
St. John's, A1B 3X5

Abstract

The measurement of acoustic intensity has been carried out extensively in air using a microphone pair and an Intensity analyzer (Brüel & Kjær Type 3360) which relies on a finite difference approximation in Eulers equation to calculate the intensity [1] and digital filtering to produce a real-time intensity spectrum. An important aspect of the accuracy of this measurement technique arises from phase errors in the transducers used [2,3].

In order to apply acoustic intensity measurement underwater, phase matched hydrophone pairs are necessary. These are obtained by measuring the phase difference between a number of hydrophones, and selecting pairs with the closest phase matching possible. This was done at C-CORE using a high pressure chamber belonging to Brüel & Kjær Ltd. (Denmark) which was designed specifically for this purpose, and loaned to Dr. Jacques Guigné.

Three pairs of Brüel & Kjær 8105 hydrophones were tested. The procedures involved in the testing are outlined in this technical note, along with the results obtained.

This propriety report can be requested from:

Nordco Ltd.
P.O. Box 8833
St.John's, Newfoundland

References

[1] Rasmussen, G., "Measuring Intensity", Intensity Measurements- The Analysis Technique of the Nineties, Brüel & Kjær BA 7196-13, 1987

[2] Rasmussen, P., "Phase Errors in Intensity Measurements", Intensity Measurements- The Analysis Technique of the Nineties, Brüel & Kjær BA 7196-13, 1987

[3] Rasmussen, G., Brock, M., "Transducers for Intensity Measurements", 11th ICA, 1983

Accepted for Oral Presentation
at WCNDT, Amsterdam (1989).

DETECTION OF IN-SERVICE FATIGUE DAMAGE IN OFFSHORE STRUCTURES USING DYNAMIC ACOUSTIC INTENSITY SCANNING

BY

J. Y. Guigné, P. G. Williams and J.G.Adams

Centre for Cold Ocean Resources Engineering,
Memorial University of Newfoundland,
St. John's, A1B 3X5

Introduction

Dynamic Acoustical Intensity Scanning (DAIS) has been shown to have great potential as a technique for non-destructive fatigue crack detection in air [1,2]. The technique is based on the fact that any vibrating structure will radiate acoustic energy from its surface. DAIS measures acoustic intensity (a vector quantity) at various locations over a structure. The flow of acoustic energy over the structure can then be mapped out using an innovative application of acoustic intensity mapping. Changes in the flow of this acoustic energy are related to changes occurring within the structure, such as the onset of fatigue cracking.

Many applications, particularly in the field of offshore development require that non-destructive testing methods be suitable for underwater use. This paper presents the results obtained from the measurement of acoustical intensity in an underwater environment. The measurements were made using a hydrophone pair submerged in a cylindrical water tank.

Laboratory Setting

Specimens

The specimen used was fabricated from 19 mm thick 1024 steel plate with dimensions 600 mm by 100 mm. Two 12 mm diameter loading holes were machined on the centre line, 30 mm from each end. On the plate, a measurement grid of six columns and four rows was marked. The grid and plate dimensions are illustrated in Figure 1.

Set-up

The specimen was suspended freely in a servo-hydraulic test frame (Figure 2). A cylindrical tank with a diameter of 1 m. and a depth of 1 m. was mounted around the specimen and filled until the water level was just below the level of the specimen grip. The test system (set for stroke control) was vibrated using a pseudo-random excitation with a band width of 10 kHz. Although the actual displacement of the specimen was negligible, significant acoustical energy was produced. This energy, flowing through the actuator, linkage and specimen, was the target of the intensity scans.

The transducers used in the experiment were a pair of omni-directional hydrophones mounted side by side in a bracket. Phase matching of the hydrophones, necessary to reduce residual intensity errors [3], was performed using an FFT analyzer and a calibrated pressure chamber. The hydrophone bracket was suspended by a bench support system which was adjustable in three directions and allowed rotation in the vertical direction.

The hydrophones were connected through charge amplifiers to the intensity analyzer. A dedicated computer system was used to control the analyser and to record the data (Figure 3).

Scanning Methodology

The support system was adjusted such that the acoustical centre of the hydrophone pair was located approximately 10 cm in front of the first grid location. Once the first point was found, scales on the support system allowed the location of the subsequent points even though visual verification of the positioning could not be done. Because of this, inaccuracies in the positioning system may have introduced slight point location errors.

Two scans of the plate were performed in each of the y (across the plate) and z (normal to the plate) directions. At each grid location, the acoustic intensity spectrum was measured using a real time digital filtering analyser. This device measures the component of the acoustic intensity vector in decibels along the line of the transducer pair. The output is an intensity spectrum over a frequency range of 200 Hz. to 2 kHz. with a one-third octave bandwidth. The directionality of the vector component is indicated by the sign of the intensity level - a positive intensity level represents energy flowing in the +y or +z direction; a negative intensity level represents energy flowing in the -y or -z direction. The spectra were transferred to a computer for post processing.

Data Processing

At each measured frequency, linear interpolation between the intensity

levels (in dB) at each grid location was performed. This data set was then used to produce graphical plots of acoustic energy flow to facilitate the visual comparison of data. Intensity levels less than the base level of 90 dB were omitted from these plots (treated as zero). Two types of data presentation are used: contour mapping of the intensity levels over the structure (e.g. Figure 4 (a)), and a three-dimensional plot of the intensity levels. For the second plot, the positive and negative intensity values are displayed separately (e.g. Figures 4 (b) and 4 (c)).

Results and Interpretation

A comparison was performed between data sets taken in the same directions. Table 1 summarizes this data. A "C" was assigned to frequencies that gave a good correlation, "P" to those that partially correlated and "N" to those that did not correlate. From Table 1, it can be seen that a relatively high number of the frequency bands showed correlation. The importance of this stationarity under constant conditions has been discussed by the authors [4]. For frequencies in which data pairs matched in both directions, a comparison was made between data measured in different directions. Table 2 summarizes the results. Only at 100 Hz was there correlation between different directions. As both of these plots were very flat, this is probably due to the high reactivity of the sound field at this frequency. The lack of correlation, particularly in the frequency bands which matched in the same direction, is a significant result. This displayed directionality confirms that the measured quantity is indeed intensity and not sound pressure. Figures 4 and 5 are examples of plots of the same frequency which correlated in the same direction but were unlike in different directions.

Conclusions

The measurement of sound intensity by hydrophones submerged in a cylindrical tank has been verified. Since the high reactivity in such a tank (represented by a high pressure) is a worst case in comparison with practical applications, these results are very encouraging.

The frequent correlation between trials measured in the same direction is also significant. Stationarity between trials is extremely important if the method is to be effective as an indicator of fatigue cracking.

References

1. J.Y. Guigné, P.G. Williams, and V. Chin. A Concept for the Detection of Fatigue Cracks in Welded Steel Nodes, Marine Technology, Vol. 18, No. 4, (1987).

2. J.Y. Guigné, P.G. Williams, and V. Chin. Analysis of the Deformation in a Partially Cracked Welded T-Plate, Marine Technology, Vol. 18, No. 4, (1987).

3. T. Jacobsen. Calibration of Sound Intensity Measurements, Brüel and Kjaer, Denmark, (1988).

4. J.Y. Guigné, P.G. Williams, and J.G. Adams. Stationarity of Acoustic Intensity Measurements on Steel Plates, for submission to: Journal of Sound and Vibration, (1988).

Comparison Results		
Freq. (Hz)	Between Two Trials In Y-Direction	Between Two Trials In Z-Direction
25	N	N
32	N	N
40	D	N
50	N	D
63	D	N
80	D	N
100	D	D
125	D	P
160	D	D
200	D	D
250	D	P
315	P	P
400	P	D
500	P	D
630	D	D
800	D	D
1000	D	D
1250	D	D
1600	N	P
2000	D	N

TABLE 1. COMPARISON BETWEEN TWO TRIALS OF INTENSITY MEASURED IN THE SAME DIRECTION

Freq. (Hz)	Comparison Result Between Y & Z
25	-
32	-
40	-
50	-
63	-
80	-
100	D
125	-
160	N
200	P
250	-
315	-
400	-
500	-
630	N
800	N
1000	P
1250	N
1600	-
2000	-

TABLE 2. COMPARISON BETWEEN TWO TRIALS IN DIFFERENT DIRECTIONS

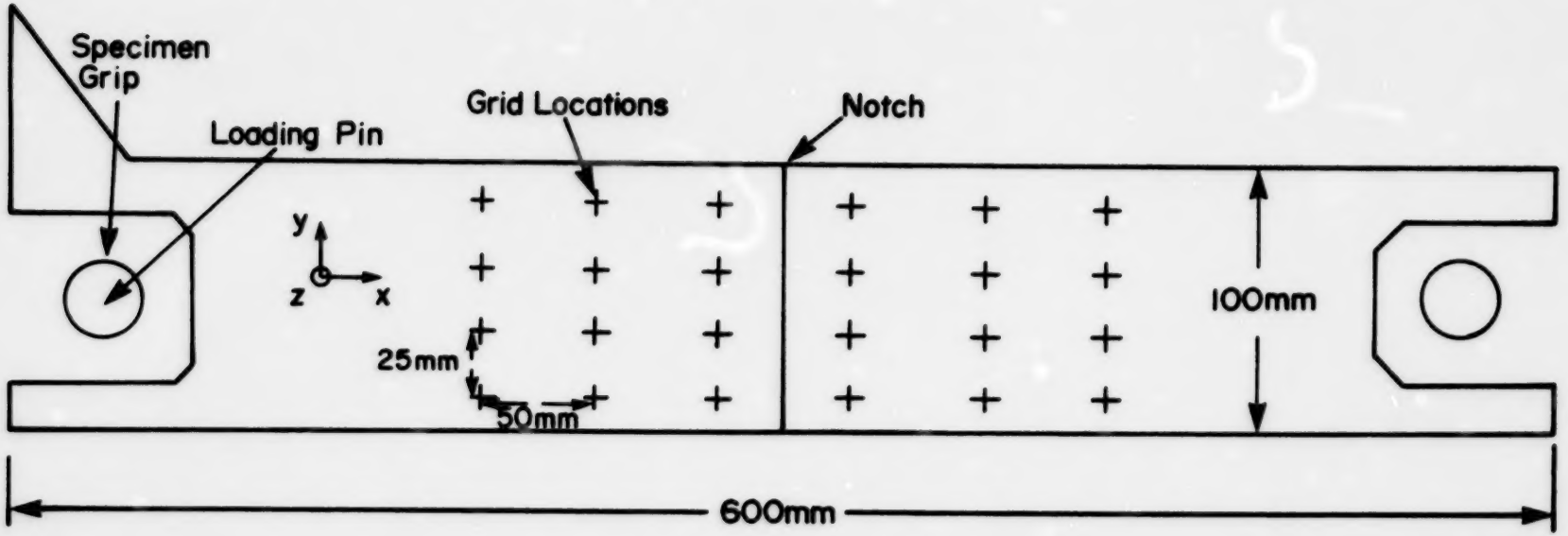

Figure 1. Specimen Dimensions.

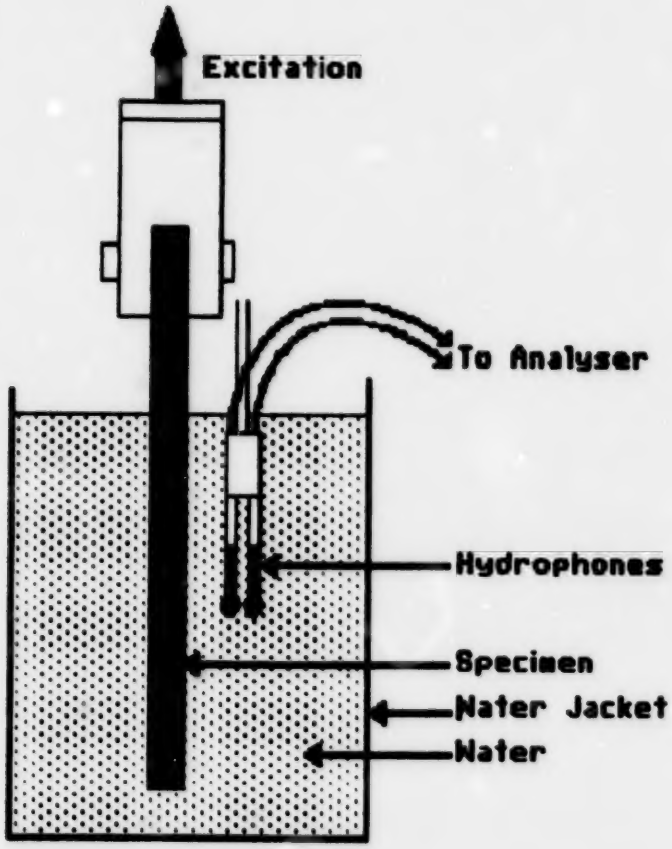

Figure 2. Measurement Set-up

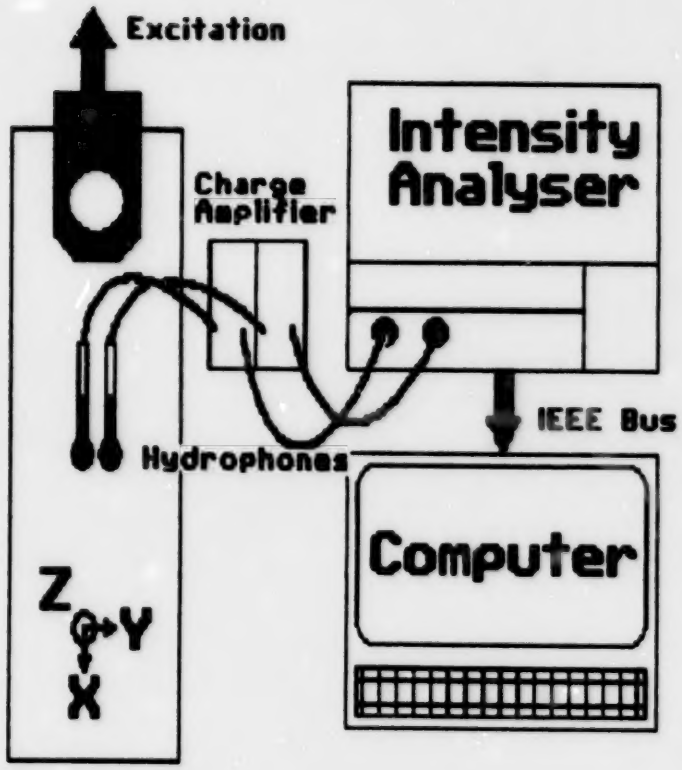

Figure 3. Instrumentation Set-up

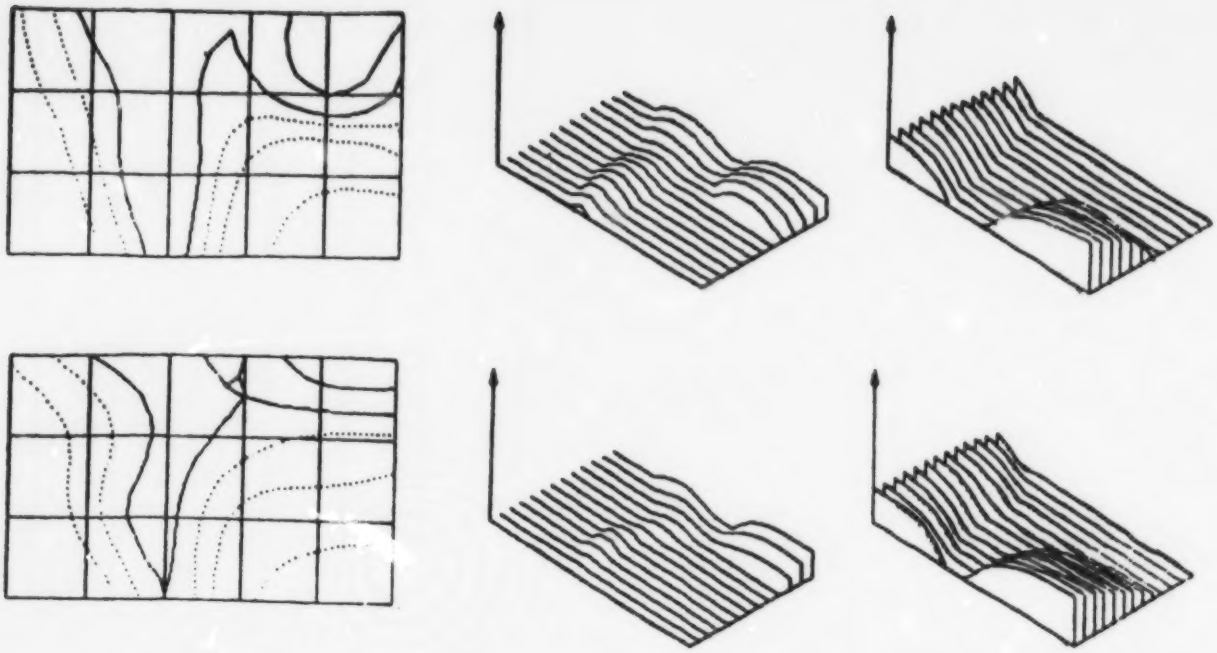

Figure 4. Energy flow in Z-direction at 800 Hz. (a) Contour Map, (b) Three dimensional plot (negative intensity) (c) Three-dimensional plot (positive intensity).

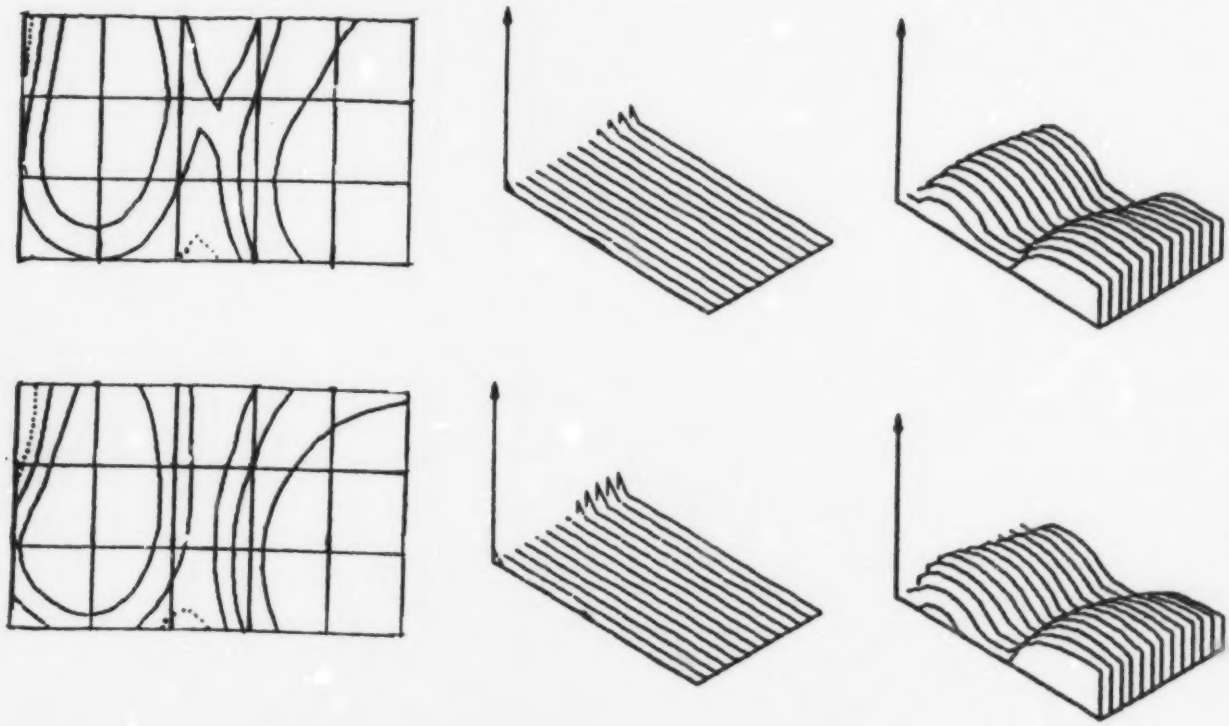

Figure 5. Energy flow in Y-direction at 800 Hz. (a) contour map, (b) Three-dimensional plot (negative intensity) (c) Three-dimensional plot (positive intensity)

In Preparation for Submission to
Canadian Metallurgical Quarterly.

CHARACTERIZATION OF STEEL PLATES CONTAINING MACHINED DEFECTS USING THE DAIS TECHNIQUE

BY

J. Y. Guigné, P. G. Williams and D. K. Mak*

Centre for Cold Ocean Resources Engineering,
Memorial University of Newfoundland,
St. John's, A1B 3X5

---

* Metals Technology Laboratories, 568 Booth Street, Ottawa

Introduction

This paper presents the DAIS characterization of steel plates containing different machined defects as imaged in air. The intensity scans are displayed and evaluated, and the remnant factors displayed.

Dynamic Acoustic Intensity Scanning (DAIS) measures the flow of acoustic energy over a structure. It makes use of a real time digital filtering processor which captures the acoustic intensity spectrum at a point. By measuring the intensity spectrum at a number of points over the surface of a structure, DAIS is able to map the energy flow over this area. From preliminary data samples the DAIS identifies the appropriate measurement parameters, such as transducer type and instrument settings, through its adaptive logic. The data collected is manipulated to provide contour maps, three-dimensional plots, and two-dimensional vector representations of the energy flow in each frequency band. By comparing data sets collected at different times over the same area, the appearance and growth of defects such as fatigue cracks can be monitored through the changes that occur in the energy flow. This change in energy flow is quantified by a parameter called the Remnant Factor.

The (DAIS) technique is being engineered as a non-destructive testing tool with its ultimate application being the underwater detection of fatigue cracking in offshore steel structures [1,2]. The DAIS technique has been applied in both air [3,4] and water [5].

Measurement Technique

Specimens

Six specimens were fabricated from 19 mm thick 1024 steel plate. The specimen dimensions were 600 mm by 100 mm, with 12 mm diameter loading holes machined on the centre line, 30 mm from each end (Figure 1). Three different defects were introduced: a machined notch 4 mm wide by 12.5 mm deep, a weld bead, and a flat bottomed hole with diameter 10 mm. and depth 12.5 mm. Table 1 shows the defects associated with each specimen.

Load Frame

Each specimen was mounted in a servo-hydraulic test frame (Figure 2)

and loaded in tension to a static load of 75 kN.

Intensity Scanning

The intensity probe consisted of two 1/4" microphones, phase matched for intensity measurement. The probe was mounted on a movable column that allowed consistent, repeatable positioning (Figure 3). The intensity measurements were made using a digital filtering intensity analyser. This device measures the component of the acoustic intensity vector in decibels along the line of the transducer pair. The output is an intensity spectrum over a frequency range of 100 Hz. to 4 kHz. with a one-third octave bandwidth (Figure 4). The directionality of the vector component, with respect to the transducer pair, is indicated by the sign of the intensity level.The spectra were transferred to a computer for post processing.

The complete system was calibrated for pressure, intensity and particle velocity using a reference intensity source.

The acoustic energy which flowed through the specimen and was targeted by the acoustic scanning was provided by a pseudo-random excitation with a bandwidth of 10 kHz applied through the servo-hydraulic actuator. This excitation is in addition to the static load on the specimen.

The first step in the DAIS procedure involves the determination of the stationarity of the acoustic source. This is done by measuring the variation in the acoustic intensity spectrum at a single location over a period of 20 seconds. This data was stored on the computer, for use during the post-processing.

A measurement grid was marked onto each specimen (Figure 1) and the intensity scanning performed by reading the intensity spectrum at each grid location. The component of the intensity vector normal to the plate was measured. The scans were carried out twice so that the repeatability of the scanning process could be determined.

Post Processing

The signal stationarity data were analyzed by calculating the mean and standard deviation of the intensity-time data, for each frequency band [4]. When the standard deviation exceeded a value of 2, the data for that

frequency band was ignored during subsequent data analysis.

For the frequency bands with acceptable stationarity based on this criterium, the data were presented in the form of contour maps for visual analysis and comparisons. The contour maps are created by interpolating between the measured data points using a cubic spline algorithm. This data set is then used to create a contour map, with solid lines connecting points of equal positive intensity, and dashed lines connecting points of equal negative intensity. The sign indicates directionality, with positive being radiated out from the plate and negative flowing towards the plate (see Figure 5).

Remnant Factors were calculated for three of the specimens containing defects (Plates 1, 4 and 5) with reference to the defect free specimen (Plate 6). The Remnant Factor is calculated as the absolute difference between the magnitude of the intensity levels measured at the same grid location on two different specimens. This difference is displayed as a contour map (see Figure 14).

Results

Stationarity Measurements

The mean and standard deviation data for the stationarity measurements over the frequency range of 100 Hz. to 4000 Hz. are displayed in tables 2 to 7. Each table also lists the number of negative (directional) intensity values, and the number of values that lie at or below the threshold intensity level of 40 dB set in the analyser. These parameters are useful in determining the quality of the source in each frequency band. For example, if all values lie at or near the threshold level then there is no measurable energy flow within that frequency band. If the sign changes frequently, then the measurement point may be in an area over which the direction of energy flow is changing rapidly.

Figure 5 shows the variation of the intensity levels with time for three different standard deviation levels. The solid line shows the mean value of the data set; the dashed lines show +/- one standard deviation from the mean. Figure 5 (a) shows the variation for a high standard deviation of 3.90, above the cut-off level. Figure 5 (b) shows a low standard deviation

of 0.67, and Figure 5 (c) shows the variation for a standard deviation of 1.43, just below the cut-off level of 2.

Intensity Mapping

Figures 6 to 13 show the contour maps for the frequency bands 800 Hz to 4000 Hz for each specimen. Negative (directional) intensity values are connected by dashed lines; positive by solid lines. The contour lines are separated by 3 dB intervals.

The frequency bands were selected based on the stationarity measurement results described in the previous paragraph. Table 8 shows a comparison between the stationarity measurement results and a visual comparison between repeated measurements over the complete frequency range of measurement (100 Hz. to 4 kHz.). P indicates partial coherence, N shows no coherence and C is complete coherence between intensity maps of repeated readings. A dash is used where the standard deviation in the intensity measurements exceeded the set value.

Remnant Factor

The Remnant Factor contour maps between three of the specimens containing defects (specimens 1, 4 and 5), and the defect free specimen (6) are illustrated in figures 14 to 21. Again, dashed lines connect negative directional values and solid lines connect positive directional values. Contour line interval is 3 dB.

Interpretation

From the comparison between the stationarity measurements and the visual comparison (Table 8) it can be seen that there is a very clear cut-off at 800 Hz. Above this frequency, the stationarity measurements provide a good indication of repeatability in the data sets. Below this frequency, the results are not as consistent as only 25% of the acceptable stationarity measurements are shown to give repeatable visual comparisons. This may be due to the variation in the background noise levels present in the laboratories during measurements, and further investigations into this may be necessary. For example, the results for Plate 4 show that only two frequencies below 800 Hz. had acceptable stationarity values whereas all but

two of the frequencies for Plate 5 were acceptable.

From the contour maps presented in figures 6 to 13, we can see how the acoustic energy flow normal to the plate varies between frequencies and between specimens. In particular, the plots for 1600 Hz. show a similar patterning for plates 1, 2, and 3 with a sink along the fifth column (Figures 9 (a),(b), and (d)). These three plates all contain notches. The fourth notched plate, plate 4, shows a shift in the location of this sink from column five to column four (Figure 9 (c)). Plate 5 (Figure 9 (e)), containing the hole, shows a pronounced sink along the fifth column, as well as a less pronounced sink along the second column. The defect free plate, Plate 6 (Figure 9 (f)) delineates two features along columns one and five which are symmetrical and equally pronounced. These patterns may be attributable to the machined defects.

Plots for the 1250 Hz. frequency band (Figure 8) and the 2500 Hz. frequency band (Figure 11) exhibit similar features regardless of the defect. At 1250 Hz., all plots show two sinks running across the measurement grid at columns 2 and 5. At 2500 Hz, all images show a sink running across the measurement grid between columns three and four. These particular patterns are associated with the modal deformation or flexing of the plates. At 3150 Hz (Figure 11) and 4000 Hz (Figure 12), the contour maps are difficult to interpret. If, however, we look at the remnant factor contour maps (Figures 17 and 18) we see distinct similarities between the two notched specimens and differences with the specimen containing the hole.

Conclusions

The intensity time measurements have been shown to be a good indicator of the stationarity of different frequency bands in order to determine which frequency bands give repeatable intensity maps. These frequencies are from 800 Hz. to 4000 Hz.

The contour maps of the energy flow normal to the plate at certain frequency bands, notably 1600 Hz. and 4000 Hz., show that the presence of machined defects does alter the energy flow through the plates. Other frequencies, for example 1250 Hz. and 2500 Hz., demonstrate a consistent patterning independent from the machined defects. These patterns are associated with the modal deformation of the plate.

The Remnant Factor contour maps show that similar patterns can be detected when two different specimens containing the same defect are compared with a defect free specimen, for example 3150 Hz. and 4000 Hz.

The visual analysis of the contour maps for comparison purposes is a less than satisfactory approach. The development of a neural networking model for the evaluation of the energy flow data is currently being carried out to enhance the analysis of the data. It is expected that this will provide better discrimination between patterns associated with different defects and with modal deformation, as well as determining 'mixed mode' patterns arising from multiple defects. Once this has been implemented, the location of defects through knowledge of their associated energy flow patterns will be possible. It is not yet known what the resolution of the detection will be in terms of defect sizing.

It should be remembered that with fatigue cracking, the work required for crack propagation occurs during the testing and therefore becomes a part of the measurement process. The resultant intensity patterns reveal this work as a distinct energy sink. In the case of machined defects the work associated with the creation of the notch is carried out in the machine shop and thus the patterns are not as distinct. However, if the resultant intensity vectors are differentiated into orthogonal components, then the perturbation of energy flow by defects, in terms of damping and reverberation, can be highlighted [3].

The DAIS technique is still in its early developmental stages but these results show that intensity mapping does have the potential to become a valuable tool in the evaluation of structural integrity.

References

1. Guigne, J.Y., Williams, P.G. and Chin, V.H. A Concept for the detection of fatigue cracks in welded steel nodes. Marine Technology, Vol 18 No. 4 Dec 1987

2. Guigne, J.Y., Williams, P.G. and Chin, V.H. Analysis of the deformation in a partially cracked welded T-plate. Marine Technol gy, Vol. 18 No. 4 Dec 1987

3. Guigne, J.Y., Williams, P.G. and Mak, D.K. Acoustical imaging using a DAIS technique for non-destructive testing. Proceedings of 17th International Symposium on Acoustical Imaging, Publ. Plenum 1988

4. Guigne, J.Y., Williams, P.G. and Adams, J.G. Stationarity of

acoustical intensity measurements on steel plates. Under review

5. Guigne, J.Y., Williams, P.G. and Adams, J.G. A note on the directionality of intensity measurements made in a cylindrical tank. Presented at the 12th World Conference on Non-Destructive Testing. Amsterdam, 1989

Plate No.	Defect	Dimensions
1	Notch	4 mm. wide x 12.5 mm. deep
2	Notch	4 mm. wide x 12.5 mm. deep
3	Notch & Weld	4 mm. wide x 12.5 mm. deep
4	Notch	4 mm. wide x 12.5 mm. deep
5	Hole	10 mm. dia. x 12.5 mm. deep
6	No defect	-

Specimen Numbers and Associated Defects

Table 1

Frequency (Hz)	Mean (dB)	Std. Devn.	No. Neg. Values	No. Base Level
800	64.17	.25	0	0
1000	63.92	.22	0	0
1250	50.87	1.92	0	0
1600	55.79	.24	0	0
2000	59.31	.15	0	0
2500	57.92	.14	0	0
3150	49.30	.23	0	0
4000	45.57	.36	0	0

Intensity - Time Statistics for Plate 1

Table 2

Frequency (Hz)	Mean (dB)	Std. Devn.	No. Neg. Values	No. Base Level
800	56.65	1.35	0	0
1000	33.57	43.21	4	0
1250	54.55	1.20	0	0
1600	51.80	.65	0	0
2000	41.86	1.20	0	3
2500	54.83	.22	0	0
3150	57.29	.23	0	0
4000	52.18	.25	0	0

Intensity - Time Statistics for Plate 2

Table 3

Frequency (Hz)	Mean (dB)	Std. Devn.	No. Neg. Values	No. Base Level
800	57.88	.53	0	0
1000	57.11	1.58	0	0
1250	39.28	30.25	2	1
1600	54.55	.23	0	0
2000	53.71	.13	0	0
2500	53.75	.14	0	0
3150	53.97	.12	0	0
4000	44.64	.22	0	0

Intensity - Time Statistics for Plate 3

Table 4

Frequency (Hz)	Mean (dB)	Std. Devn.	No. Neg. Values	No. Base Level
800	64.23	.24	0	0
1000	-61.60	.49	20	0
1250	-29.76	39.29	16	1
1600	57.73	.35	0	0
2000	55.08	.55	0	0
2500	65.26	.14	0	0
3150	57.84	.13	0	0
4000	54.34	.11	0	0

Intensity - Time Statistics for Plate 4

Table 5

Frequency (Hz)	Mean (dB)	Std. Devn.	No. Neg. Values	No. Base Level
800	55.49	.67	0	0
1000	-54.56	1.43	20	0
1250	-49.92	.84	20	0
1600	35.42	28.01	2	3
2000	58.56	.11	0	0
2500	59.26	.15	0	0
3150	50.03	.07	0	0
4000	47.80	.15	0	0

Intensity - Time Statistics for Plate 5

Table 6

Frequency (Hz)	Mean (dB)	Std. Devn.	No. Neg. Values	No. Base Level
1000	-60.33	.56	20	0
1250	-55.39	.55	20	0
1600	50.35	.43	0	0
2000	56.02	.16	0	0
2500	54.54	.22	0	0
3150	48.89	.23	0	0
4000	47.96	.15	0	0

Intensity - Time Statistics for Plate 6

Table 7

Frequency	Plate 1	Plate 4	Plate 5	Plate 6
100	P	-	P	-
125	N	-	C	C
160	C	-	C	C
200	-	-	N	N
250	-	-	N	N
315	-	-	-	P
400	-	-	-	-
500	N	N	P	-
630	P	N	P	-
800	C	C	-	C
1000	C	C	C	C
1250	C	-	C	C
1600	C	C	C	-
2000	C	C	C	C
2500	C	C	C	C
3150	C	C	C	C
4000	C	C	C	C

Comparison between Stationarity Measurements and Visual Comparison
(- indicates that standard deviation in stationarity values exceeds 2)

Table 8

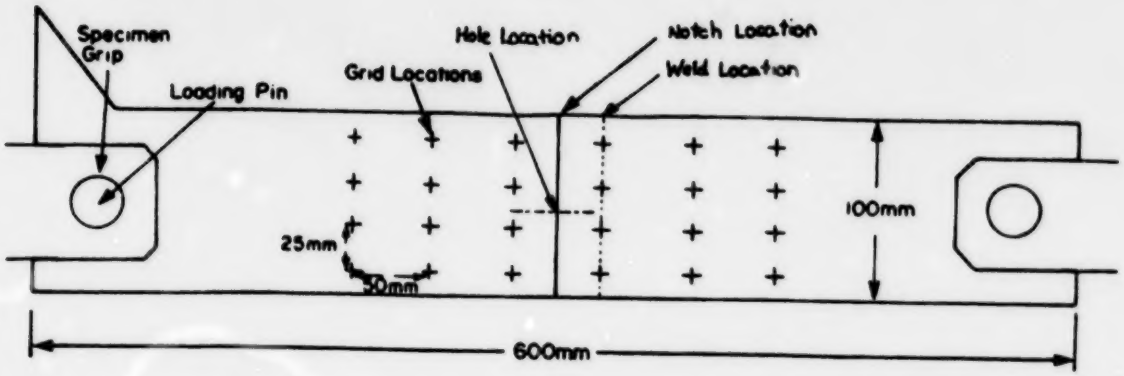

Figure 1. Specimen Dimensions

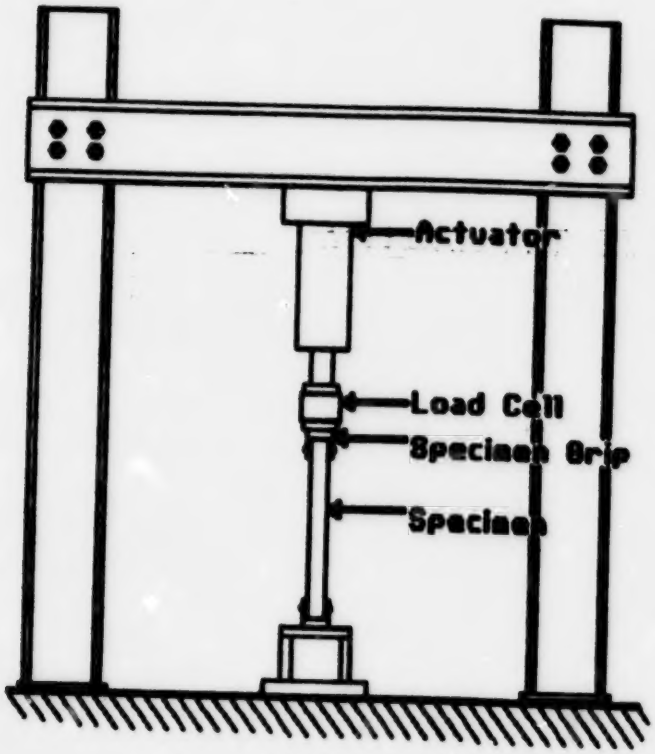

Figure 2. Load Frame

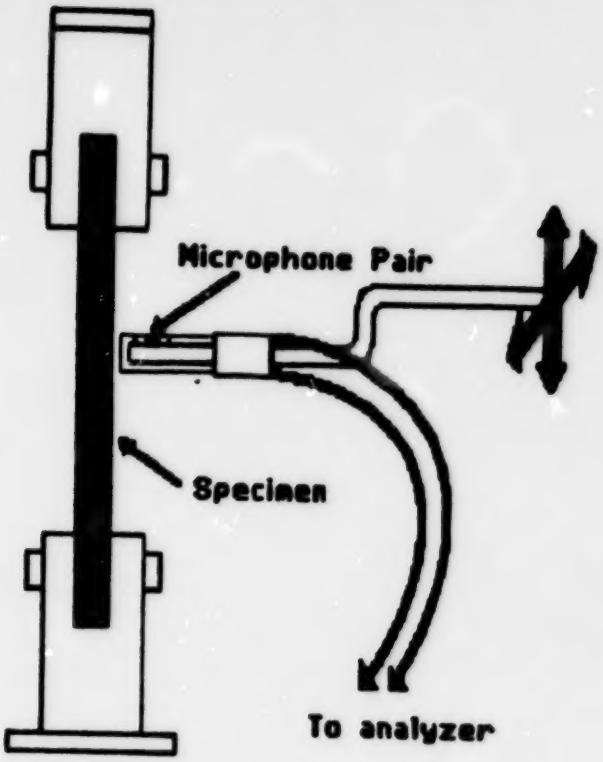

Figure 3. Intensity Probe

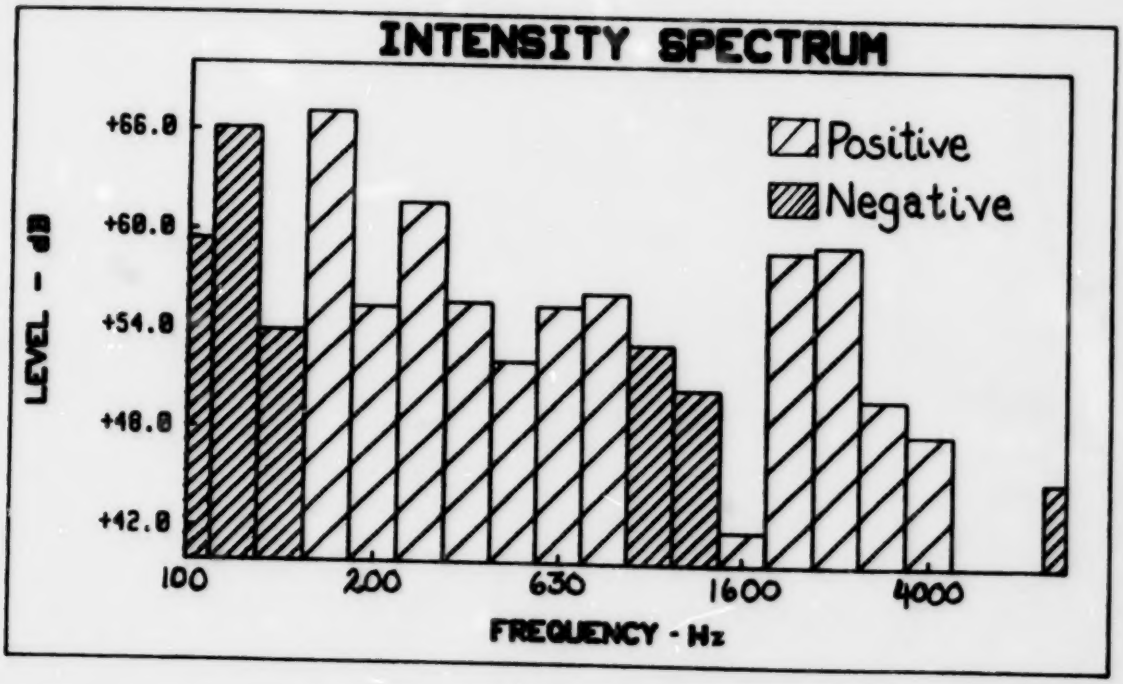

Figure 4. Example of 1/3 Octave Intensity System

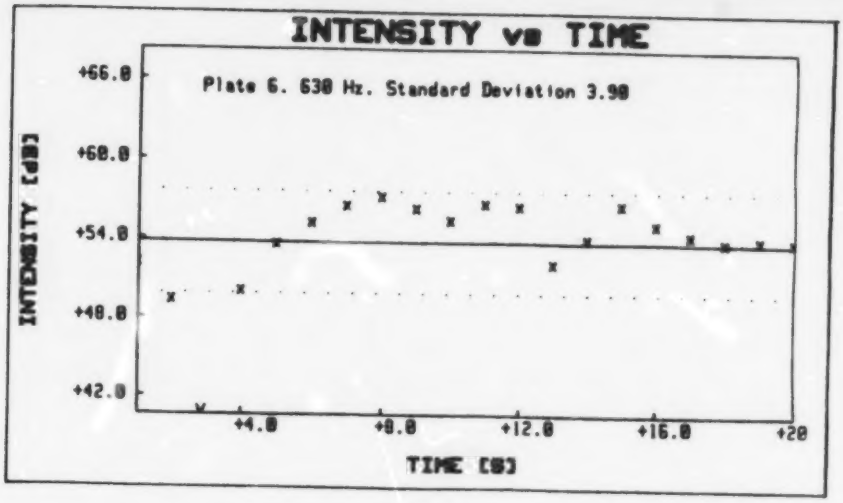

(a)

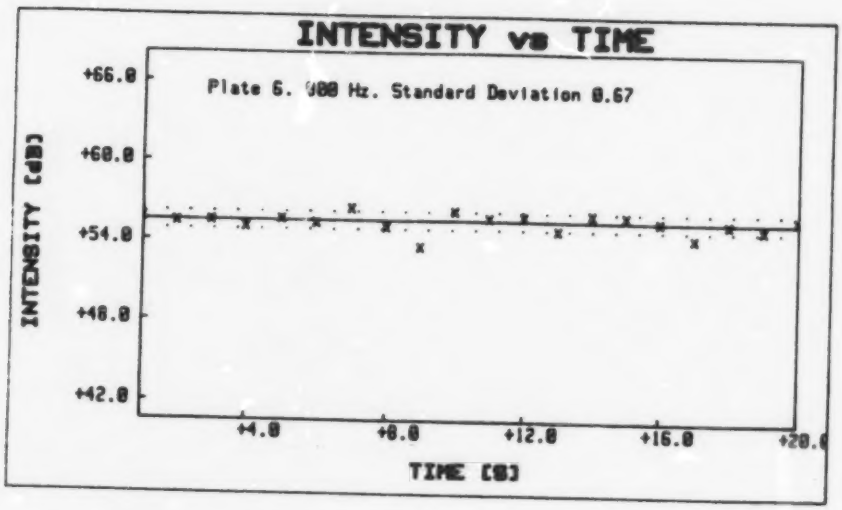

(b)

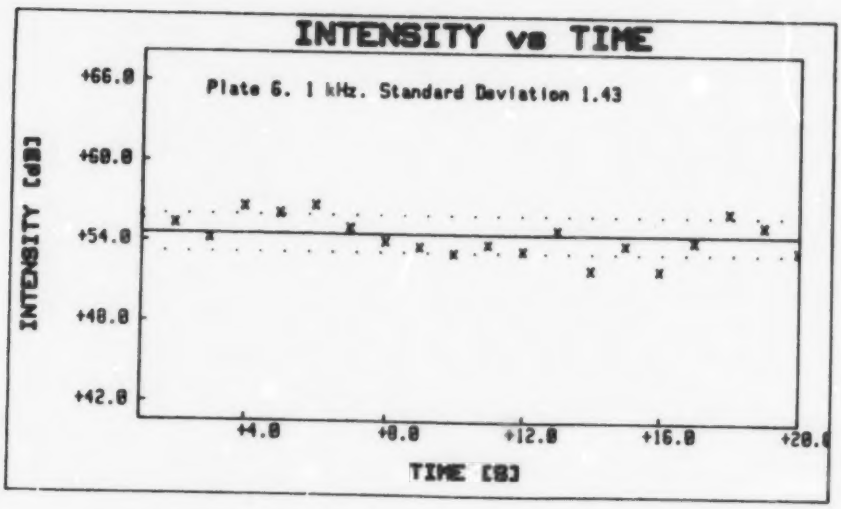

(c)

Figure 5. Intensity - Time Variation

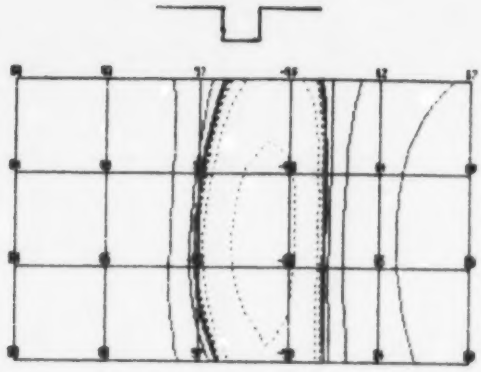

(a) Plate 1

12.5mm Notch

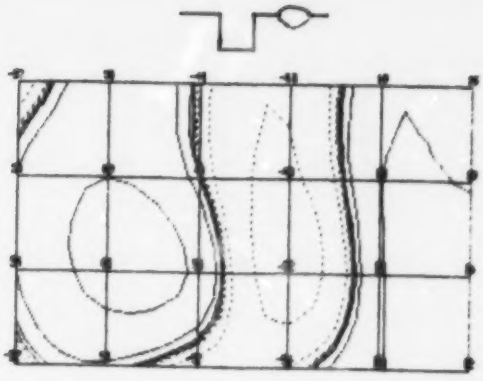

(d) Plate 3

12.5mm Notch
& Weld Bead

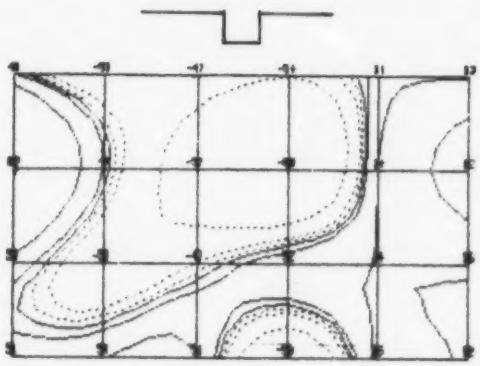

(b) Plate 2

12.5mm Notch

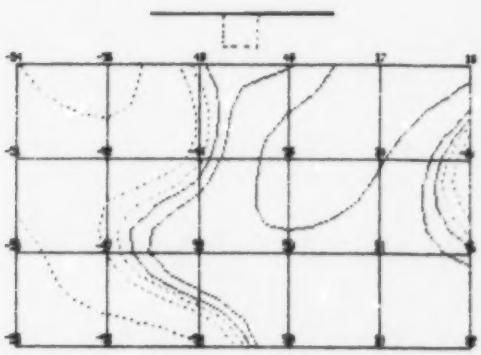

(e) Plate 5

12.5mm Deep Hole

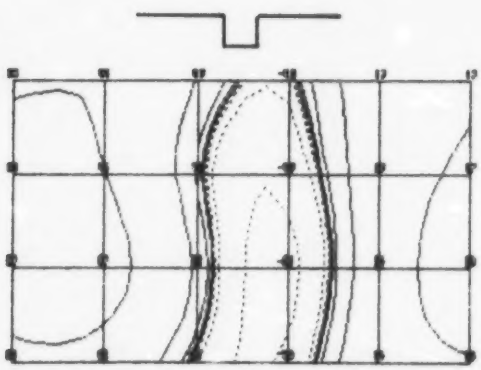

(c) Plate 4

12.5mm Notch

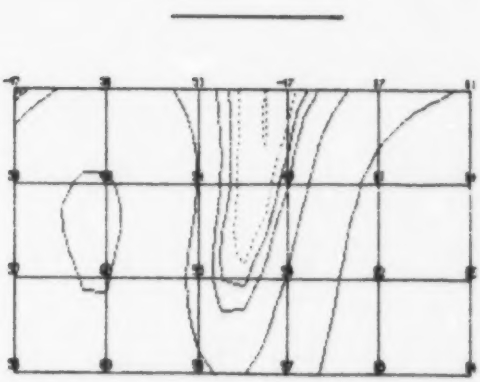

(f) Plate 6

No Defect

Figure 6. 800 Hz Contour Maps.

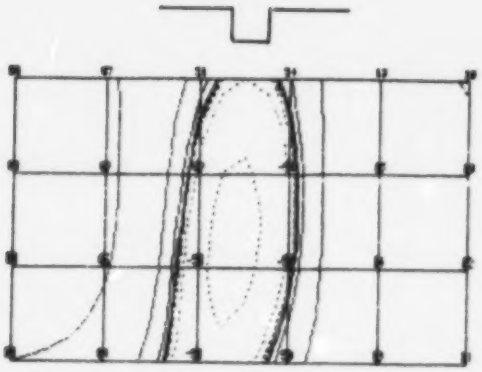

(a) Plate 1
12.5mm Notch

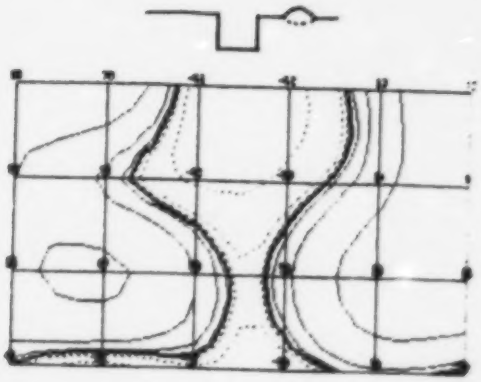

(d) Plate 3
12.5mm Notch
& Weld Bead

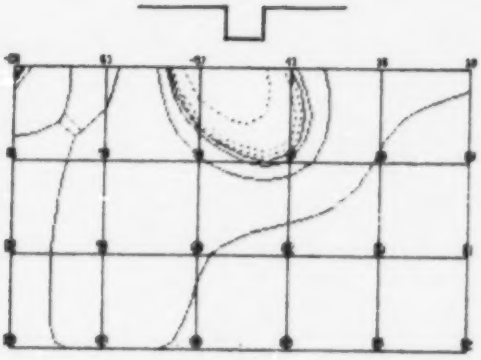

(b) Plate 2
12.5mm Notch

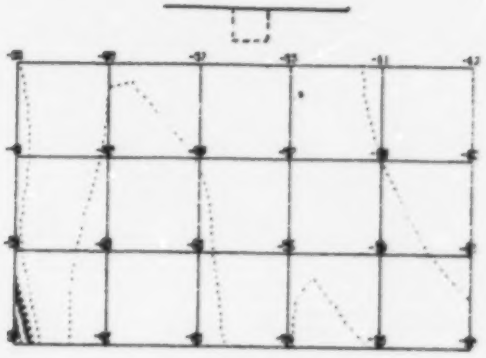

(e) Plate 5
12.5mm Deep Hole

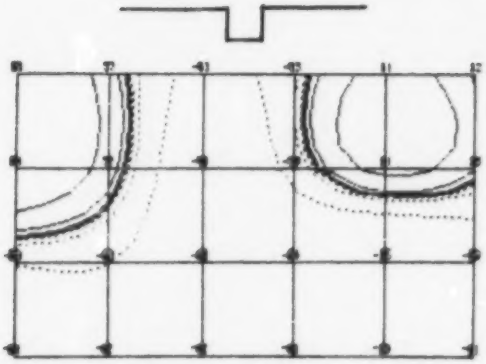

(c) Plate 4
12.5mm Notch

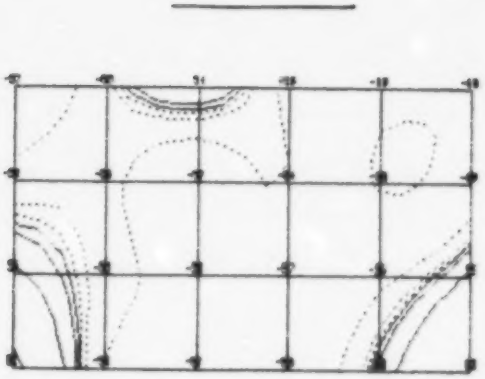

(f) Plate 6
No Defect

Figure 7. 1000 Hz Contour Maps.

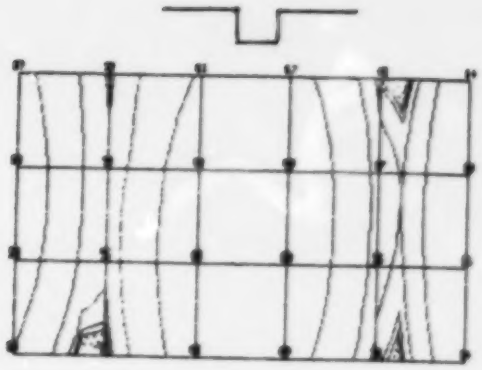

(a) Plate 1

12.5mm Notch

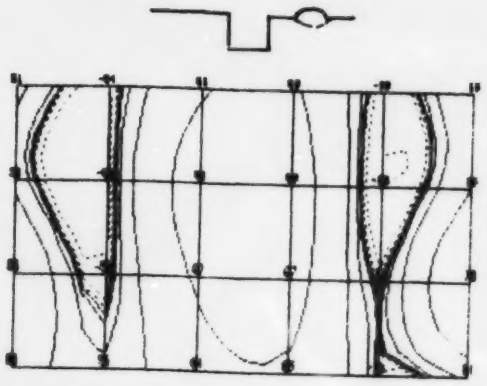

(d) Plate 3

12.5mm Notch
& Weld Bead

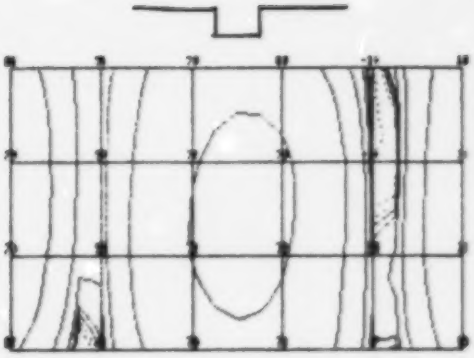

(b) Plate 2

12.5mm Notch

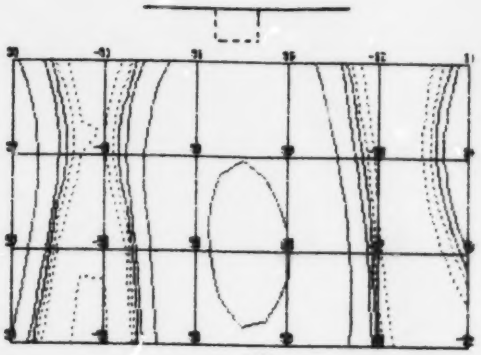

(e) Plate 5

12.5mm Deep Hole

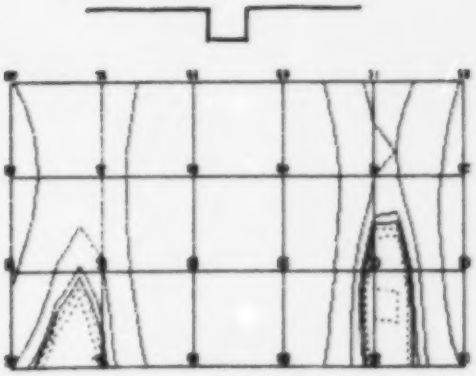

(c) Plate 4

12.5mm Notch

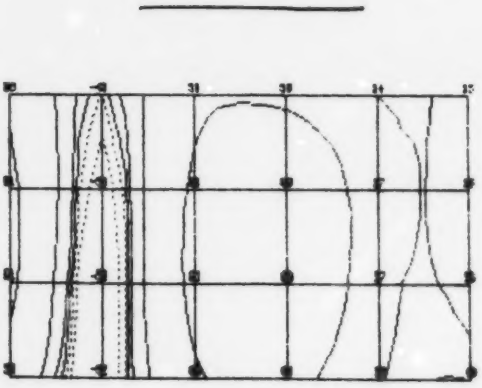

(f) Plate 6

No Defect

Figure 8. 1250 Hz Contour Maps.

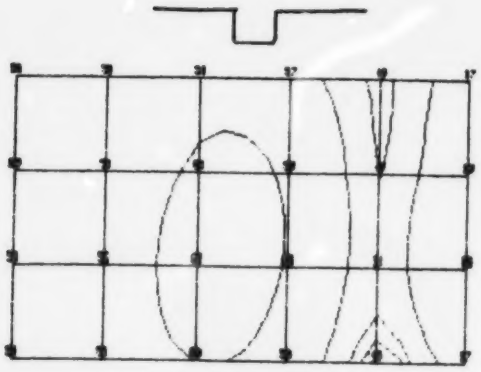

(a) Plate 1

12.5mm Notch

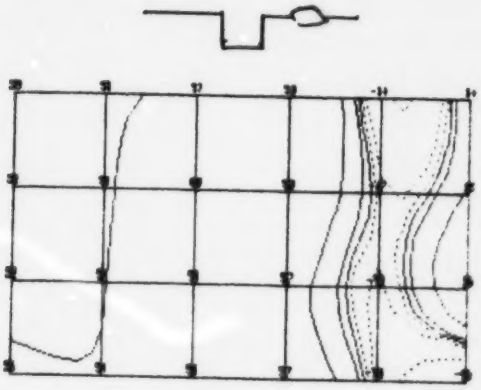

(d) Plate 3

12.5mm Notch
& Weld Bead

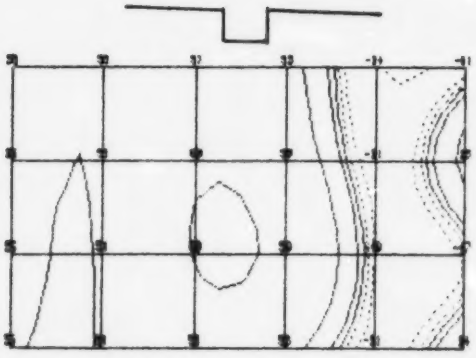

(b) Plate 2

12.5mm Notch

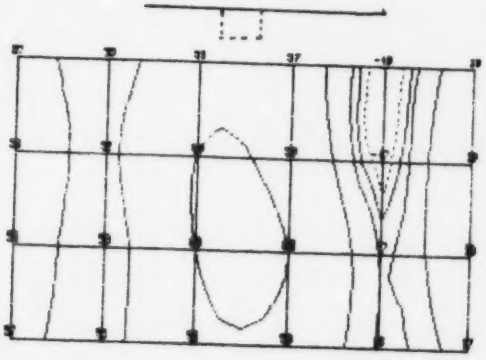

(e) Plate 5

12.5mm Deep Hole

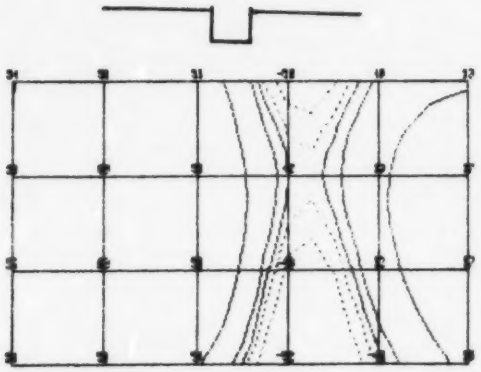

(c) Plate 4

12.5mm Notch

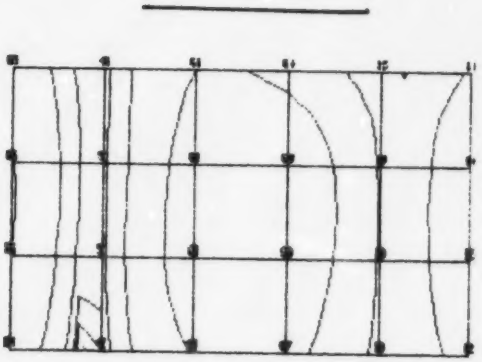

(f) Plate 6

No Defect

Figure 9. 1600 Hz Contour Maps.

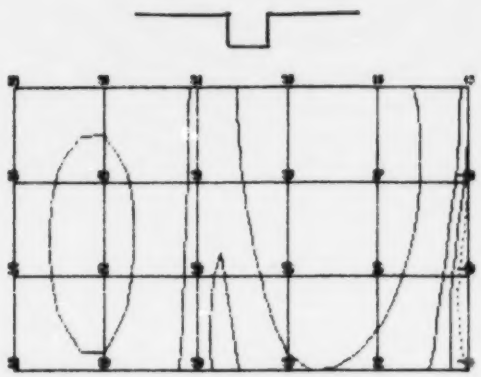

(a) Plate 1

12.5mm Notch

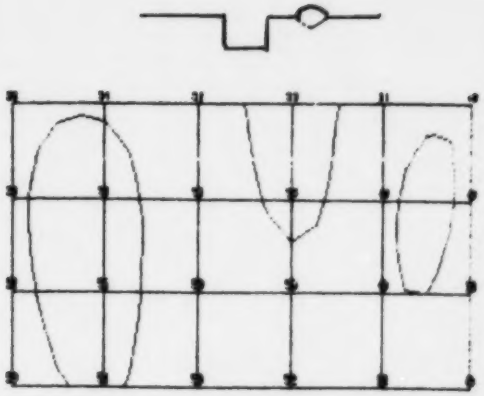

(d) Plate 3

12.5mm Notch
& Weld Bead

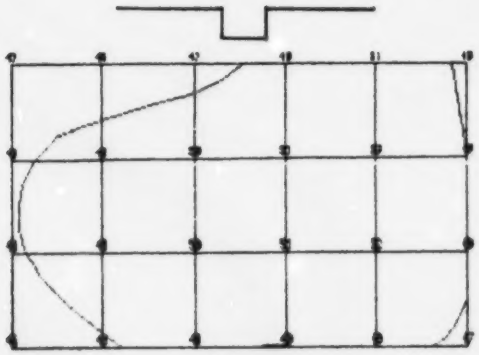

(b) Plate 2

12.5mm Notch

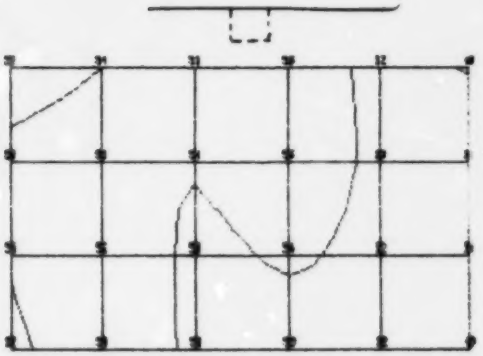

(e) Plate 5

12.5mm Deep Hole

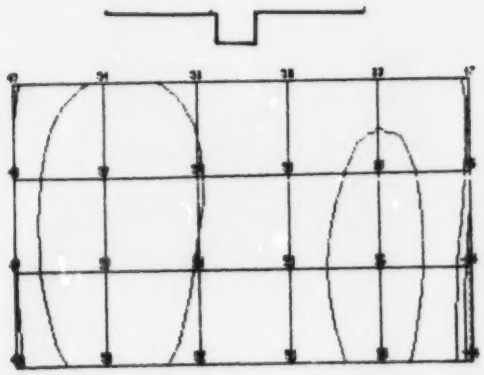

(c) Plate 4

12.5mm Notch

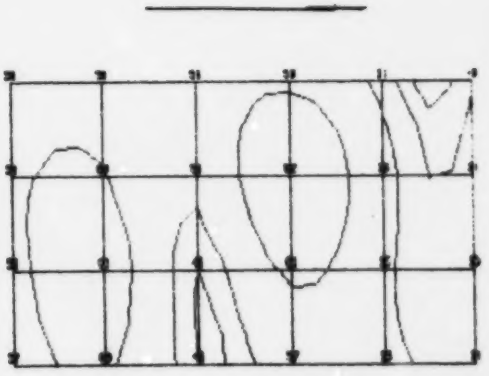

(f) Plate 6

No Defect

Figure 10. 2000 Hz Contour Maps.

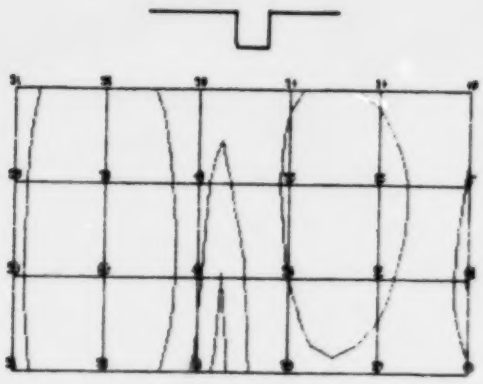

(a) Plate 1

12.5mm Notch

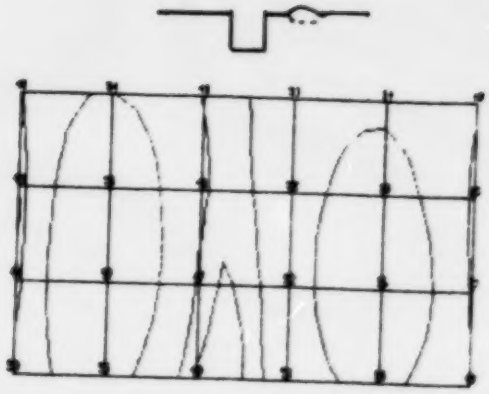

(d) Plate 3

12.5mm Notch
& Weld Bead

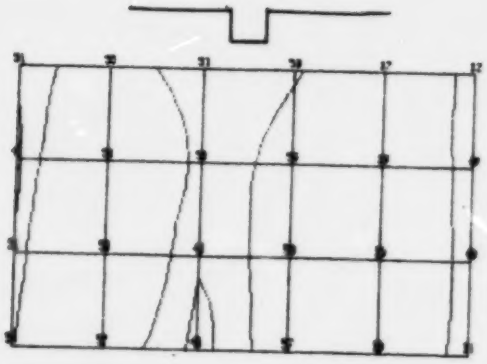

(b) Plate 2

12.5mm Notch

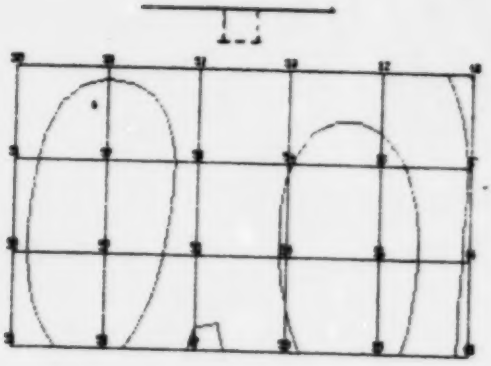

(e) Plate 5

12.5mm Deep Hole

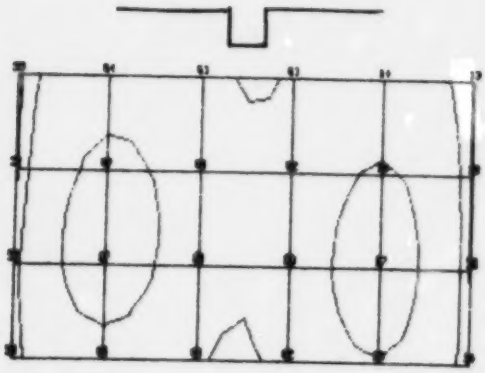

(c) Plate 4

12.5mm Notch

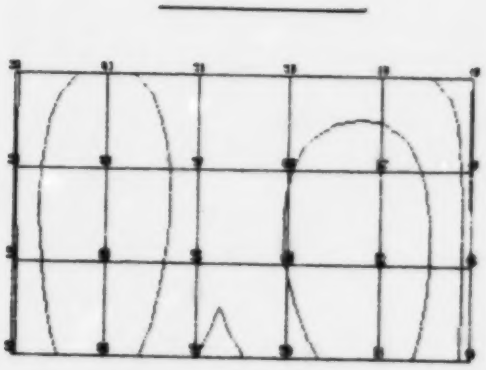

(f) Plate 6

No Defect

Figure 11. 2500 Hz Contour Maps.

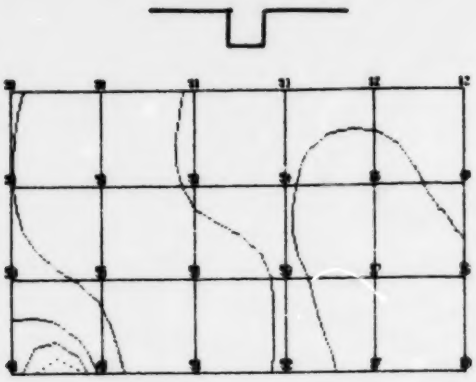

(a) Plate 1

12.5mm Notch

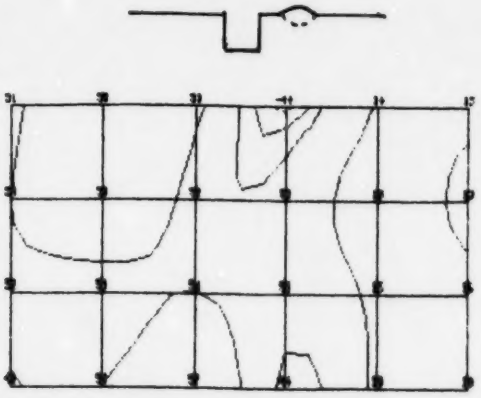

(d) Plate 3

12.5mm Notch
& Weld Bead

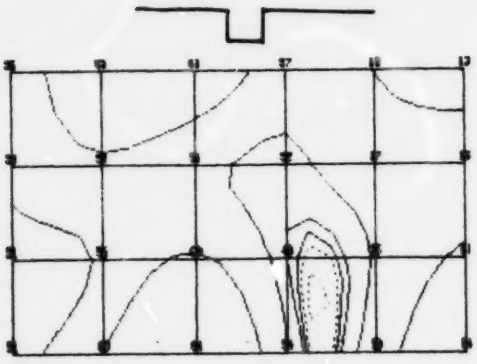

(b) Plate 2

12.5mm Notch

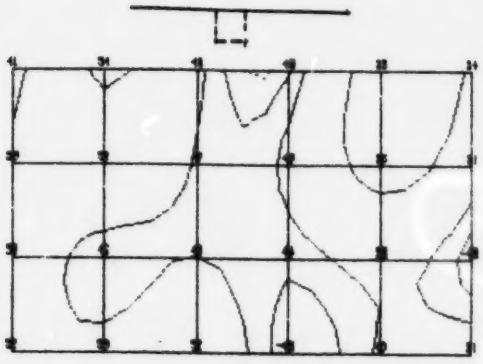

(e) Plate 5

12.5mm Deep Hole

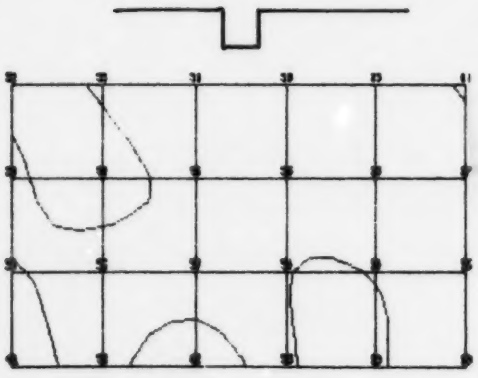

(c) Plate 4

12.5mm Notch

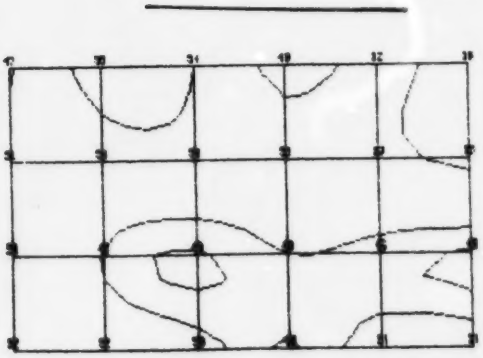

(f) Plate 6

No Defect

Figure 12. 3150 Hz Contour Maps.

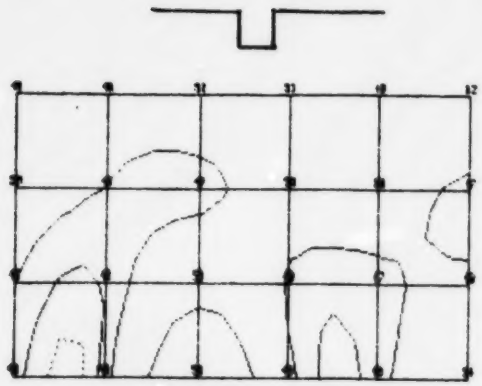

(a) Plate 1

12.5mm Notch

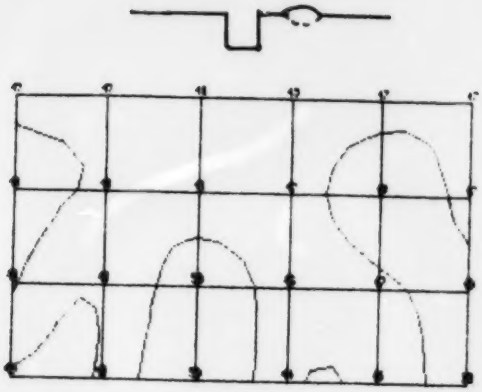

(d) Plate 3

12.5mm Notch
& Weld Bead

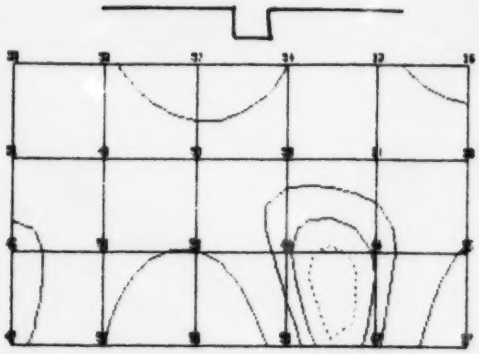

(b) Plate 2

12.5mm Notch

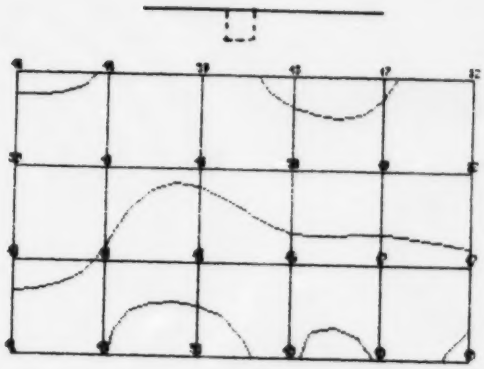

(e) Plate 5

12.5mm Deep Hole

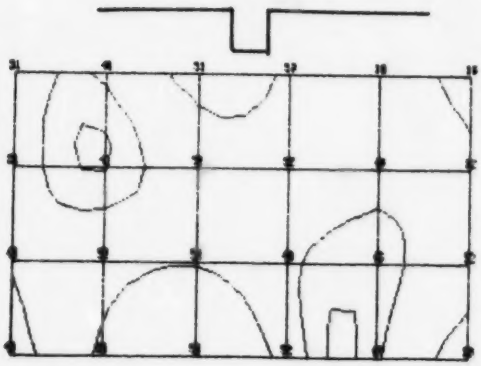

(c) Plate 4

12.5mm Notch

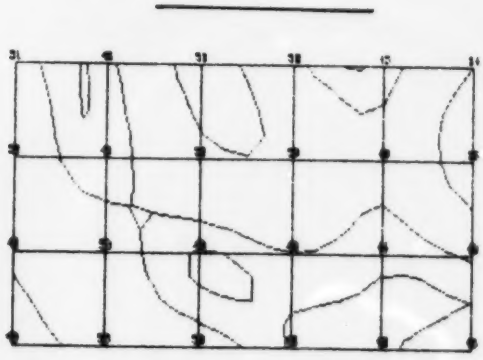

(f) Plate 6

No Defect

Figure 13. 4000 Hz Contour Maps.

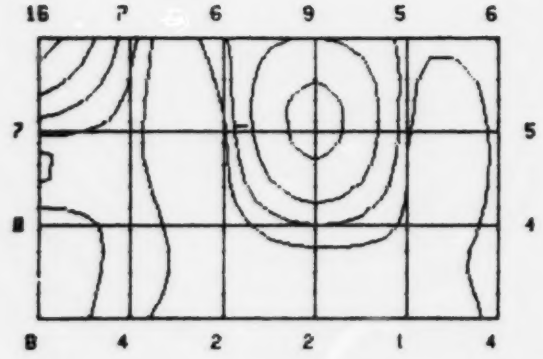

Plate 1 - Notch
(a)

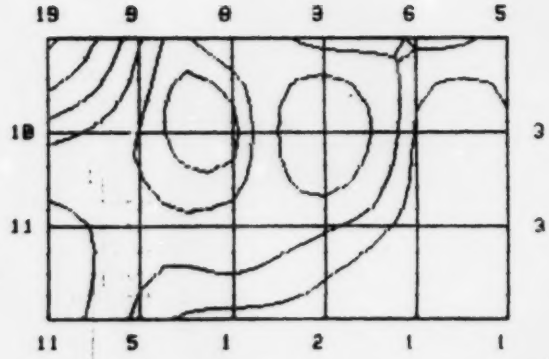

Plate 4 - Notch
(b)

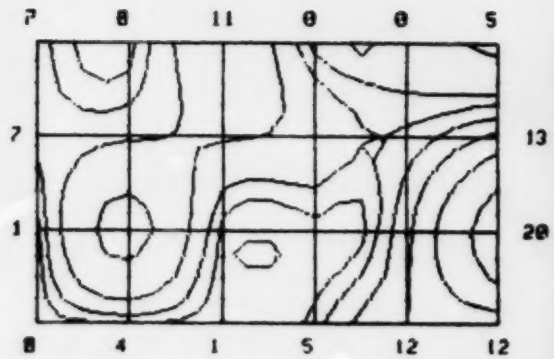

Plate 5 - Hole
(c)

Figure 14 800 Hz Remnant Factor Contour Maps
Referenced to Plate 6

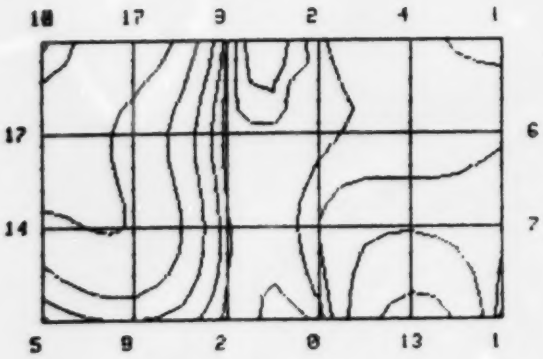

Plate 1 - Notch
(a)

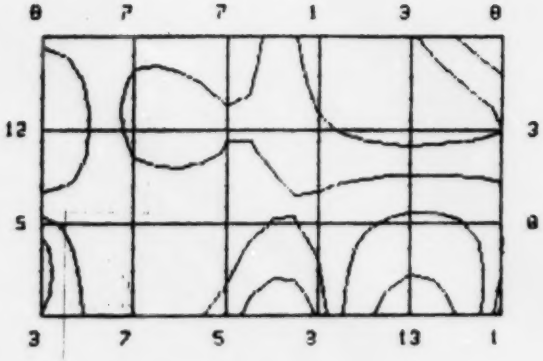

Plate 4 - Notch
(b)

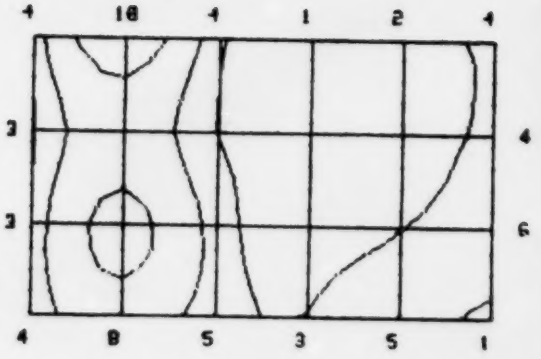

Plate 5 - Hole
(c)

Figure 15 1000 Hz Remnant Factor Contour Maps
Referenced to Plate 6

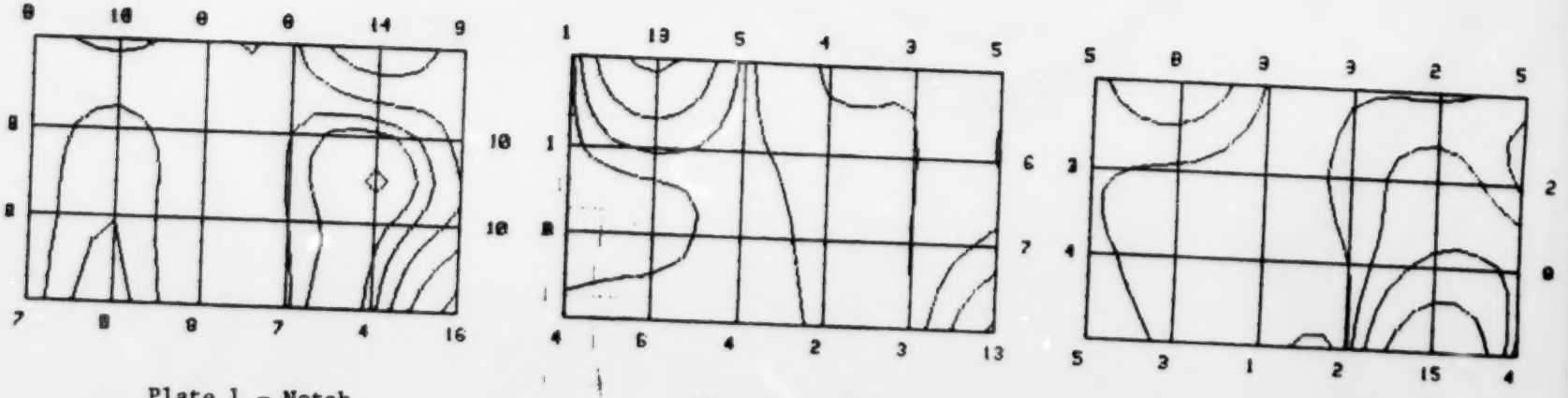

Plate 1 - Notch
(a)

Plate 4 - Notch
(b)

Plate 5 - Hole
(c)

Figure 16 1250 Hz Remnant Factor Contour Maps
Referenced to Plate 6

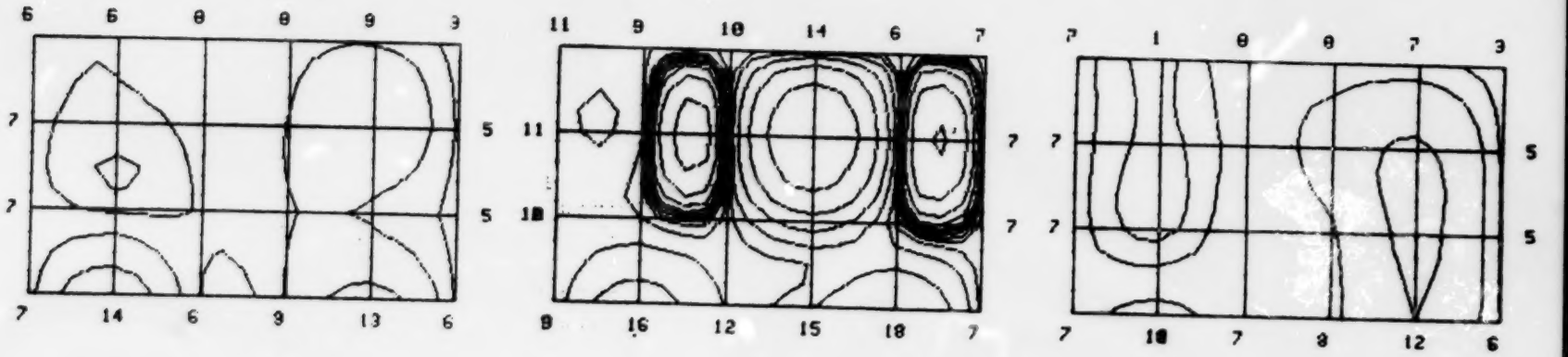

Plate 1 - Notch
(a)

Plate 4 - Notch
(b)

Plate 5 - Hole
(c)

Figure 17 1600 Hz Remnant Factor Contour Maps
Referenced to Plate 6

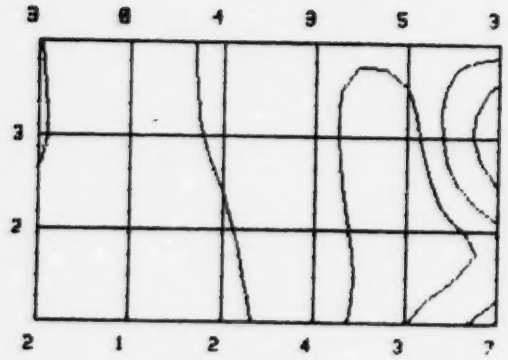

Plate 1 - Notch
(a)

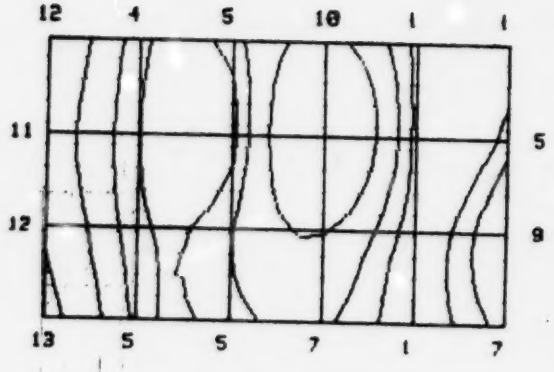

Plate 4 - Notch
(b)

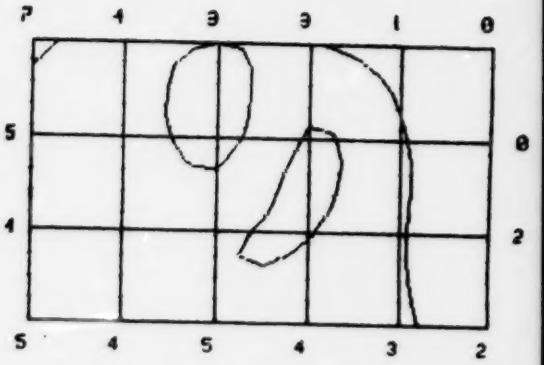

Plate 5 - Hole
(c)

Figure 18. 2000 Hz Remnant Factor Contour Maps
Referenced to Plate 6

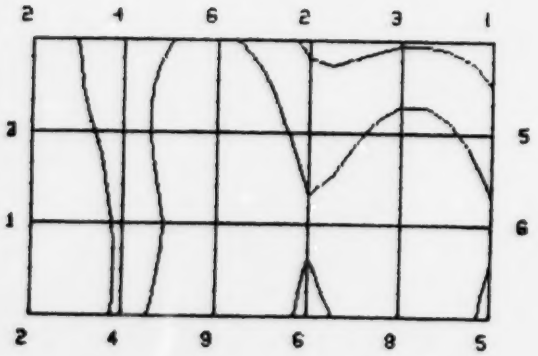

Plate 1 - Notch
(a)

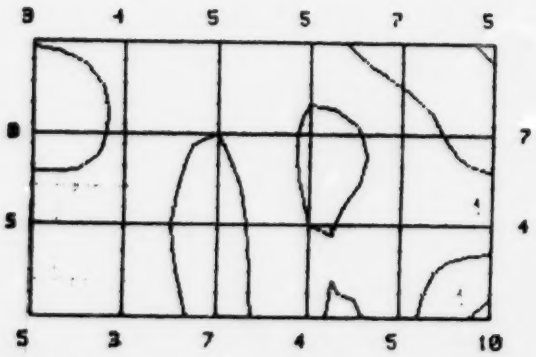

Plate 4 - Notch
(b)

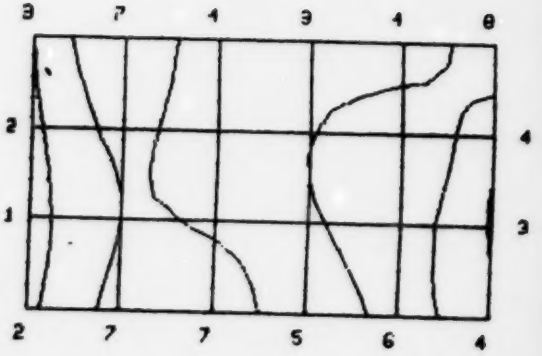

Plate 5 - Hole
(c)

Figure 19 2500 Hz Remnant Factor Contour Maps
Referenced to Plate 6

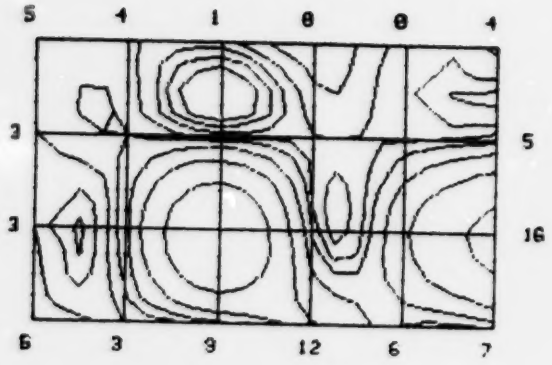

Plate 1 - Notch
(a)

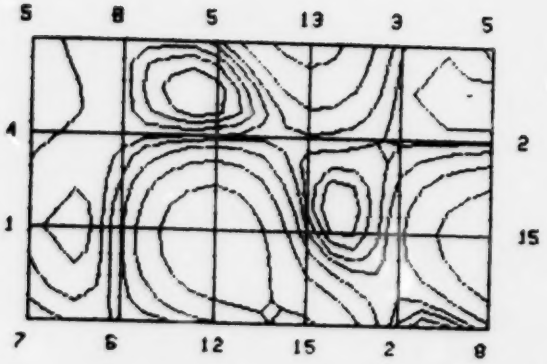

Plate 4 - Notch
(b)

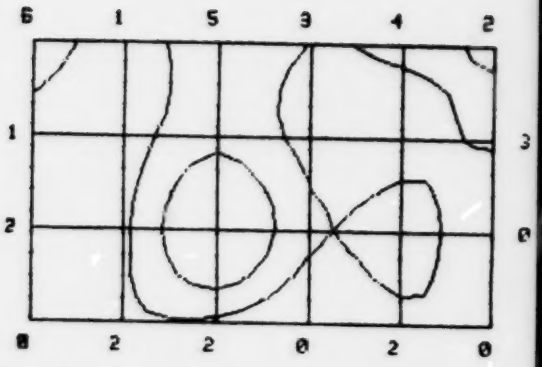

Plate 5 - Hole
(c)

Figure 20 3150 Hz Remnant Factor Contour Maps
Referenced to Plate 6

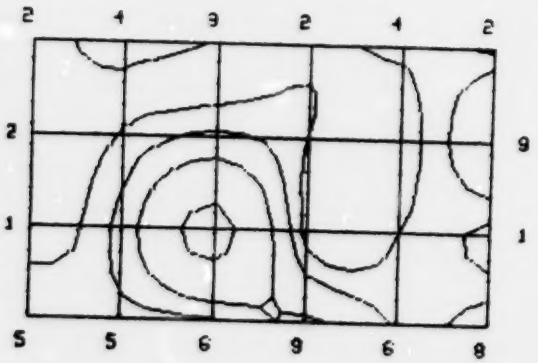

Plate 1 - Notch
(a)

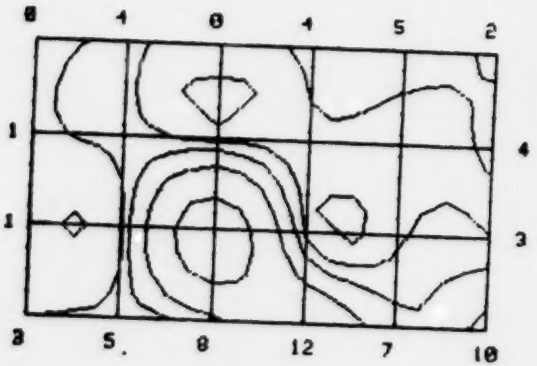

Plate 4 - Notch
(b)

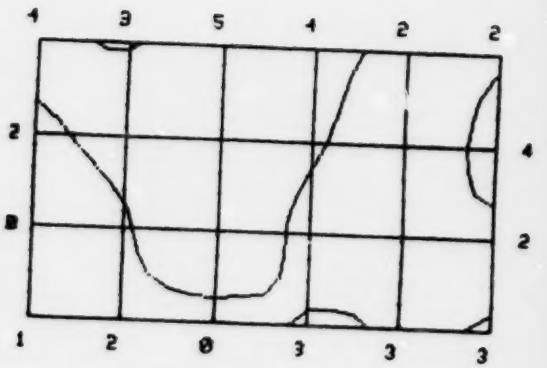

Plate 5 - Hole
(c)

Figure 21 4000 Hz Remnant Factor Contour Maps
Referenced to Plate 6

APPENDIX A LABORATORY EQUIPMENT AND PROCESSORS

For the work carried out to date, propriety calibrated equipment was purchased from Brüel & Kjaer Ltd. Software for the data collection and analysis of the DAIS has been developed at C-CORE by Mr. Gareth Williams.

Work is currently being undertaken by NORDCO Ltd., with supportive research by C-CORE, to develop a compact real time areal intensity receiver. This will permit the simultaneous real-time measurement of all three components of the intensity vector at several points over a measurement grid.

Robotic manipulators for the implementation of the scanning process are also being considered by The Faculty of Engineering and Applied Science here at Memorial University of Newfoundland.

A.1 INTENSITY ANALYZER

The Brüel & Kjaer type 3360 is a digital filtering, real time intensity analyzer, designed for use with microphones or hydrophones to measure acoustic intensity; with accelerometers to measure surface intensity, or with a combination of accelerometer and microphone to measure surface intensity. When used with a calibrated microphone pair, the device can measure pressure from either microphone and the component of the intensity vector in the direction of the microphone pair. In addition, the device used in this investigation has been modified to permit the measurement of the magnitude of the particle velocity.

The output of the device is a 1 or 1/3 octave spectrum which is presented in real time on the screen of the unit. In addition, a 1/12 octave spectrum can be measured in four passes when the instrument is being controlled via the IEEE interface. The unit has 42 real time digital filtering channels which be set to give a 1/3 octave bandwidth with centre frequencies from 1.6 Hz. to 20 kHz., a 1 octave bandwidth with centre frequencies from 2 Hz. to 16 kHz. and a 1/12 octave bandwidth. The filtering is carried out on the input pressure signals, and these can then be displayed directly, or can be used to calculate the intensity as follows:

The time averaged intensity vector, I, is given by the product of the instantaneous pressure, p and the particle velocity, v:

$$\bar{I} = \overline{p\,v}$$

where the bar denotes a time average. With a two transducer measurement probe, the particle velocity is calculated by using a finite difference approximation in Eulers equation. The intensity is calculated from:

$$I = \overline{\frac{P_a + P_b}{2\,\rho\,\Delta r} \int (P_b - P_a)\,dt}$$

where ρ is the density of the acoustic medium, and Δr is the transducer spacing.

For intensity measurements, the directionality of the reading is indicated in each frequency band. Figures A1 (a), A1 (b) and A1 (c) show examples of a pressure spectrum measured using the 1, 1/3rd and 1/12th octave bandwidth respectively. The sound pressure spectrum for the 1/3rd octave spectrum is shown in Figure A2, and the particle velocity spectrum is shown in Figure A3.

The data values for the measured spectra can be transferred to an external device via an IEEE-488 interface bus, allowing downloading of data to a computer for further processing.

A.2 TRANSDUCERS

A.2.1 Microphones

A sound intensity probe, Brüel & Kjaer type 3519, was used to measure the sound intensity in air. This probe consists of a phase matched pair of free-field microphones. One 1/4" pair and one 1/2" pair are provided along with spacers to maintain the correct microphone separation for calibrated intensity measurements. The useful frequency range of the probe is determined by the microphone size and the microphone spacing chosen (Figure A4). The microphones used are phase matched to minimize the phase errors of the system.

A.2.2 Hydrophones

Brüel & Kjaer Type 8105 hydrophones were used in the underwater

investigations. These are omnidirectional spherical hydrophones, with a working depth of 1000 m. Measurement is made through the use of piezolectric ceramic sensing elements.

A.3 CALIBRATION

The microphones are supplied as a factory calibrated, phase matched pair and as such, must be used together as supplied. No adjustments are made to these microphones or their pairings.

The 8105 hydrophones are also supplied as factory calibrated units, but are not phase matched. This was carried out at C-CORE using a pressure chamber calibration system loaned to Dr. Guigné by Brüel & Kjaer Ltd., Denmark. For details, see Paper VI, "Hydrophone Phase Matching for Underwater Intensity Measurement" in Section III of this report.

The complete system for measurement in air can be calibrated for pressure measurement by the use of a pistonphone (B & K Type 4220), which provides a calibrated sound pressure level of 124 dB at 250 Hz. In addition, the intensity and particle velocity calibrations can be checked by the use of the pistonphone and an intensity coupler (B & K Type UA 0914). The coupling element causes a phase change between the two microphones which simulates calibrated sound-intensity and particle-velocity levels.

The phase matching of the system when used with the 1/2" microphone pair can be checked by measurement of the residual intensity index. This is done by using the intensity coupler with a pink noise source (B & K 0055).

For measurement in water, the system is calibrated with the hydrophones by using a hydrophone calibrator (B & K Type 4223).

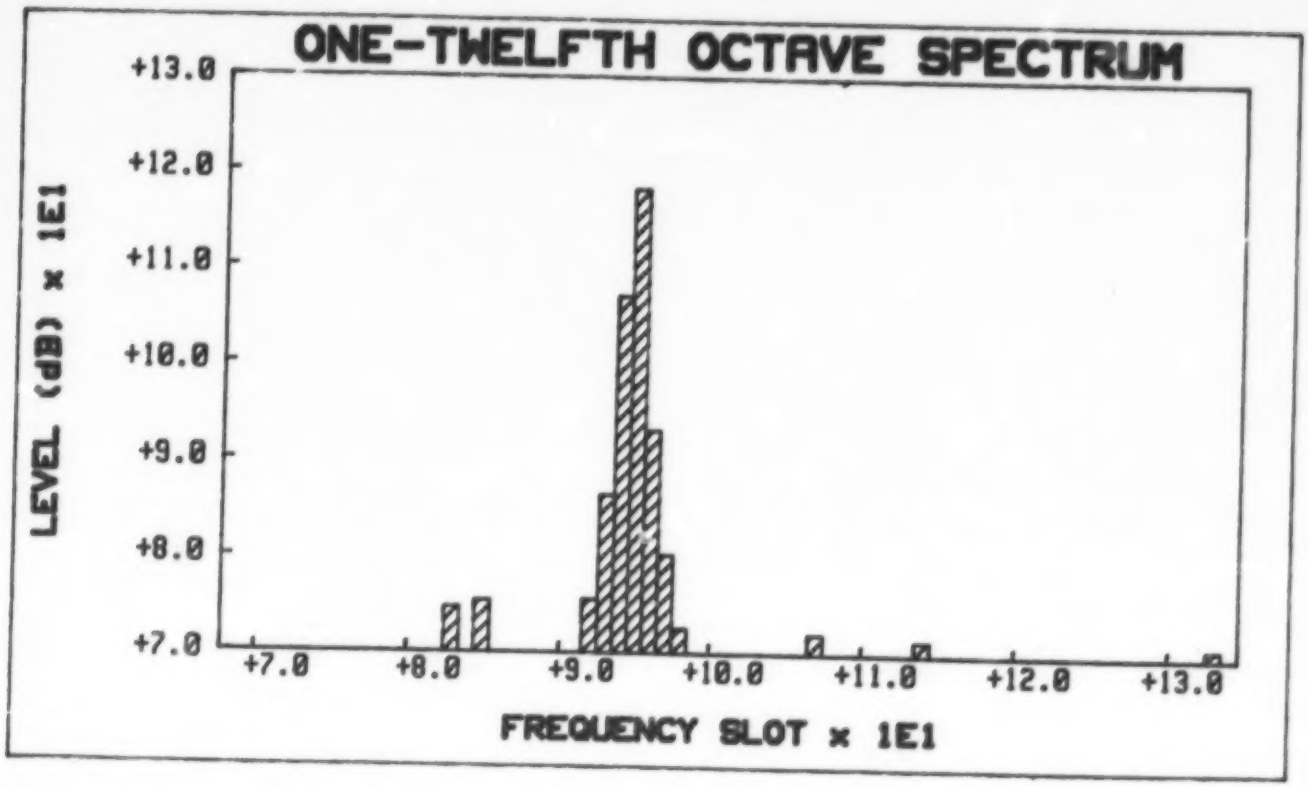

Figure A1 (a)

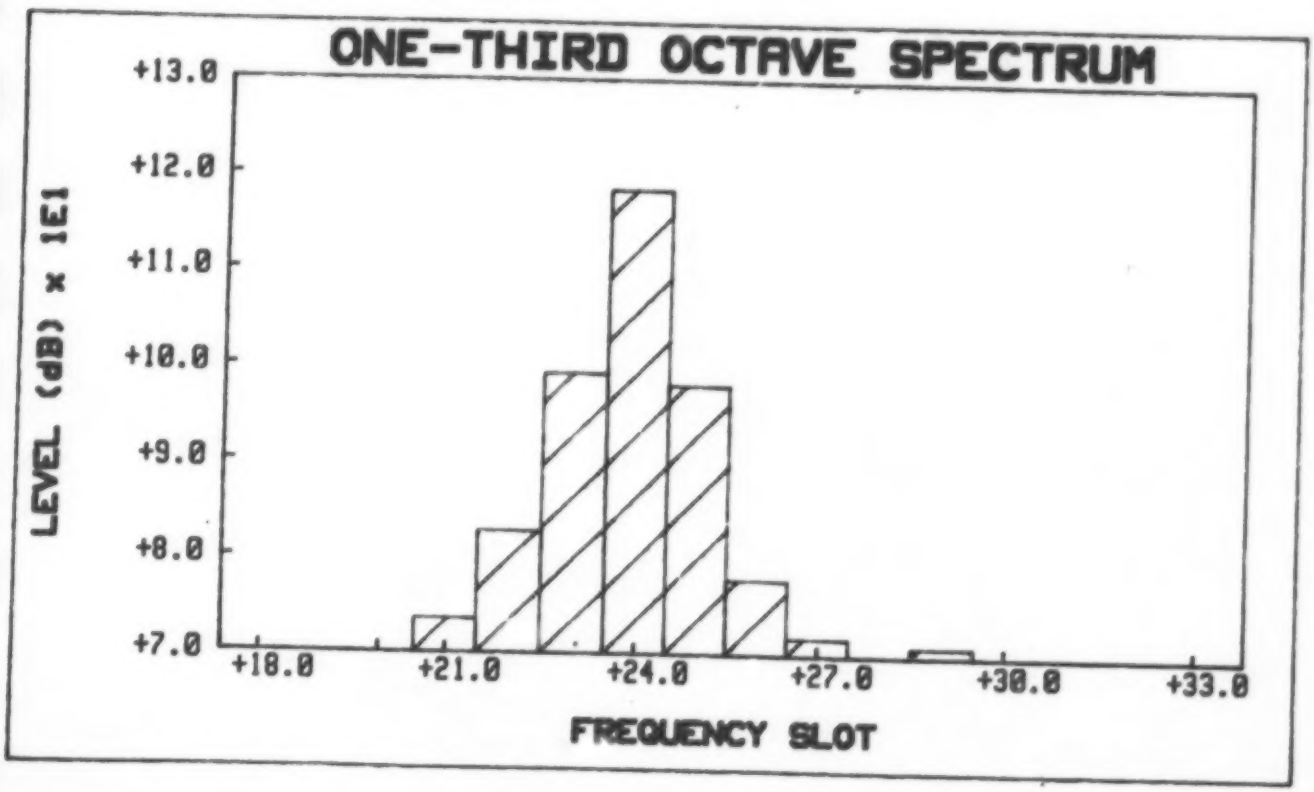

Figure A1 (b)

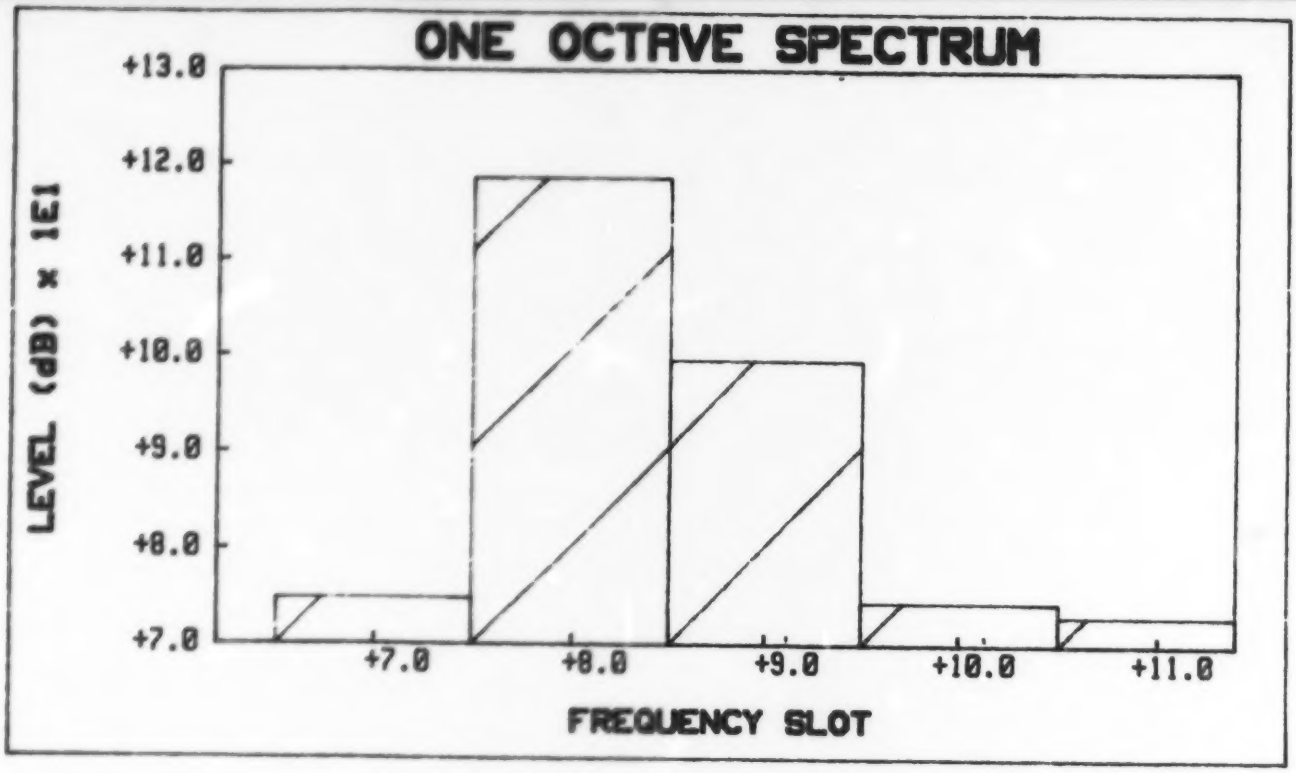

Pure Tone (250 Hz.) Pressure Spectra.
Figure A1 (c)

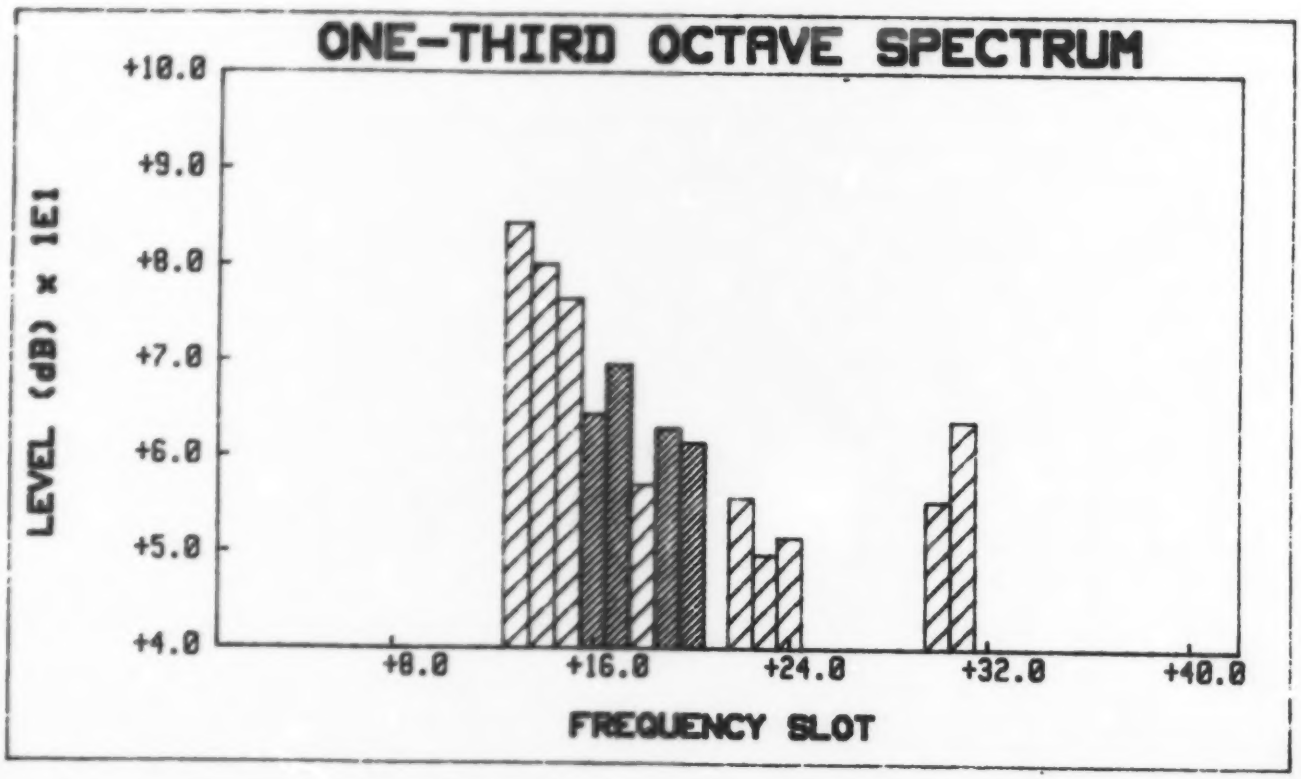

Intensity Spectrum
Figure A2

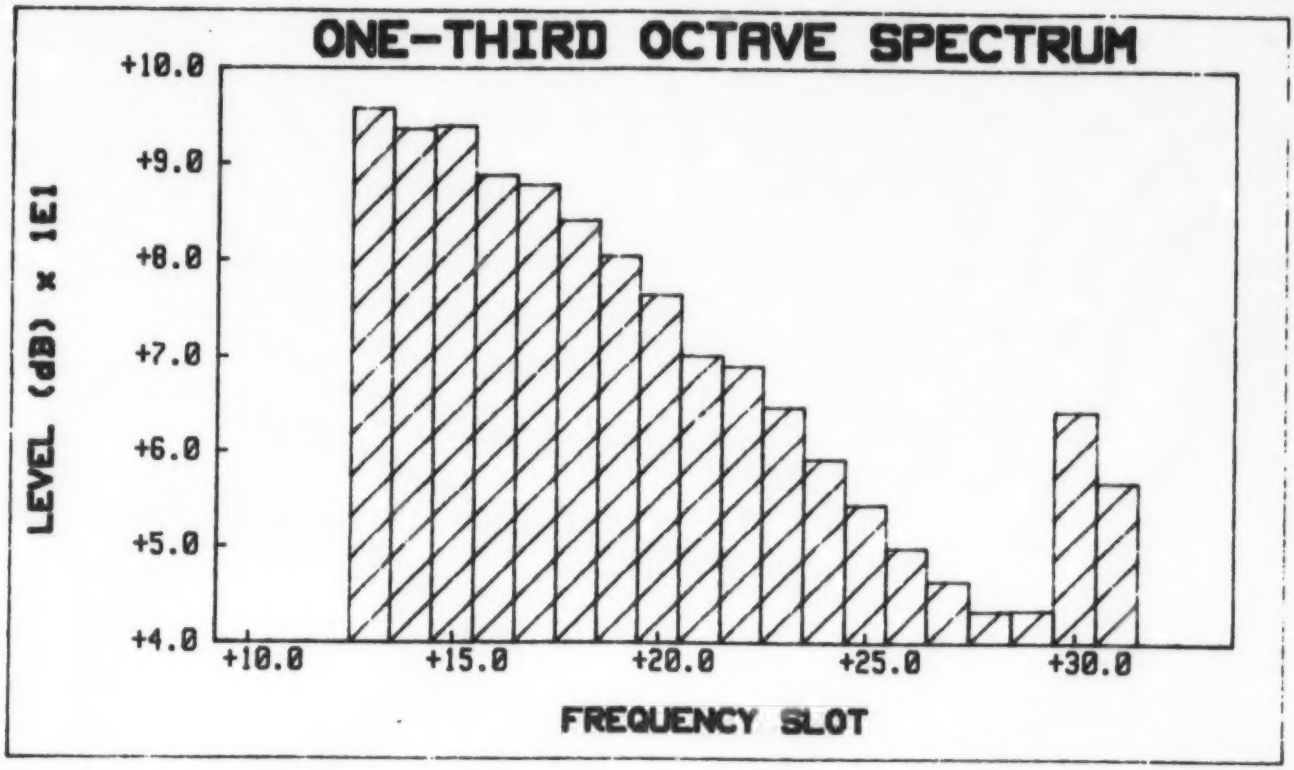

Velocity Spectrum
Figure A3

Δr	6 mm	12 mm	50 mm
1/4"	250 Hz – 10 kHz (250 Hz – 12,5 kHz)	125 Hz – 5 kHz	–
1/2"	–	125 Hz – 5 kHz	31,5 Hz – 1,25 kHz

Useful Frequency Ranges for Variuos Microphone Configurations
Figure A4